# A STUDY ON NUCLEAR STRUCTURES OF TRANSITIONAL NUCLEI AROUND A = 100

A THESIS

*Submitted by*

**T. ASHOK KUMAR**
**(Reg. No. 10612)**

**PHYSICS**

*in partial fulfillment of the requirements for the degree of*

**DOCTOR OF PHILOSOPHY**


**MANONMANIAM SUNDARANAR UNIVERSITY**
**TIRUNELVELI- 627 012**

**NOVEMBER 2018**

# MANONMANIAM SUNDARANAR UNIVERSITY
# TIRUNELVELI - 627 012

## CERTIFICATE

The research work embodied in the present Thesis entitled "**A STUDY ON NUCLEAR STRUCTURES OF TRANSITIONAL NUCLEI AROUND A = 100**" has been carried out in the Department of Physics, S.T. Hindu College, Nagercoil. The work reported herein is original and does not form part of any other thesis or dissertation on the basis of which a degree or award was conferred on an earlier occasion or to any other scholar.

I understand the University's policy on plagiarism and declare that the thesis and publications are my own work, except where specifically acknowledged and has not been copied from other sources or been previously submitted for award or assessment.

**T ASHOK KUMAR**
RESEARCH SCHOLAR

**Dr. G. Suresh**
SUPERVISOR
Assistant Professor
Physics Wing, DDE
Annamalai University
Chidambaram.

# ACKNOWLEDGEMENT

First of all I thank my Lord Almighty for showering his blessings on me and giving me this opportunity.

My foremost thanks go to my Guide **Dr. G. Suresh**, Assistant Professor, Physics wing, DDE, Annamalai University, Chidambaram, for his interest, personal care, expert and enthusiastic guidance in my research work.

I convey my gratitude to **Dr. Chidambara Thanu** Principal, S.T. Hindu College Nagercoil for giving motivation and valuable suggestions.

I am thankful to **Dr. Elampari**, head, Department of Physics. S.T Hindu College for extending the facilities provided to carry out my research work.

I would like to express my gratitude to my parents **Mr. K. Thasa Rajan** and **P. Selvi** for their warm guidance led me to be what I am now.

I extend my heartful thanks to my wife Mrs. S.V. Anisha for her encouraging support. I am thankful to my children Anash and Ashan for their good wishes for my work.

It is my pleasure to thankful staff members of the S.T Hindu College Nagercoil for their valuable help

I would like to express my gratitude to all my relative, friends and well wishers for their constant encouragement.

**ASHOK KUMAR.T**

# CONTENTS

# LIST OF FIGURES

# LIST OF ABBREVIATIONS

| | | |
|---|---|---|
| IBM | - | Interacting boson Model |
| STHR | - | Statistical theory of hot rotating Nuclei |
| CNM | - | Cranked Nilsson oscillator Model |
| LDP | - | Level density parameter |
| HFB | - | Hartree-Fock-Bogoliubov |

# CHAPTER I
# INTRODUCTION

## 1.1 Introduction

The study of structural changes in hot rotating nuclei at high excitation energy is an area of current interest in nuclear structure studies. The investigation of nuclear shape transitions at finite temperature and angular momentum continues to be one of the more demanding aspects in excited nuclei. The atomic nucleus is undergoing a variety of shape transitions with increasing temperature and angular momentum. Experimental confirmation of such shape transitions in hot rotating nuclei promises to open up new outlook in our efforts to realize the response of the nuclear many-body system at finite temperature and angular momentum.

Nuclear models representing the nature of ever intriguing nuclear force can be robust if they render applicability over various domains, including the extremes of temperature (T), spin (I), and density. Hence, extending the nuclear models to study nuclei at these extremes also gains significance, particularly in the light of current progress in the experimental facilities with which these nuclear states are becoming more accessible. An experimental investigation on the possibility of heating the nucleus to a finite temperature opens for us a new dimension in the study of nuclear structure. The primary experimental technique of constituting hot nuclei is via heavy ion reactions. Recent development in detector systems are making it possible to study the properties of nuclei under extreme conditions of temperature and spin [Snover, 1986, Gaardhoje 1988].

The combined effect of spin and temperature has created a variety of shape transition phenomena in nuclei. The interplay between rotational motion and intrinsic excitations reveals fundamental properties of atomic nuclei. The rotation is a collective motion of the deformed shape, whereas intrinsic energy is mainly generated by the excitation of individual nucleons. Rotational energy correlations, while the valley is formed by $\gamma$ rays from the region of damped rotational motion at higher excitation energy.

The study of structural properties of nuclei with mass number A ~ 100 is receiving considerable attention in nuclear structure physics. As an outcome of the inconspicuous interplay between single-particle and collective degrees of freedom, nuclei in this mass region of the nuclear chart display a huge variety of exciting phenomena. A few experimental [Gaardhoje 1988, Heyde K. and J. L. Wood 2011, Albers 2012, Albers 2013, Thomas 2013, Park 2016, Sieja 2009] and theoretical studies have already been report on the structure of those nuclei. The ground stat properties of nuclei around the mass number A = 100 has been studied extensively [Rodriguez-Guzman 2010, Mei 2012, Browne 2015, Sarriguren 2015, Federman and S. Pittel 1977, Xiang 2012, Rodriguez 2014, Federman and Pittel 1978, Skalski 1997, Sumikama 2011, Clement 2016, Lalkovski S. and P. Van Isacker 2009, Boyukata, 2010, Rodriguez-Guzm2010].

It is known that this mass region represents a classic example of dramatic shape changes with particle number. The deformed sub-shell gap at N=60 plays an important role in shape transition of Sr, Zr and Mo nuclei. The shape transition for Sr and Zr is sharp while in Mo, it is smooth. This region is particularly interesting

because of the sudden onset of deformation at N = 60 making it one of the most dramatic shape changes on the nuclear chart. The study of nuclear deformation in neutron rich nuclei around mass numbers A~100 helps on to understand the collective motion occurring in these nuclei. A first experimental trace of the deformation of these nuclides was given in the work of Johansson in 1965. Since this discovery, impressive endeavours have been made, both experimentally and theoretically, to comprehend the properties of the nuclides in the region [Johansson 1965, Cheifetz 1970, Azuma 1993, Hotchkis 1991, Ebert 2012, Smith 2012].

There is considerable interest in the study of the structure of nuclei in the mass region A≈100 due to the onset of deformation in the neutron rich nuclei [Sirag 2015, Mamta Aggarwal 2016, Kirchuk 1993, Sotty 2015, Vidya DEVI 2013, Rodriguez-Guzman 2014]. These neutron rich nuclei are of special interest because they are just at the border between a rather spherical and a well deformed shape. Theoretically, the region has been studied using interacting boson model [Sirag 2015], Nilsson Strutinsky Cranking method [Mamta Aggarwal 2016], statistical theory[Mamta Aggarwal 2016, Santhosh Kumar 2015] and and Hartree-Fock-Bogolyubov [Kirchuk 1993]. Most of these methods correspond to cold nuclei and are applicable strictly speaking only to yrast spectroscopy. In these investigations of the nuclear shape at high excitation energies are absent, and the statistical properties of fast rotating nuclei have not been given proper consideration.

In recent times, shape transitions induced by temperature and angular momentum one of the trust area of research. Experimentally, such responses to the thermal excitations have been studied from the shapes of the giant dipole resonances

(GDR) built on excited states [Gaardhoje 1992, Nanal 1999, Snover 1986]. Theoretically, they have been studied earlier in a finite temperature non-relativistic microscopic Hartree-Fock [Quentin 1978, Goodman 1986] and Hartree-Fock Bogoliubov (HFB) framework [Goodman 1988 Goodman 1986 Egido 1986] with a pairing plus quadrupole (P+Q) interaction.

In order to understand the equilibrium deformation in these hot and rotating systems around A = 100, in the present work, a calculation was performed for estimating the equilibrium shape of a nucleus by minimizing the free energy under the framework of temperature dependent rotating cranked Nilsson oscillator model (CNM) of hot rotating nuclei for a given temperature and angular momentum [Rajasekaran 1988, Rajasekaran 1981, Rajasekaran 1987, Rajasekaran 1988, Rajasekaran 1988].

**1.2 Literature Review**

Nomura 2018, investigate the structure of even-even neutron-rich Ru, Mo, Zr and Sr nuclei in the A ~100 mass region by using the interacting boson model (IBM) with microscopic input from the self-consistent mean-field approximation based on the Gogny-D1M energy density functional. The deformation energy surface in the quadrupole deformation space ($\beta$ and $\gamma$), computed within the constrained Hartree-Fock-Bogoliubov framework, is mapped onto the expectation value of the appropriately chosen IBM Hamiltonian with configuration mixing in the boson condensate state. The mapped IBM Hamiltonian is used to study the spectroscopic properties of $^{98\text{-}114}$Ru, $^{96\text{-}112}$Mo, $^{94\text{-}110}$Zr and $^{92\text{-}108}$Sr. Several cases of -soft behavior are predicted in Ru and Mo nuclei while a pronounced coexistence between strongly-

prolate and weakly-oblate deformed shapes is found for Zr and Sr nuclei. The method describes well the evolution of experimental yrast and non-yrast states as well as selected B(E2) transition probabilities. Their calculations describe well the rapid structural change between N = 58 and 60 in Zr and Sr nuclei. The analysis of the Gogny-D1M and mapped IBM energy surfaces as well as the wave functions of the $0^{+1}$ and $0^{+2}$ states reveals that the sudden lowering of the energy levels from N = 58 to 60 in those nuclei is the consequence of the onset of large prolate deformations.

Dudouet 2017, studied neutron-rich $^{96}$Kr by γ-ray spectroscopy, produced in transfer- and fusion-induced fission reactions, has been performed using the combination of the Advanced Gamma Tracking Array and the VAMOSþþspectrometer. They observed a second excited state for the first time, assigned to $J^{\pi} = 4^{+}$, and a previously reported level energy of the first $2^{+}$ excited state is confirmed. The measured energy ratio $R_{4/2} = E(4^{+})/E(2^{+})$ =2.12(1) indicates that this nucleus does not show a well-developed collectivity contrary to that seen in heavier N =60 isotones. This new measurement highlights an abrupt transition of the degree of collectivity as a function of the proton number at Z =36, of similar amplitude to that observed at N = 60 at higher Z values. A possible reason for this abrupt transition could be related to the insufficient proton excitations in the $g_{9/2}$, $d_{5/2}$, and $s_{1/2}$ orbitals to generate strong quadrupole correlations or to the coexistence of competing different shapes. An unexpected continuous decrease of $R_{4/2}$ as a function of the neutron number up to N = 60 is also evidenced. This measurement establishes the Kr isotopic chain as the low-Z boundary of the island of deformation for N = 60 isotones. A comparison with available theoretical predictions using different beyond mean-field approaches shows that these models fail to reproduce the abrupt transitions at N = 60 and Z = 36.

Petrovici 2011 investigated the shape transition from moderate deformation in $^{98}$Zr to large deformation in $^{104,106,110}$Zr, shape coexistence and variable shape mixing at low as well as intermediate and high spins in Zr isotope. The influence of the shape mixing on the structure and dynamics of the investigated Zr isotopes is discussed and comparison with the available data is presented. They found that, the $0h_{11/2}$ spherical orbital is responsible for the onset of deformation and neutron alignment in the prolate deformed bands. The $0g_{9/2}$ protons are aligning faster in the oblate bands. Also found that the changes in the renormalization of the effective interaction could influence the oblate and prolate mixing in the structure of the wave functions as well as the corresponding electromagnetic properties.

Roubin 2017, performed an extension of the atomic mass surface in the region $A \approx 100$ via measurements of the $^{100-102}$Sr and $^{100-102}$Rb masses with the ion-trap spectrometer ISOLTRAP at CERN-ISOLDE, including the first direct mass determination of $^{102}$Sr and $^{101,102}$Rb. These measurements confirm the continuation of the region of deformation with the increase of neutron number, at least as far as N= 65. To interpret the deformation in the strontium isotopic chain and to determine whether an onset of deformation is present in heavier krypton isotopes, a comparison is made between the experimental values and mean-field and beyond mean-field results available in the literature. To complete this comparison Hartree-Fock-Bogoliubov calculations for even and odd isotopes were performed, illustrating the competition of nuclear shapes in the region.

Sirag 2015 investigated the first and second order shape phase transitions (SPTs) in even-even heaviest nuclei in the A~100 mass region with neutron number

$N \geq 52$, by analyzing the potential energy surfaces (PESs) within the interacting boson model (IBM). He considered the consistent-Q Hamiltonian with control parameter within the IBM coherent state formalism. The SPTs are explored with variation of the control parameter. The validity of the model is examined for two neutron-rich isotopic chains, Zirconium ($^{40}$Zr) isotopes for the SPT from a spherical vibrator U(5) to an axially deformed rotor SU(3) called the X(5) symmetry, and Ruthenium ($^{44}$Ru) isotopes for the SPT from a spherical vibrator U(5) to a -soft rotor O(6) called the E(5) symmetry. Relatively flat PESs are obtained for nuclei showing the E(5) symmetry, while in nuclei corresponding to the X(5) case, PESs with a bump are obtained.

Pinston 2005 investigated, odd and odd-odd *N*=59 istones, using a combination of two experimental techniques. They established that three shapes coexist in odd $^{97}$Sr and $^{99}$Zr, while two different shapes were seen in odd-odd $^{98}$Y and $^{96}$Rb. These new data demonstrate that the spectroscopy of odd-*A* and odd-odd nuclei, provides much more information on the structure of the different shapes than even-even nuclei. The theoretical interpretation of these collective excitations is based on the Nilsson diagram in the *N*=58 region and it shows that the spherical unique-parity state plays a very important role in the shape coexistence mechanism. In conclusion, a great wealth of nuclear structure information was recently gained for these odd and odd-odd *N*=59 isotones and they hope that these new results will trigger new calculations for this mass region.

Clement 2016, investigated the structure of neutron-rich $^{96,98}$Sr nuclei by low-energy safe Coulomb excitation of radioactive beams at the REX-ISOLDE facility,

CERN, with the MINIBALL spectrometer. A rich set of transitional and diagonal *E*2 matrix elements, including those for non-yrast structures, has been extracted from the differential Coulomb-excitation cross sections. Their results support the scenario of a shape transition at $N = 60$, giving rise to the coexistence of a highly deformed prolate and a spherical configuration in $^{98}$Sr, and are compared to predictions from several theoretical calculations. The experimental data suggest a significant contribution of the triaxal degree of freedom in the ground state of both isotopes.

Santhosh Kumar 2015, presents results of statistical calculations of single-particle characteristics of nuclei, excitation energies and shape transition in the Sn isotope with neutron number 50, which is the extremely neutron deficient isotope. Their study revealed the following conclusions: At all temperatures the ground state deformation is spherical ($\delta = 0.0$). 2. The excitation energy is smooth growing with angular momentum and is increased for increasing temperature and at spin, $J \approx 2$ 6h, there is a shape change from spherical to oblate ($\gamma$ = -180o). The decrease of proton separation energy with increasing spin at E* = 14MeV is due to the transition from $S_n$ to $I_n$ via the transformation of a proton in $^{100}$Sn to a neutron via nuclear decay. The neutron separation energy decreases with increasing temperature and spin, which shows the stability of the nucleus $^{100}$Sn against temperature and angular momentum.

Mamta aggarwal 2016, theoreticaly investigated the shape transitions in A = 100 isobars of Z = 42 to 50. They observed a variety of shape transitions, while moving from neutron rich $^{100}$Mo to proton rich $^{100}$Sn with predominant triaxiality. Temperature and spin induced shape transitions are explored within the microscopic theoretical framework of statistical theory of hot rotating nuclei. Prolate non-

collective – a rare shape phase is reported in this mass region on the proton rich side of the nuclear chart. In ground state, triaxiality is predominant shape phase with high deformation on the neutron rich side with shape transition to prolate deformations while moving towards proton rich side while approaching shell closure Z = 50 where equilibrium deformation reduces to zero. She predict for the first time the rarely seen shape phase of prolate non-collective in A=100 isobars on the neutron deficient side of the nuclei at low spin with a shape transition to usually seen shape phase of oblate non-collective. A = 100 isobars of Mo, Tc, Ru do not exhibit this rare shape phase whereas Rh, Pd, Ag, Cd, In and Sn nuclei are predicted to have prolate non collective shape as the predominant shape phase over a large angular momentum range.

Sotty 2015, for the first time presents the excited states of the neutron-rich nuclei $^{97;99}$Rb using the multistep Coulomb excitation of radioactive beams. Comparisons of the results with particle-rotor model calculations provide clear identification for the ground-state rotational band of $^{97}$Rb as being built on the $\pi g_{9/2}[431]\ 3/2^{+}$ Nilsson-model configuration. The ground-state excitation spectra of the Rb isotopes show a marked distinction between single-particle-like structures below N =60 and rotational bands above. Their study defines the limits of the deformed region around A ~ 100 and indicates that the deformation of $^{97}$Rb is essentially the same as that observed well inside the deformed region. It further highlights the power of the Coulomb-excitation technique for obtaining spectroscopic information far from stability.

### 1.3 Objective of the Thesis

The objective of this thesis is to illustrate the use of statistical theory in the study structural changes in the nuclei around mass number A ~ 100.

In this work, the structural properties of Krypton ($_{38}$Kr) Zirconium ($_{40}$Zr) and Molybdenum ($_{42}$Mo) are investigated as a function of different degrees of freedom such as angular momentum, deformation and temperature. Further the structural changes in $^{90, 92, 94, 96, 98, 100}$Sr isotopes are studied. Furthermore we also investigated the odd-even and odd-odd effect in nuclei around mass A = 100. The single particle level density parameter, excitation energy, entropy and neutron and proton separation energy were extracted as a function of angular momentum, deformation and temperature for the above systems.

**1.4 Layout of the Thesis**

A statistical theory [Rajasekaran 19888, Rajasekaran 1981, Rajasekaran 1987, Rajasekaran 1988, Rajasekaran 1988], which incorporates deformation, collective and non-collective degrees of freedom and shell effects, is developed to study the single particle level density parameter, rotational energy, entropy and neutron and proton separation energy and is given in Chapter II. This chapter describes the statistical theory proposed by Morreto and modified by Rajasekaran. The use of the statistical theory of nuclei in these investigations, and its success in explaining asymptotic fission which is a consequence of the shell structure of nuclei, provide enough proof of its utility [Rajasekaran 1988]. Soon after Strutinsky [Strutinsky 1967] prescribed a method of extracting shell correction of liquid drop energies so that ground state masses of nuclei could be estimated correct to ±0.5MeV, Ramamoorthy et al. [Ramamoorthy 1907, 1980, 1983] put forth a statistical method, which yielded results as accurate as the former method. This infused more faith on the practitioners of the statistical model and disproved the wrong notion that statistical models yield only macroscopic details.

The basic constituent in the statistical theory is a suitable shell model level scheme [Nilsson 1969, Eisenberg 1976, Soloviev 1976, Irvine 1972, Seeger 1970] generated for various nuclear deformations. substantial consideration has been given to the selection of the various parameters involved in the deformed harmonic oscillator Hamiltonian [Rajasekaran 19888, Rajasekaran 1981, Rajasekaran 1987, Rajasekaran 1988, Rajasekaran 1988, Strutinsky 1967, Ramamoorthy 1907, 1980, 1983, Nilsson 1969, Eisenberg 1976, Soloviev 1976, Irvine 1972, Seeger 1970, Shanmugam 1978,79] for a rotating nucleus. Triaxial deformations [Eisenberg 1976] are assumed for the purpose of diagonalization of the Hamiltonian depending upon the situation.

In all calculations reported in this thesis, single particle data obtained by diagonalizing the cranked Nilsson Hamiltonian were used. The methods of obtaining the triaxial and cranked Nilsson oscillator [Inglis 1954] levels are presented in Chapter III. In this chapter we describe the nuclear shapes and deformation parameters within the framework of cranked Nilsson model. It is expected that changes in nuclear shape may occur as a consequence of fast nuclear rotation. In the present study the rotation is based on the changes in characteristic harmonic oscillator frequencies $\omega_1$, $\omega_2$ and $\omega_3$ (Nilsson parameterization). Nilsson parameterization corresponds to basic vibrations $\omega_1$, $\omega_2$ and $\omega_3$ in the principal axes with requirement the constant volume be enclosed by the equipotential surface. This condition may be written as $\omega_1\omega_2\omega_3 = \omega_0$ for the harmonic oscillator potential.

Chapter IV of the thesis contains the study of structural properties of $^{94,96,98}$Kr, $^{98,100,102}$Zr and $^{102,104,106}$Mo as a function of different degrees of freedom such as

angular momentum, deformation and temperature. The statistical theory is used to study the structural properties, which incorporates deformation, collective and non-collective rotational degrees of freedom and shell effects. The inputs for the statistical theory are the microscopic single particle levels and single particle spins corresponding to the triaxially deformed Nilsson harmonic oscillator potential. Naturally, the results reflect the effect of the shell structure of the nucleus at different deformations. The $\kappa$, $\mu$ pair used for generating the single particle level scheme is as given in Ref. [Shanmugam 1978,79, Diebel 1980]. These parameters are appropriate since an agreement between Strutinsky's smoothed moment of inertia and the rigid rotor value is obtained by Diebel et al. [Diebel 1980]. The deformation parameter $\varepsilon$ is varied from $\varepsilon = 0.0$ to 1.2 with $\Delta\varepsilon = 0.1$ for $\gamma = -180°$ corresponds to an oblate shape (rotating about the symmetry axis) and $\gamma = 120°$ corresponds to the prolate shape (rotating about an axis perpendicular to the symmetry axis). Calculations are carried out by minimizing the free energy for equilibrium deformation.

The different parameters akin to single particle temperature dependent shell energy $E_{shell}$ [Andersson 1978, Nerlo-Pomorska 2005, Pomorski 2004, Pomorski 2000, Brack 1997 Egido 2000], level density parameter `a` [Bohr 1961, Bloch 1977, Baba 1970, Carjan 1979, Arunachalam 1997, Chakrabarty 1995 Agrawal 1994], and rotational energy ($E_{rot}$) [Rajasekaran 1988] have been evaluated as functions of angular momentum and temperature for Mo,Kr and Zr. It is establish that at low temperatures the effect of angular momentum on the single particle level density parameter 'a' is prominent due to the shell effects. However, at high temperatures the empirical value of 'a' (a = A/8) is reproduced.

Chapter V of the thesis contains the study of structural changes of Sr isotopes. The statistical method is used, which incorporates deformation, collective and non-collective rotational degrees of freedom and shell effects.

Chapter VI of the thesis described the study of odd, odd-odd effects in hot nuclei around A ~ 100. The various nuclear parameters are extracted as function of deformation, angular momentum and temperature.

In the last chapter a brief summary and conclusion are presented. The scope of future work also mentioned.

# CHAPTER II
# STATISTICAL THEORY

## 2.1 Introduction

The exploration of nuclear physics has usually been restricted to fairly low energy states. Unquestionably the best investigated and clarified marvels are those which happen close to the ground state and have either a collective or single particle nature. In this area, the nuclear level density is very low, and discrete levels might be distinguished. Theoretical models like the shell model or the IBA can foresee the spectra and inter level transitions well, and these properties are genuinely simple to gauge experimentally. But when higher energy excitations are considered, there are various issues. States with a high degree of non-collectivity may show up, as new degrees of freedom open up with the accessible energy. The creation of states leads to level densities that are neither theoretically nor experimentally resolvable. On the theoretical side, regardless of whether just a single or two shells are viewed as, the quantity of states a couple of several MeV over the ground state may number into the millions. Tentatively, the widths of the states end up analogues to or larger than their spacing, and a continuum type of spectrum results.

Nuclei in states having both high spin and excitation energy can be formed in heavy ion collisions. In such collisions, nuclei can join together, and then start to lose energy through neutron evaporation. Once the evaporation threshold has been crossed, nuclei lose energy through $\gamma$-ray de-excitation, from states which are still quite high in energy. The transition rates can be calculated by using Fermi's Golden Rule, which requires knowledge of the level density in the region of the transition. Thus to really understand the behaviour of the nuclei in this region, the level density must be known. The high level density of hot nuclei warrants a statistical treatment.

The compound nucleus formed in heavy ion reaction may be described as a thermodynamical system of fermions with several degrees of freedom like deformation, collective and non-collective rotation, particle number fluctuation etc. The quantal aspects of the systems are important in single particle level spectrum of the Nilsson type or Wood-Saxon potentials, which include deformation and shell structure. The grand partition function about the statistical average of energy, particle number, angular momentum and entropy determines the phase-space or probability of finding system with a particular set of observables. The development of statistical theory by Bethe [Bethe 1936], Ericson [Ericson 1960], Ignatyuk [Ignatyuk 1960], Ramamoorthy [51], Moretto [Moretto 1972] and Rajasekaran [Rajasekaran 19888, Rajasekaran 1981, Rajasekaran 1987, Rajasekaran 1988, Rajasekaran 1988] has resulted in successful application to high spin nuclei.

**2.2 Statistical Theory**

Since the level density is so large, it is hopeless to look at the properties of individual states, since they will not be resolvable. Only average properties such as the average shape and level density should be significant in this regime. In order to average over a set of states, their distribution must be known. Statistical methods are used in many branches of physics to perform such averages, and in combination with thermodynamics, give a framework in which to calculate them. The level density is the partition function for the microcanonical ensemble.

The statistical theory of the deformed nuclear system of N neutrons and Z protons begins with the partition function $\Omega(\alpha, \beta, \gamma)$. The grand canonical partition function of the system is written in terms of single particle energy eigenvalues $\varepsilon_i$ and

the z component of spin projection $\pm m_i$ of the deformed oscillator potential of the Nilsson-Hamiltonian type diagonalized in cylindrical basis [Huizenga 1972]. The grand canonical partition function $\Omega$ contains the statistical properties of the system [Feynman 1972].

$$e^{\Omega} = \sum_{N',Z',E'} \exp\left(\alpha_Z Z' + \alpha_N N' - \beta E'\right) \tag{2.1}$$

where $\alpha_Z$, $\alpha_N$ and $\beta$ are the Lagrangian multipliers conserving the total number of nucleons, the total energy for a system of $N'$ neutrons and $Z'$ protons, at a temperature $T = 1/\beta$. The quantity $T = 1/\beta$ is known as the statistical temperature. The total energy is the sum of the single particle energies occupied by fermions. The summation is over all nuclei with $N'$ neutrons and $Z'$ protons, and over all energy eigenvalues $E'$ of each nucleus.

$$e^{\Omega} = \sum_{N',Z',E'} \rho(N', Z', E') \exp\left(\alpha_Z Z' + \alpha_N N' - \beta E'\right) dE' \tag{2.2}$$

The summation over the energy can be replaced by an integration [Huizenga 1972, Huizenga 1972] as the nuclear levels exhibit a continuous spectrum even for few MeV of excitation energy. The quantity $\rho(Z', N', E')$ represents the density of states of A ($N'$ neutrons and $Z'$ protons) nucleons at the energy $E'$, at a finite statistical temperature. From Eq. (2.2), it is obvious that the grand partition function $\Omega$ can be considered as a Laplace transform of the state density $\rho(Z', N', E,T')$. Consequently $\rho(Z', N', E', T)$ can be obtained by taking inverse Laplace transform of the above equation. Williams [William 1969] has used recursive relation for finding the exact state density. However, the more general method makes use of the inverse Laplace transform for Eq. (2.2):

$$\rho(N', Z', E') = \frac{1}{(2\pi i)^3} \oint d\alpha_N \oint d\alpha_Z \oint d\beta e^S \qquad 2.3$$

where the quantity $S = \Omega + \beta E - \alpha_Z Z - \alpha_N N$ is called the entropy of the system. The above integrals are the well-known Darwin-Fowler integrals [Feynman 1972, Fowler 1936]. The only approximation so far introduced in the formalism is the continuous approximation in which the level density is considered is a continuous function. On the other hand, the simplification of the method arises from a significant approximation called the saddle point approximation. It is establish that the integrand in Eq. (2.3) has a saddle point whose location is defined by the equation

$$\frac{\partial S}{\partial \alpha_Z} = 0 \; ; \; \frac{\partial S}{\partial \alpha_N} = 0; \frac{\partial S}{\partial \beta} = 0 \qquad 2.4$$

or, in other words

$$\frac{\partial \Omega}{\partial \alpha_Z} = Z \; ; \; \frac{\partial \Omega}{\partial \alpha_N} = N; \frac{\partial S}{\partial \beta} = -E \qquad 2.5$$

The path of the integration can be chosen to pass through this point. By expanding the exponent S in a Taylor series about the saddle point and maintaining only up to the quadratic term the integrals in Eq. (2.3) give up

$$\omega(Z, N, E) = \frac{e^S}{(2\pi)^{3/2} D^{1/2}}, \qquad 2.6$$

where D is a 3×3 determinant specified by

$$D = \begin{vmatrix} \frac{\partial^2 \Omega}{\partial \alpha^2} & \frac{\partial^2 \Omega}{\partial \alpha \partial \beta} & \frac{\partial^2 \Omega}{\partial \alpha \partial \gamma} \\ \frac{\partial^2 \Omega}{\partial \beta \partial \alpha} & \frac{\partial^2 \Omega}{\partial \beta^2} & \frac{\partial^2 \Omega}{\partial \beta \partial \gamma} \\ \frac{\partial^2 \Omega}{\partial \gamma \partial \alpha} & \frac{\partial^2 \Omega}{\partial \gamma \partial \beta} & \frac{\partial^2 \Omega}{\partial \gamma^2} \end{vmatrix}$$

whose elements are the second derivative of $\Omega$ with respect to the Lagrangian multipliers and evaluated at the saddle point. Equation (2.6) is an excellent approximation and it almost yields correct results at high excitation energies. Still at the low excitation energies the conformity is reasonably good [William 1969]. The sophistication of this method lies in the fact that it can be generalized for arbitrary number of constants of motion $C_i$. If n constants are introduced, the density of states retains the form of Eq. (2.6) with entropy replaced by

$$S = \Omega + \beta E - \sum_{i=1}^{n-1} \alpha_i C_i \qquad 2.7$$

with the exponent of $2\pi$ in Eq. (2.6) equal to n/2.

**2.2.1 Dependence of level density on finite dimensions of the vector space**

The dependence of the level density on the finite dimension of vector space [Rajasekaran 1982] is best obtained by defining the entropy S(E) in terms of the configurations W(E) available for a given energy of the system [Glasstone 1973]

$$W(E) = e^{S(E)} \qquad 2.8$$

in view of the fact that W(E) is the number of eigenstates for a given energy E of the system, the density of states can be achieved by differentiating it with respect to E, remembering that S(E) is a smooth function of E:

$$\rho(E) = \frac{\partial W}{\partial E} = e^{S(E)} \frac{\partial S}{\partial E} \qquad 2.9$$

The entropy of a system of N fermions characterized by the chemical potential $\mu$ and the temperature T is given by

$$S = \ln Q + \beta E - \alpha N \qquad 2.10$$

where Q is the grand canonical partition function, $\alpha = \mu\beta$ the Lagrangian multiplier, and E is the total energy of the system. The partition function with regard to the single particle energies $\varepsilon_i$ is

$$\ln Q = \sum_i \ln[1 + \exp(\alpha - \beta\varepsilon_i)] \qquad 2.11$$

The chemical potential $\mu$ for a particular value of $\beta$ is determined by the particle number conservation:

$$N = \sum_i n_i$$

with

$$n_i = \sum_i [1 + \exp(\alpha - \beta\varepsilon_i)]^{-1} \qquad 2.12$$

The total energy E and the excitation energy $E^*$ are given by

$$E = \sum_i n_i \varepsilon_i$$

$$E^* = E - E_0 \qquad 2.13$$

where the ground state energy $E_0$ of the N particle system is denoted by

$$E_0 = \sum_{i=1}^{N} \varepsilon_i \qquad 2.14$$

If we now differentiate Eq. (2.10) with respect to the excitation energy taking into the account the Eqns. (2.12) and (2.13)

$$\frac{\partial S}{\partial E} = \frac{\partial S}{\partial E^*}$$

$$\frac{\partial \ln Q}{\partial \alpha}\frac{\partial \alpha}{\partial E^*} + \frac{\partial \ln Q}{\partial \beta}\frac{\partial \beta}{\partial E^*} + \beta + E\frac{\partial \beta}{\partial E^*} - N\frac{\partial \alpha}{\partial E^*} \qquad 2.15$$

because

$$\frac{\partial \ln Q}{\partial \alpha} = N \quad \text{and} \quad \frac{\partial \ln Q}{\partial \beta} = -E$$

one would obtain

$$\frac{\partial S}{\partial E} = \frac{\partial S}{\partial E^*} = \beta = \frac{1}{T} \tag{2.16}$$

which is the standard thermodynamic definition of temperature. Therefore, the level density expression (2.9) turns out to be

$$\rho(E) = \beta e^{S(E)/T} \tag{2.17}$$

We have to note that W(E) has to be normalized to succumb the total probability using the definition for the partition function

$$Q = \sum_{N'} \rho(E) e^{\beta E + \alpha N'} dE' \tag{2.18}$$

If the dimensionality of phase space is restricted [Inglis 1954], then the upper limit of the integrand is no longer infinity but a finite value depending on the number of single particle states N accessible. In this context, the entropy of the system has a maximum value [Pathria 1972] $N_0 \ln_2$ which is obvious from the expression

$$S = \sum_i \left[ n_i \ln n_i + (1 - n_i) \ln (1 - n_i) \right], \tag{2.19}$$

evaluated in the first limit of $\beta \to 0$.

For a system of N particles, the normalized constants can be obtained by substituting Eq. (2.9) in Eq. (2.18)

$$Q = C \int e^s e^{-\beta e + \alpha N} \frac{\partial S}{\partial E} dE \,, \tag{2.20}$$

substituting for $e^S$ from Eq. (2.10) and remembering that Q is not a function of E by definition, equation (2.20) give way

$$1 = C \int_0^{S_{max}} dS, \qquad 2.21$$

As a result the normalization constant turns into

$$C = \frac{1}{N_0 \ln 2} \qquad 2.22$$

through this normalization $\rho(E)$ appears as

$$\rho(E) = \frac{\beta e^s}{N_0 \ln 2} \qquad 2.23$$

We observed that the exponential term in the expression for the level density is the identical one as in all the earlier works but only by the factors multiplying it differ. It demonstrates an explicit dependence on the finite dimension of the vector space [Chan 1982 William 1969, Fowler 1936, Glasstone 1973, Gottschalk 1977, Rajasekaran1987] establish that for large values of $N_0$, the level density calculations are the same with the earlier formula. The present formula used in our calculations avoids the monotonous procedure of evaluating a determinant whose elements are second derivatives of the function and assuage the computational work.

**2.3 Two Methods of Generating High Spins**

There are two techniques of producing high spin states in the statistical theory. In one method [Rajasekaran [Rajasekaran 19888, Rajasekaran 1981, Rajasekaran 1987, Rajasekaran 1988, Rajasekaran 1988], triaxially deformed single particle spectrum is bring into play an input and the collective rotation can be produced by introducing a Lagrangian multiplier into the partition function of the super-fluid

nucleus [Rajasekaran [Rajasekaran 19888, Rajasekaran 1981, Rajasekaran 1987, Rajasekaran 1988] to conserve the total angular momentum of the system. Another technique [Rajasekaran [Rajasekaran 19888, Rajasekaran 1981, Rajasekaran 1987, Rajasekaran 1988, Rajasekaran 1988] the term corresponding to collective rotation $-\vec{\omega}\cdot\vec{j}_z$ is included in the Hamiltonian [Shanmugam 1978] of the system itself. The matrix elements of $-\vec{\omega}\cdot\vec{j}_z$ generate the spin by splitting ±mz states. The two methods are as follows:

1. The statistical theory of hot rotating nuclei (STHR) and
2. The cranked Nilsson oscillator model (CNM) of hot rotating nuclei.

In the present work second methods was used.

**2.4 Cranked Harmonic Oscillator Method**

**2.4.1 Without Pairing Correlation**

The eigenvalues produced by Cranked Nilsson Hamiltonian with finite values of the collective frequency ω are used here. The analogous partition function is given by

$$Q(\omega,\alpha_z,\alpha_n,\beta)=\sum_{E_i N_i,Z_i}\exp(\alpha_z Z_i+\alpha_n N_i-\beta\varepsilon_i^n(\omega)) \qquad 2.38$$

The Lagrangian multipliers $\alpha_z$, and $\alpha_n$ conserve the number of proton and number of neutron and total energy at a given temperature T = 1/β. The resultant equations in terms of the single particle energies $\varepsilon_i(\omega)$ are given by

$$\langle N\rangle=\sum_i n_i^n=\sum_i 1+\exp(-\alpha_n N_i+\beta\varepsilon_i^n(\omega))^{-1} \qquad 2.39$$

$$\langle Z\rangle=\sum_i z_i^n=\sum_i 1+\exp(-\alpha_z Z_i+\beta\varepsilon_i^z(\omega))^{-1} \qquad 2.40$$

The total angular momentum is obtained by

$$M = M_z + M_n$$

where

$$M_z = M(\varepsilon_i^z(\omega)) = \sum_i n_i^z m_i^z$$

and

$$M_n = M(\varepsilon_i^n(\omega)) = \sum_i n_i^n m_i^n \qquad 2.41$$

The simultaneous non-linear Equations (2.39), (2.40) and (2.41) has to be solved to establish $\alpha_z$, and $\alpha_n$ for every value of $\omega$ and T. The total energy of the system is attained as

$$E = E_z + E_n$$

where

$$E_z = E_z(\varepsilon_i^z(\omega)) = \sum_i z_i^z \varepsilon_i^z(\omega) + \hbar\omega \sum_i n_i^z m_i^z$$

and

$$E_n = E_n(\varepsilon_i^n(\omega)) = \sum_i n_i^n \varepsilon_i^n(\omega) + \hbar\omega \sum_i n_i^n m_i^n \qquad 2.42$$

The excitation energy of the system is obtained by

$$E^* = E_n^* + E_z^*$$

where

$$E_z^* = \sum_i n_i^z \varepsilon_i^z(\omega) - \sum_i \varepsilon_i^z(0)$$

and

$$E_n^* = \sum_i n_i^n \varepsilon_i^n(\omega) - \sum_i \varepsilon_i^n(0) \qquad 2.43$$

The requirement of renormalizing the total energy does not arise here, because we are paying attention only in the energy difference among the excited and the ground states of the system and not in the real magnitude of the energies. The entropy of the system is then achieved as

$$S = \frac{\partial(T \ln Q)}{\partial T}$$

$$S = S_z + S_n$$

where

$$S_z = \sum_i [n_i^z \ln n_i^z + (1 - n_i^z) \ln(1 - n_i^z)],$$

and

$$S_n = \sum_i [n_i^n \ln n_i^n + (1 - n_i^n) \ln(1 - n_i^n)], \qquad 2.44$$

It is understandable from Eqs. (2.39) and (2.40) that the occupational probability $n_i$ are dissimilar for $+m_z$ and $-m_z$ states, because the eigenvalues $\varepsilon_i(\omega)$ are different for these states. The thermodynamical potential is specified by

$$F = -T \ln Q$$

**2.4.2 With Pairing Correlation**

The logarithm of grand canonical partition function for the Z protons of the superfluid nuclei at a temperature T, using the BCS formulation [Brack 1997, Bardeen 1957, Decowski 1968, Sano 1963, Bengtsson 1975], is given by [Rajasekaran 1987].

$$\ln Q_{BCS}(\omega) = -\beta \sum_k [\varepsilon_k^z(\omega) - \lambda_z - E_k^z(\omega)] + \sum_k \ln 1 + \exp[-\beta(E_k^z(\omega)] - \beta \frac{\Delta_z^2}{G_z} \qquad 2.45$$

where $E_i^n = [(\varepsilon_i^n - \lambda_n) + \Delta_i^2]^{1/2}$ are the proton quasi particle energies. $G_Z$ is the pairing strength and $\Delta_Z$ is the gap parameter. The quantity $\lambda_z$ is the proton chemical potential. The particle number equations for protons, the equation for energy E, and angular momentum M are given below:

$$Z = \sum \{1 - \frac{(\varepsilon_i^z - \lambda_z)}{2E_i^z} [\tanh \frac{1}{2} \beta(E_i^z(\omega))]\} \qquad 2.46$$

$$M_z = \sum_k \frac{m_k^z}{[1+\exp\beta_i^n(\omega))]} \qquad 2.47$$

$$E_z = \sum_k \varepsilon_k \{1 - \frac{(\varepsilon_k^z(\omega) - \lambda_n)}{2E_k^z(\omega)}[\tanh\frac{1}{2}\beta(E_k^z(\omega))\} - \beta \Delta_i^2 / G_z \qquad 2.48$$

The gap parameter $\Delta z$ is obtained as a function of $\lambda z$ and by solving the gap equation:

$$\sum \frac{1}{2E_i^n}[\tanh\frac{1}{2}\beta(E_i^n - \gamma m_i^n) + \tanh\frac{1}{2}\beta(E_i^n + \gamma m_i^n)] = \frac{2}{G_n} \qquad 2.49$$

along with Eq. (2.46) for given values of $\beta$ and $\omega$. These values are used to calculate $M_z$, $E_z$ and $S_z$. The entropy is then given by

$$S_z = \sum_k \ln 1 + \exp[-\beta(E_k^z(\omega)] + \beta \sum_i \frac{E_k^z(\omega)}{1+\exp(\beta(E_k^z(\omega))} \qquad 2.50$$

A similar set of equations for neutrons also exists. These values are used to calculate $M_n$, $E_n$ and $S_n$. The total angular momentum M, the total energy E, and the total entropy S are then obtained using

$$S = S_z + S_n$$

$$M = M_z + M_n$$

and

$$E = E_z + E_n \qquad 2.51$$

The procedure specified in this chapter are used in Chapter IV to extort different parameters like single particle level density parameter, proton and neutron separation energy and rotational energy to investigate the structural changes in A~100 nuclei.

# CHAPTER III
# NILSSON MODEL

## 3.1 Introduction

The first deformed potential to describe axially symmetric nuclei was introduced by Nilsson who took a single-particle potential which was based on a deformed harmonic-oscillator potential and modified by a strong spin-orbit (l. s) force and an ($l^{2-} < l^2>_N$) term to simulate the flattening of the potential at the centre of the nucleus [Nilsson 1955]. Another commonly used deformed single-particle potential is a deformed Woods-Saxon potential. The nuclear radius for deformed nuclei assuming a constant nuclear volume can be parameterized in terms of a multipole expansion :

$$R(\theta(\varphi) = c(\alpha)R_0\left[1+\sum_{\lambda=2}^{\lambda_{max}}\sum_{\mu=-\pi}^{\mu=\lambda}\alpha\lambda_\mu Y_{\lambda\mu}(\theta,\varphi)\right] \qquad 3.1$$

where $R_0$ is the radius of a sphere having the same volume as the nucleus, $\alpha_{\lambda\mu}$, are the expansion coefficients of the spherical harmonics $Y_{\lambda\mu}(\theta,\phi)$. $\lambda$ and $\mu$ determine the surface coordinates as functions of $\theta$ and $\phi$, respectively. The parameters $c(\alpha)$ are determined from the volume-conservation condition. The lowest multipole, $\lambda=2$, corresponds to quadrupole deformation. For axially-symmetric shapes the $\alpha_{\lambda\mu}$ coefficients with $\mu \neq 0$ vanish and hence the nuclear radius can be written as :

$$R(\theta(\varphi) = c(\alpha)R_0[1+\beta_2 Y_{20}(\theta\theta\rho) \qquad 3.2$$

which is indeed independent of $\theta$. The quadrupole deformation parameter $\beta_2$ ($=\alpha_{20}$) quantifies the nuclear deformation, the larger the value of $\beta_2$ the more deformed the

nucleus. Positive and negative $\beta_2$ values correspond to prolate and oblate shapes respectively. Quadrupole deformations can give rise to asymmetric shapes through triaxial distortions, hence one need to introduce additional shape parameters. The $\gamma$ shape degree of freedom describes a stretching/squashing effect at right angles to the major nuclear axis.

The basic ingredient in the theory is a suitable shell model scheme [Nilsson 1969, Eisenberg 1976, Soloviev, 1976, Irvine 1972] generated for various nuclear deformations. Considerable attention has been given to the various parameters involved in the deformed harmonic oscillator Hamiltonian [Moretto 1971, Gaardhoje 1992] for hot rotating nuclei. This Chapter of the thesis is devoted to the study of the methods available to obtain the triaxially deformed single particle levels, and cranked oscillator levels.

### 3.2 Cranked Nilsson Hamiltonian

Inglis [Inglis 1954], introduced a useful tool for the analysis of the nuclear rotational motion provided by the cranking model. Here nucleons move in a potential that is set to rotate with a rotational frequency $\omega$. This is understood by the addition of a term $-\vec{\omega}\cdot\vec{j}_z$ to the intrinsic Hamiltonian. The disturbance in the nucleons caused by the rotation could then be considered as a perturbation of the ground state intrinsic field. The first investigation of nuclei with very high angular momentum was carried out by Bengtsson et al. [Bengtsson 1975], taking the coupling between the nucleons and the rotational motion in a non-perturbative way. The quantum mechanical wobbling can be neglected at very high spins, as a result that the rotation is assumed to take place around a fixed axis The Coriolis force, which is associated with this rotation strives to align the spin vectors of the nucleons along the rotational axis.

Through increasing rotational frequency, other nucleons become aligned. Because the aligned nucleons have a density that is symmetric around the rotational axis, a prolate nucleus, revolving around an axis perpendicular to the symmetry axis will change its deformation to a triaxial form. It is clear that, by a straightforward extension of the cranking model, it is possible to describe the continuous transition from prolate shape, with rotation axis perpendicular to the symmetry axis, to oblate shapes with rotation around the symmetry axis.

A number of groups have carry out calculations in which the full cranking Hamiltonian is diagonalized for a deformed nucleus. By the use of this it is possible to map out of different regions of rotation, i.e., the shape changes and diverse ways of constructing angular momentum, collective rotation or excitation of single particle nature, as a function of spin. A complete microscopic calculations of the deformation energy was done by Faessler et al. [Faessler 1976, Faessler 1976, Poloszajctak 1977] using a many body model Hamiltonian and trial wave functions representing the different shapes at the same time as the Dubno-Rossendorf [Andersson 1978], and the Lund-Warsaw [Neergard 1975, Neergard 1978] groups carried out study based on the Strutinsky shell correction method [Strutinsky 1967]. In this thesis we used the single particle data obtained by diagonalizing cranked Nilsson Hamiltonian.

### 3.2.1 Diagonalizing the cranked Nilsson Hamiltonian

In a rotating nucleus (without internal excitations), the nucleus move in a cranked Nilsson potential with deformation described by $\delta$ and $\theta$. The cranking is execute around one of the principal axis, z-axis and the cranking frequency is given by $\omega$. The Hamiltonian for the cranked Nilsson oscillator $H^w$ is given by [Eisenberg 1976]

$$H^w = H^0 - \vec{\omega} \cdot \vec{j}_z \qquad 3.3$$

where $H^0$ is the triaxial Nilsson Hamiltonian. Here the rotation axis is assumed to be z-axis. The Hamiltonian for a single particle in the non-rotating system, and is given by

$$H^0 = \frac{p^2}{2m} + \frac{m}{2}\left(\omega_x^2 x^2 + \omega_y^2 y^2 + \omega_z^2 z^2\right) + c\hat{l}\cdot\vec{s} + D\left(\hat{l}^2 - 2\left\langle \hat{l}^2 \right\rangle\right) \qquad 3.4$$

The intrinsic spin is represented by s and l represents the angular momentum. $\omega$ is the cranking frequency or rotational frequency. Angular momentum is accounted by the addition of this cranking term $-\vec{\omega}\cdot\vec{j}_z$ to the non-rotating single particle Hamiltonian. To describe the nuclear shape two types of deformation parameters are commonly used. The first based on the harmonic oscillator frequencies based on the harmonic oscillator frequencies $\omega_x$, $\omega_y$ and $\omega_z$. The second is based on the expansion of the nuclear surface in terms of spherical harmonics. In the present work, we used the first type of parameterization. The three oscillator frequencies are given by

$$\begin{aligned}
\omega_x &= \omega_0[1 + (1/3)\varepsilon\cos\gamma + (1/\sqrt{3})\varepsilon\sin\gamma] \\
\omega_y &= \omega_0[1 + (1/3)\varepsilon\cos\gamma - (1/\sqrt{3})\varepsilon\sin\gamma] \\
\omega_z &= \omega_0[1 - (2/3)\varepsilon\cos\gamma],
\end{aligned} \qquad 3.5$$

With the constraint that the total volume remains constant such that

$$\omega_x\omega_y\omega_z = \dot{\omega}_0^3 \qquad 3.6$$

This constant is the value of $\omega_0$ at $\varepsilon = 0$ and is determined from the fit to nuclear size. The parametrization defined by Eqs. (3.5) and (3.6) is referred to as Nilsson parameterization. The parameter $\varepsilon = (a - b)/R_0$ corresponds to the elongation or flattening of the potential, while $\gamma$ describes its nonaxiality, where 'a' is the semi major axis, 'b' is the semi minor axis and '$R_0$' is the radius of equivalent sphere.

For a > b, $\varepsilon > 1$ (prolate shape)

For a < b, $\varepsilon < 1$ (oblate shape)

For a = b, $\varepsilon = 0$ (spherical shape)

The choice of variation of shape parameter extends from $\gamma = 0$ to $2\pi$. Though, in the absence of rotation one can always change the meaning of the three principal axes so that it is sufficient to consider only one sector of the whole plane ($\varepsilon$,$\gamma$), i.e., a plane with radial polar coordinate $\varepsilon$ is and angular coordinate $\gamma$ is lying between $\gamma = 0°$ (prolate ellipsoidal shape) and $\gamma = 60°$ (oblate ellipsoidal shape). If the nuclear rotation is involved, the x-axis is assumed as the axis of rotation. In this case one can consider three sectors ($-120° = \gamma = 60°$) in the deformation plane, viz., (i) from $\gamma = -120°$ to 60° (prolate non-collective to oblate collective), (ii) from $\gamma = -60°$ to 0° (oblate non-collective to prolate collective) and (iii) from $\gamma = 0°$ to 60° (prolate collective to oblate non-collective).

In the case of rotation about x-axis the sectors on the other side of the x-axis are equivalent to the sectors as indicated by the same numbers in Fig. (3.1). In the case of rotation about y-axis the three sectors to be considered in one half and the equivalent sectors in the other half is represented in Figs. (3.2). Similarly Fig. (3.3) is drawn for the rotation about z-axis.

### 3.2.2 Dimensionality of phase space

The levels generated up to shells N = 9 are found to be sufficient for the range of temperatures used in our calculations. The total number of particles for all levels up to N shells is given by the equation

$$\sum \Lambda_{\Lambda} = (1/3)(N+1)(N+2)(N+3) \qquad 3.7$$

and is equal to 440 levels for N = 9 which are sufficient for the range of temperatures used in our calculations. The single particle spin projections $m_i$ along the symmetry axis are not needed for the calculations since the angular momentum is generated by adjusting the cranking frequency $\omega$ in the Nilsson Hamiltonian.

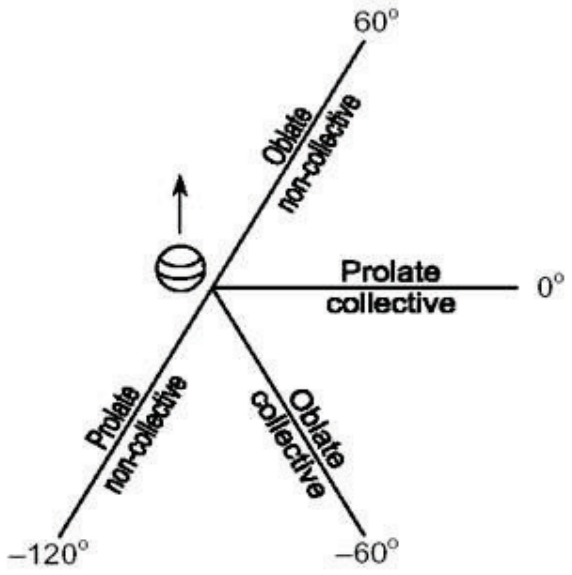


**Figure 3.1: Polar plot of nuclear deformation for rotation around x axis**

Hence, by assuming the nucleons to be moving in a triaxially deformed cranked Nilsson harmonic oscillator potential, the salient features corresponding to collective, non-collective prolate and oblate shapes of the rotating nucleus with respect to the deformation parameters are presented in this chapter.

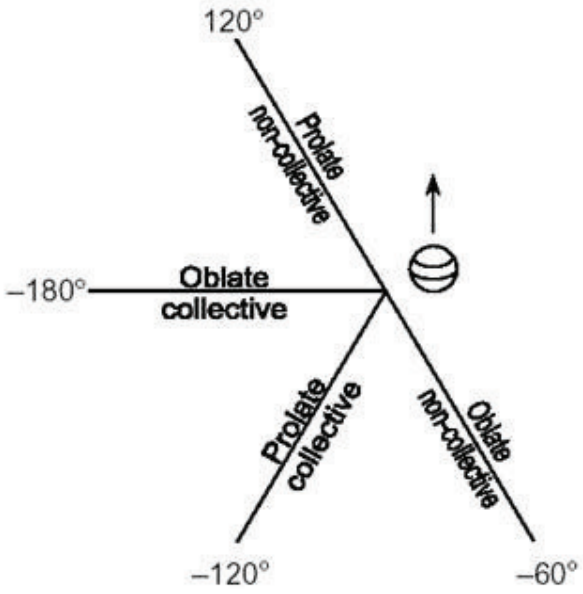


**Figure 3.2:Polar plot of nuclear deformation for rotation around y axis**

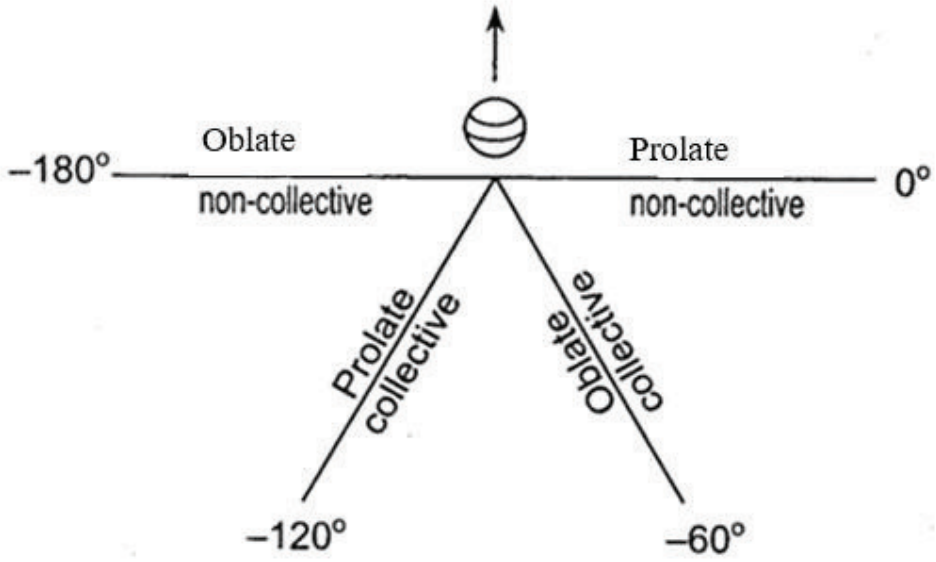


**Figure 3.3:Polar plot of nuclear deformation for rotation around z axis**

In the nuclear case, for instance, the enhancement of E2 transitions among members of rotational bands has led to the conclusion that quadrupole degrees of freedom are the most important in describing the nuclear shape and density. By choosing these quadrupole deformation parameters as the most important, the free energy will come to depend on them as well as the temperature and spin. We will thus be able to find the equilibrium free energy by extremizing the free energy with respect to the deformation. The equilibrium values of the deformation will then be interpreted as describing the average shape of the nucleus.

# CHAPTER IV

# SHAPE EVOLUTION IN $^{94,96,98}$Kr, $^{98,100,102}$Zr AND $^{100,102,104}$Mo

## 4.1 Introduction

During the last decade there have been various theoretical investigations of the A∼100 mass region. One of the very important regions of nuclear deformation is located on the nuclear chart around mass number $A$ = 100, between the isotopic chains of krypton ($Z$ = 36) and molybdenum ($Z$ = 42). This region is particularly interesting because of the sudden onset of deformation at $N$ = 60 making it one of the most dramatic shape changes on the nuclear chart [de Roubin 2017]. Nuclei with atomic masses of about 100 and neutron number of about 60 tend to undergo rapid changes in shape as the number of neutrons in the nucleus increases by just one or two. Understanding how and why these changes occur could provide important information about how nucleons (protons and neutrons) in the nucleus interact with each other – something that is not well understood.

A rapid change of quadrupole deformation is known to occur at around $N$ = 60 in the neutron-rich Zr and Sr isotopes, making this region an active area for both experimental and theoretical studies. The isotopic chain of neutron-rich zirconium nuclei offers an example of rapid transition from spherical to deformed shape with a possible identification of the sudden onset of quadrupole deformation between N=58 and 60.

The study of nuclear deformation in neutron rich nuclei around A~100 mass regions helps us to understand the nature of collective motion occurring in this region. In the ground state, a transition from spherical to deformed shape in these nuclei has been studied extensively by several theoretical [de Roubin 2017, F.K. Wohn 1983, Pinedo 2009, Skalski 1993, Sieja 2009, Skalski 1993, Lalkovski 2009, Pereira 2009, Kirchuk 1993, Cheal 2007, Boyiiukata 2010, Mamta Aggarwal 2016,Rodriguez-Guzman2010, *Sirag2015,* Rodriguez-Guzman 2010, Mei 2012, Xiang 2012, Rodriguez 2014, Sotty 2015, Sarriguren 2015, Charlwood 2009] and experimental methods [Sumikama 2011, Dudouet 2017, Albers 2012, Albers 2013, Thomas 2013, Browne 2015, Urban 2004, Clement 2016, Cheifetz 1970, Park 2016, Johansson 1965]

Most of these methods correspond to cold nuclei and are applicable strictly speaking only to yrast spectroscopy. In these investigations of the nuclear shape at high excitation energies are absent, and the statistical properties of fast rotating nuclei have not been given proper consideration.

In order to understand the equilibrium deformation in these hot and rotating $^{94,96,98}$Kr, $^{98,100,102}$Zr and $^{100,102,104}$Mo nucleus, a calculation was performed for estimating the equilibrium shape of a nucleus by minimizing the total free energy under the framework of temperature dependent rotating cranked Nilsson oscillator model (CNM) of hot rotating nuclei for a given temperature and angular momentum.

**4.2 Result and Discussion**

Figure 4.1 to 4.2 displays the shape evolution of the $^{94}$Kr nuclei as a function of angular momentum for different temperatures. With increasing angular momentum,

small triaxial deformations gradually set in at the temperature T = 0.5 MeV (fig. 4.1). From Fig. 4.1, for the nuclei $^{94}$Kr it is observed that at low spin, the nucleus is an oblate non-collective shape. As spin is increased, it changes smoothly to triaxial shape. However, above a certain critical angular momentum (M= 28ħ for T=1.0MeV, M= 30ħ for T=1.5MeV, M= 32ħ for T=2.0MeV, M= 34ħ for T=2.4MeV and M= 34ħ for T=3.0MeV) nucleus moves to non collective oblate from collective prolate. A significant effect of shape changes is observed at very low temperatures. A similar behaviour is exhibited by the nucleus for the temperature T = 1.0MeV. It is interesting to note that with increasing temperature the presence of triaxial shape vanish, the nuclei undergoes a shape transition from collective prolate to oblate shape. The effect caused by phase changes with T is more clearly seen from the plot 4.1.

The Fig. 4.1 and 4.2 shows the equilibrium shape of the system is determined by minimizing the free energy with respect to the deformation parameters $\beta$ and $\gamma$, as a function of angular momentum for different temperature for the nuclei $^{94}$Kr. It is observed from Fig. 4.2 (T = 0.5MeV) that the nucleus is found to be deformed ($\beta = 0.2$ and $\gamma = -120$) for the angular-momentum range M = 0ħ and triaxial upto 12ħ, above 12ħ the nucleus is in prolate shape up to 28ħ again oscillate between triaxial and oblate shape above 32ħ. For T = 1.0MeV the nucleus remains at spherical shape with $\beta = 0.0$ and $\gamma = -120°$ for the angular- momentum range M = 0 to 10ħ, triaxial ($\beta$= 0.2 and $\gamma = -170$ for M = 12-14 ħ and $\beta = 0.2$ and $\gamma = -140$ for M = 16ħ, $\beta = 0.0$ and $\gamma = -120$ for M = 18-20 ħ, $\beta = 0.2$ and $\gamma = -170$ for M = 22 ħ and $\beta = 0.2$ and $\gamma = -140$, $\beta = 0.0$ and $\gamma = -120$ for M = 26-28 ħ ), it reaches the oblate shape for M = 30 to 36 ħ ($\beta = 0.3$ and $\gamma = -180^{\circ}$). Above T = 1.0 Mev the nuclei

undergoes a shape transition from collective prolate to oblate shape (M = 28ħ for T = 1.5MeV, M = 28ħ for T = 2.0MeV, M = 32ħ for T = 2.5MeV and M = 34ħ for T = 3.4MeV).

Figure 4.3 to 4.4 displays the shape evolution of the $^{96}$Kr nuclei as a function of angular momentum in the (β, γ) plane for different temperatures. The shape of $^{96}$Kr is remain deformed (β=0.2) over the spin range 0ħ-16ħ. At I = 18-24ħ the shape for the nucleus suddenly changes to spherical shape. For the spin value around 26-28ħ the shape change to deformed shape (β=0.3). For the spin 20-32ħ, the deformation parameter decreases to 0.2. For the spin value 32ħ- 48ħ the nucleus continue in the deformed shape with β=0.3 and at spin value 50ħ the nucleus reaches the highest deformed state with β=0.4.

Figure 4.5 to 4.6 displays the shape evolution of the $^{98}$Kr nuclei as a function of angular momentum for different temperatures. The shape of $^{98}$Kr is spherical (β=0.0) for the spin value 0ħ. At I = 2-6ħ the shape for the nucleus suddenly changes to deformed shape (β=0.2). For the spin value around 8-20ħ the shape change to spherical shape (β=0.0). For the spin value above 22ħ the nucleus maintained its deformed shape with β=0.3 and β=0.4.

Figure 4.7 to 4.8 displays the shape evolution of the$^{98}$Zr nuclei as a function of angular momentum for different temperatures. With increasing angular momentum, small triaxial deformations gradually set in at the temperature T = 0.5 MeV (fig. 4.7). From Fig. 4.7, for the nuclei $^{98}$Zr it is observed that at low spin, the nucleus in an oblate non-collective shape. As spin is increased, it changes smoothly to triaxial

shape. However, above a certain critical angular momentum (M= 30ħ for T=1.0MeV, M= 24ħ for T=1.5MeV, M= 24ħ for T=2.0MeV, M= 24ħ for T=2.4MeV and M= 24ħ for T=3.0MeV) nucleus shift from collective prolate to non collective oblate. A significant effect of shape changes is observed at very low temperatures. A comparable behaviour is display by the nucleus for the temperature T = 1.0MeV. It is fascinating to note that with rising temperature the presence of triaxial shape disappear, the nuclei experience a shape transition from collective prolate to oblate shape. The effect caused by phase changes with T is more clearly seen from the plot 4.7. It is obvious from the figure 4.9-4.12, analogous trend of transition were observed for the nuclei $^{100}$Zr and $^{102}$Zr.

Figure 4.13 to 4.14 displays the shape evolution of the $^{100}$Mo nuclei as a function of angular momentum for different temperatures. With increasing angular momentum, small triaxial deformations gradually set in at the temperature T = 0.5 MeV (fig. 4.13). From Fig. 4.14, for the nuclei $^{100}$Mo it is found that at low spin, the nucleus in prolate collective shape. As spin is increased, it changes smoothly to triaxial shape. A similar behaviour is exhibited by the nucleus for the temperature T = 1.0MeV. It is interesting to note that with increasing temperature the presence of triaxial shape vanish, the nuclei undergoes a shape transition from collective prolate to non collective oblate shape. The effect caused by phase changes with T is more clearly seen from the plot 4.14. It is evident from the figure 4.15-4.18, similar trends of transition were observed for the nuclei $^{100}$Mo and $^{102}$Mo.

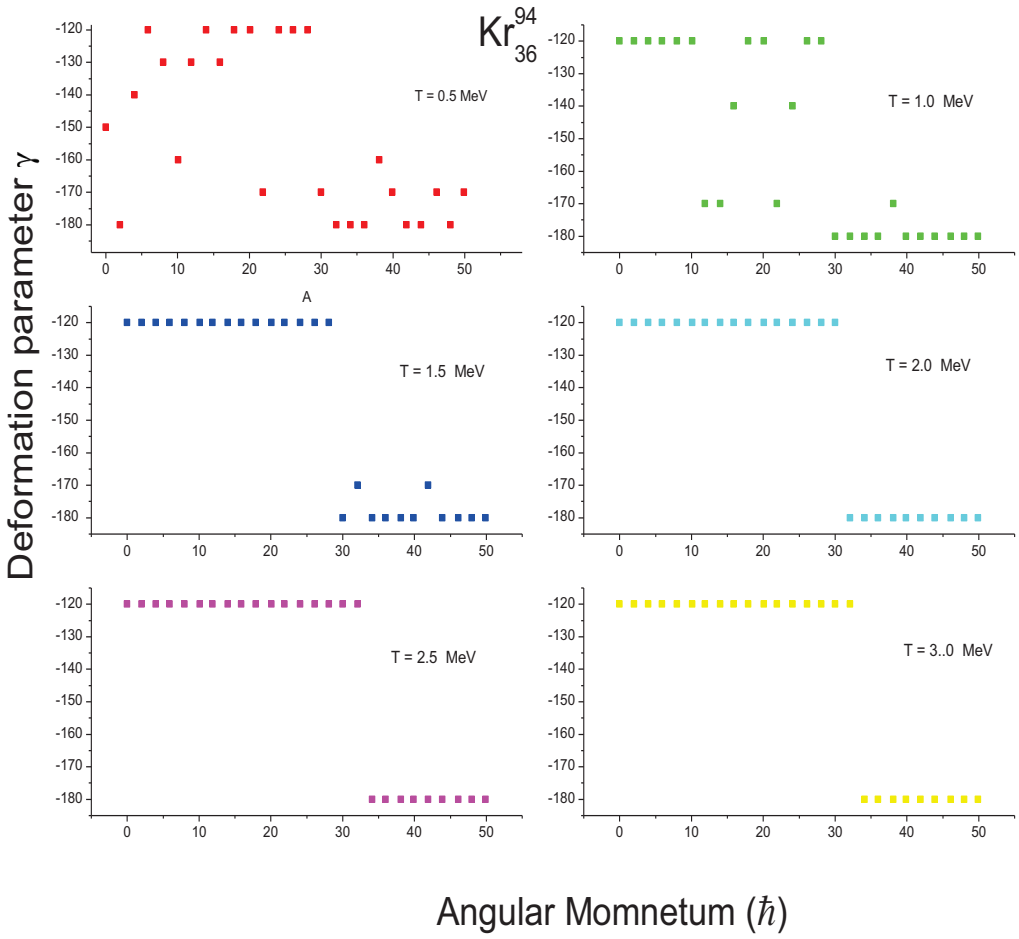


**FIG. 4.1: The deformation γ as a function of angular momentum I for the nuclei $^{94}$Kr**

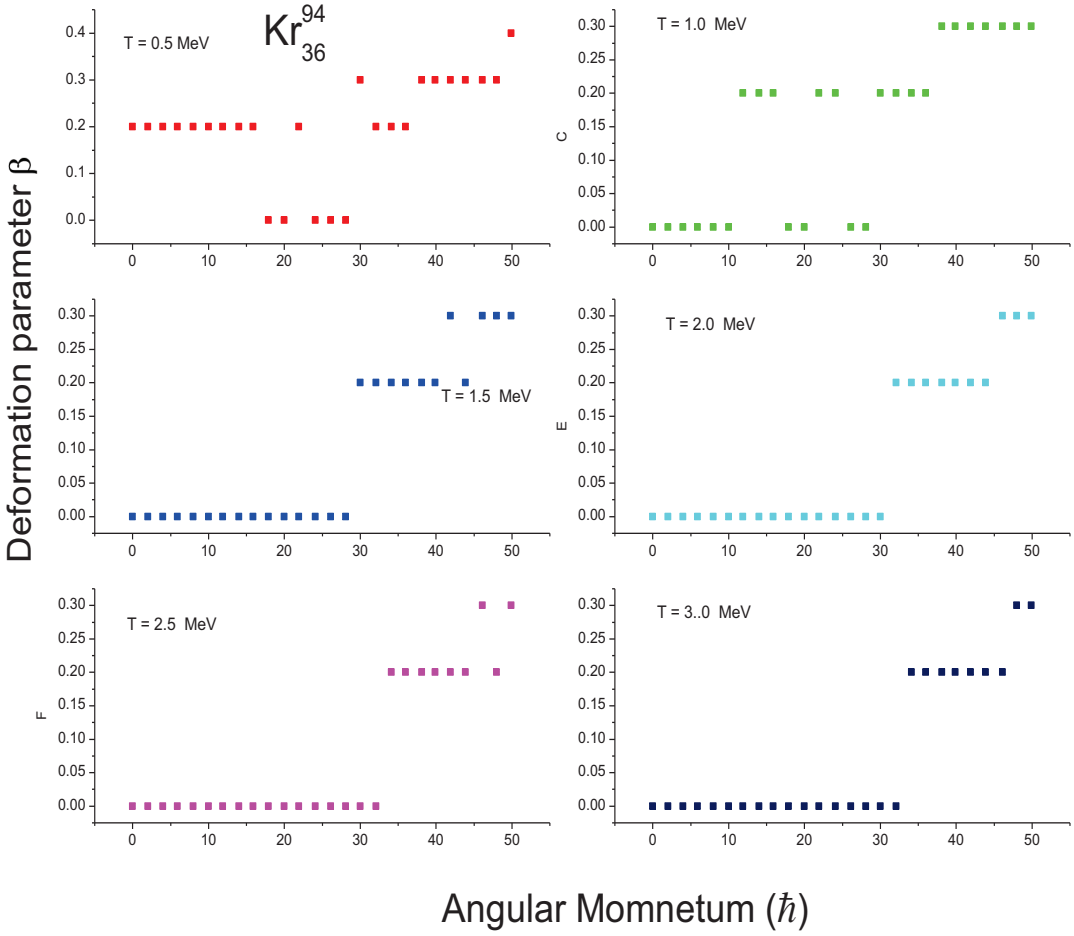


**FIG. 4.2: The deformation β as a function of angular momentum I for the nuclei $^{94}$Kr**

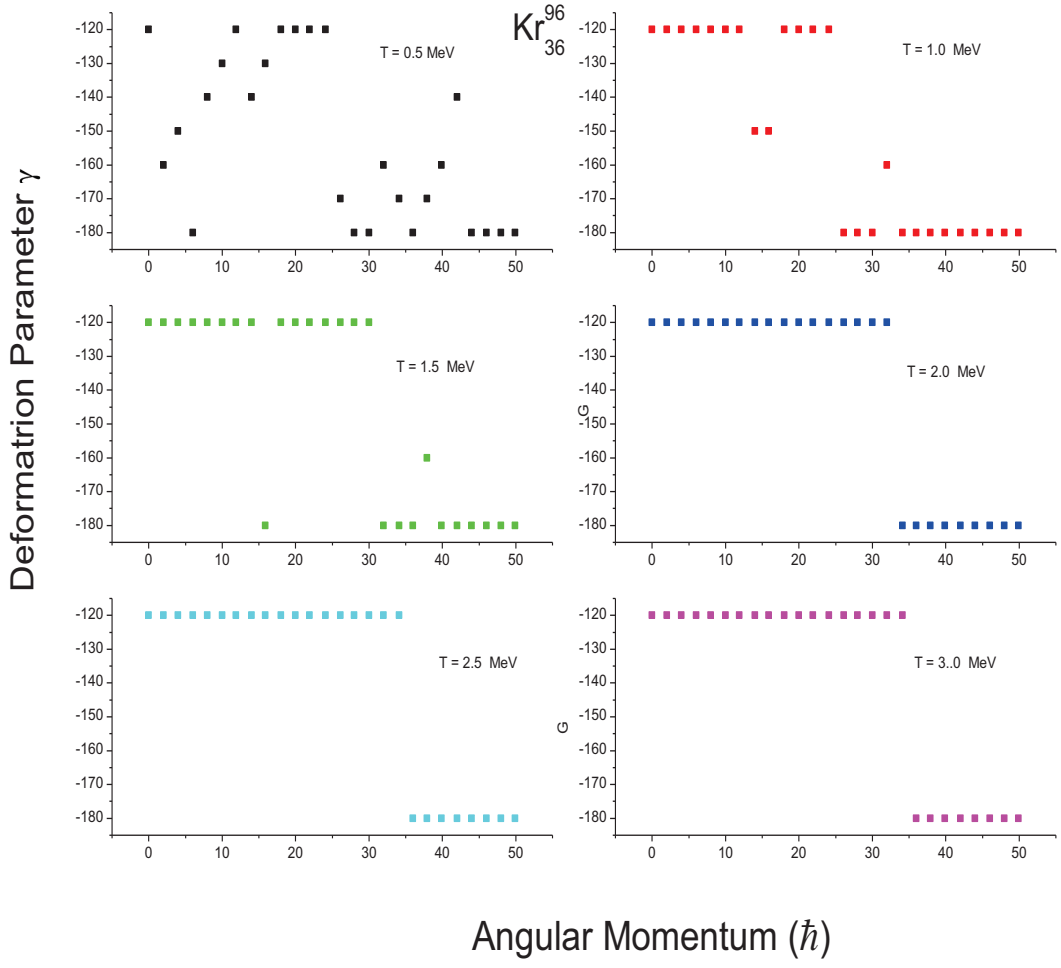


**FIG. 4.3: The deformation γ as a function of angular momentum I for the nuclei $^{96}$Kr**

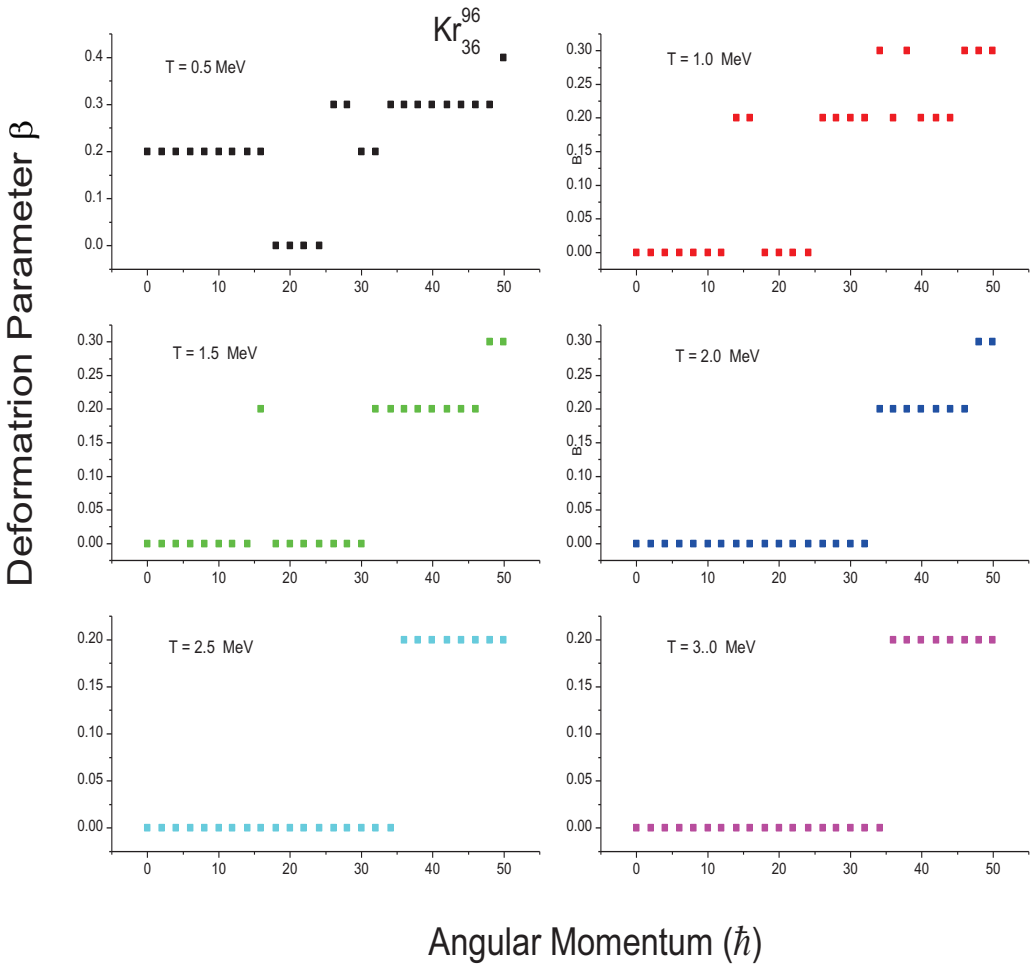


**FIG. 4.4:** **The deformation β as a function of angular momentum I for the nuclei $^{96}$Kr**

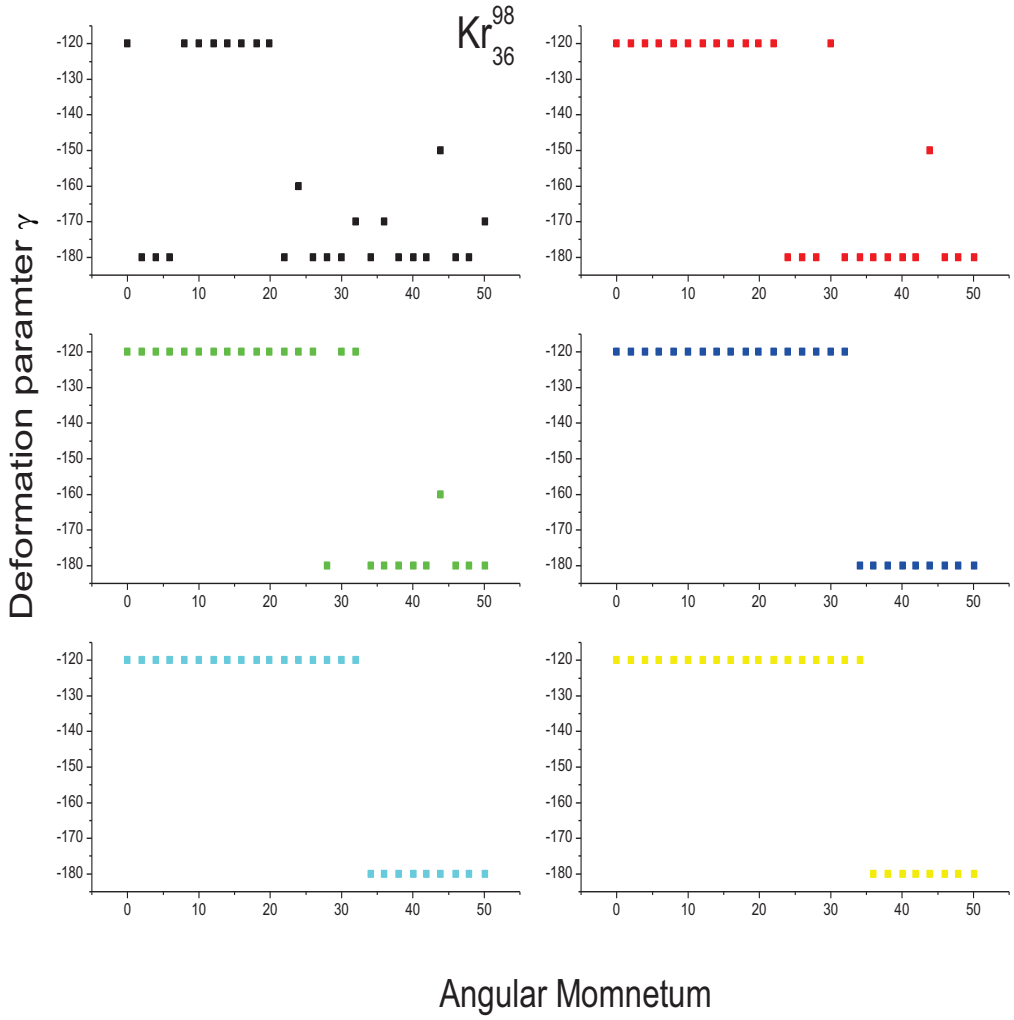


**FIG. 4.5: The deformation γ as a function of angular momentum I for the nuclei $^{98}$Kr**

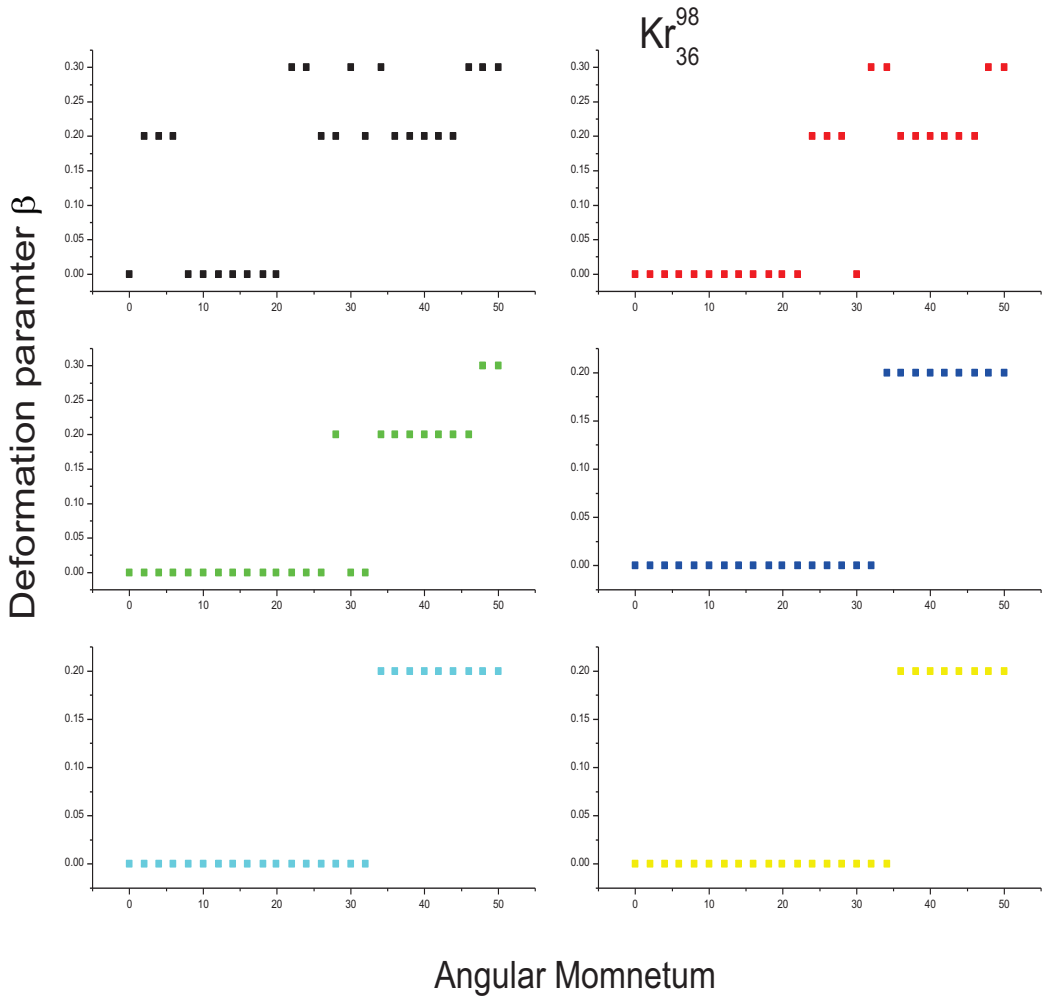


**FIG. 4.6: The deformation β as a function of angular momentum I for the nuclei $^{98}$Kr**

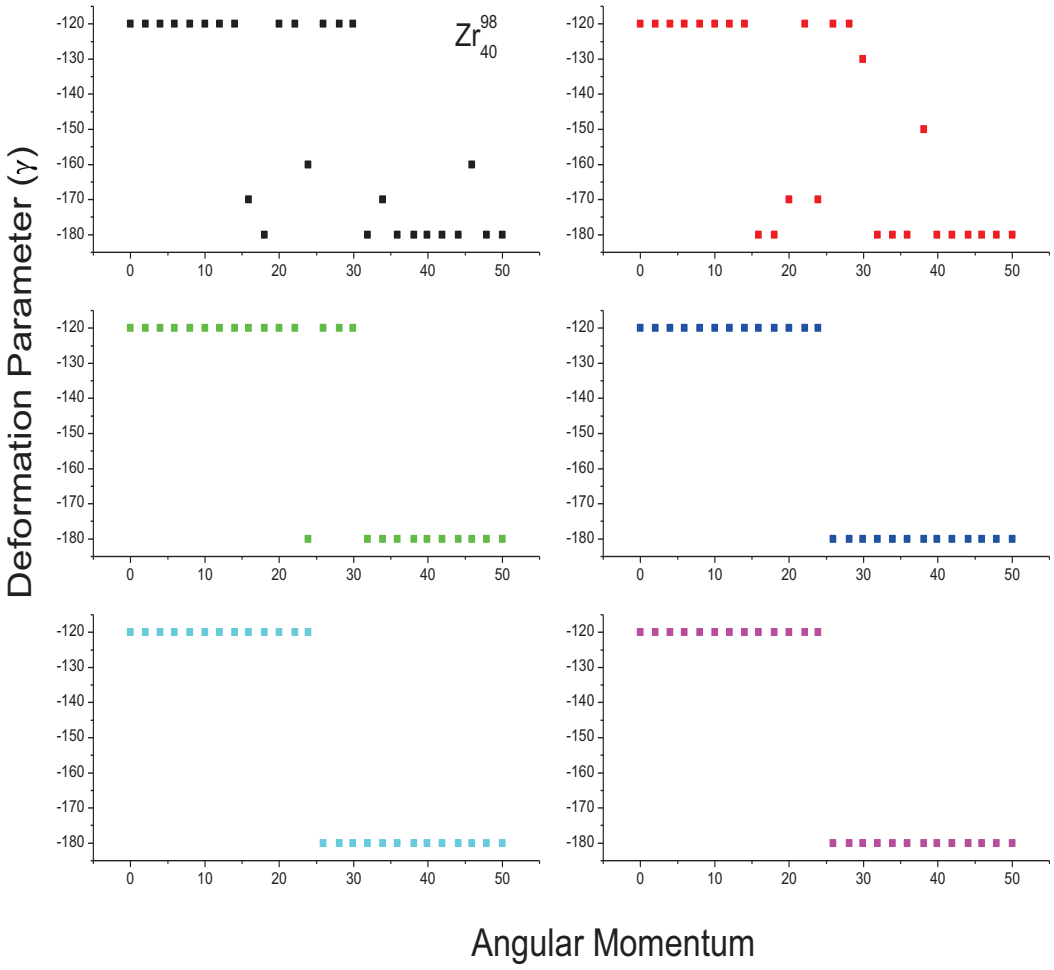


**FIG. 4.7: The deformation γ as a function of angular momentum I for the nuclei $^{98}$Zr**

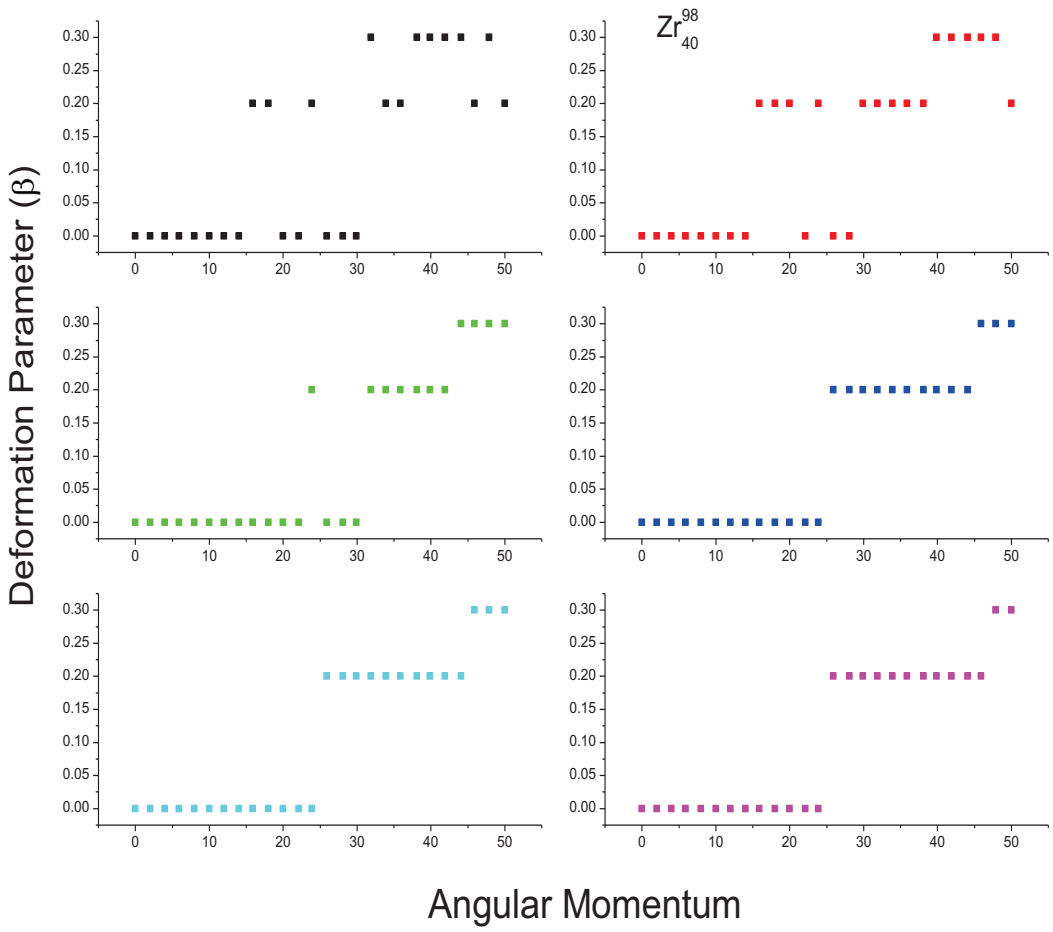


**FIG. 4.8: The deformation β as a function of angular momentum I for the nuclei $^{98}$Zr**

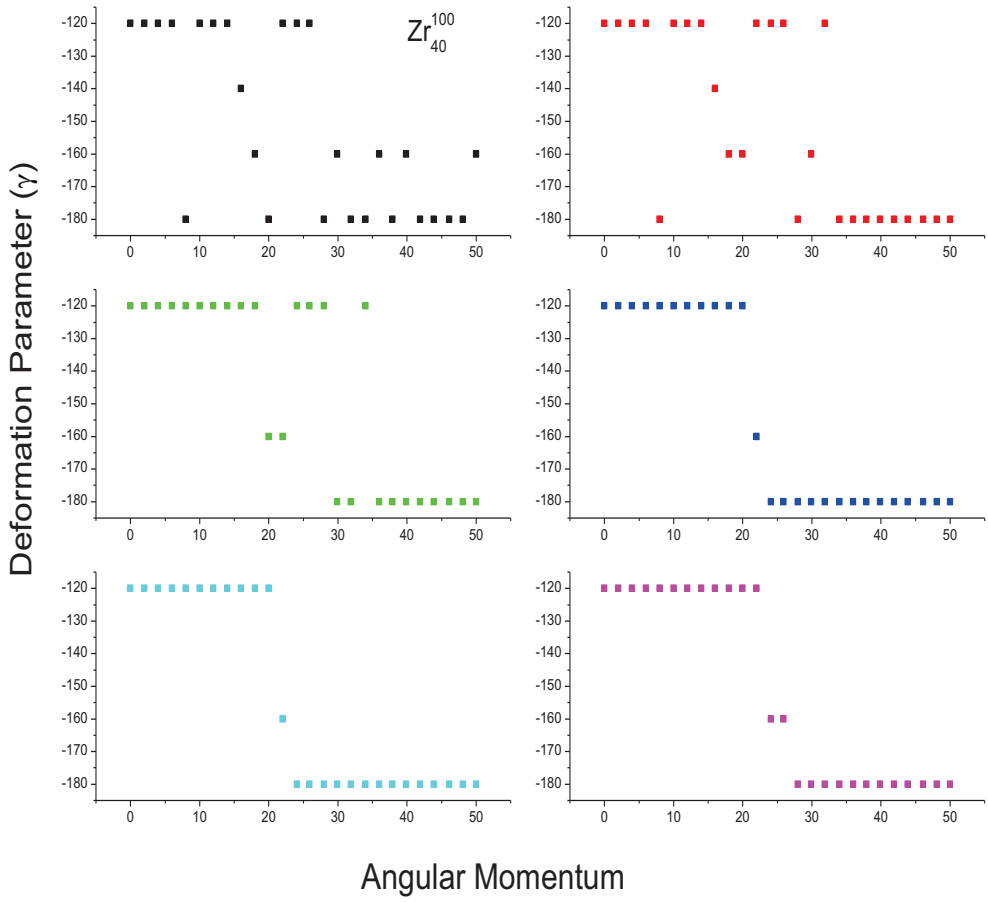


**FIG. 4.9: The deformation γ as a function of angular momentum I for the nuclei $^{100}$Zr**

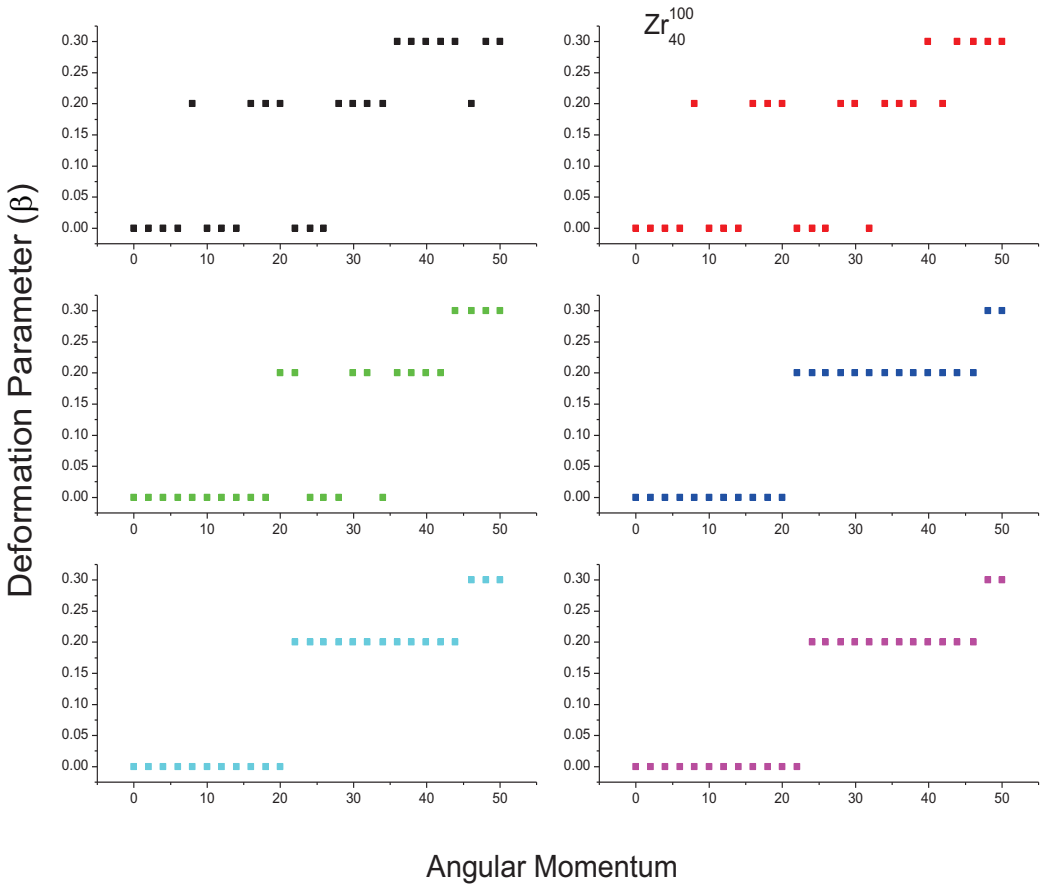


**FIG. 4.10: The deformation β as a function of angular momentum I for the nuclei $^{100}$Zr**

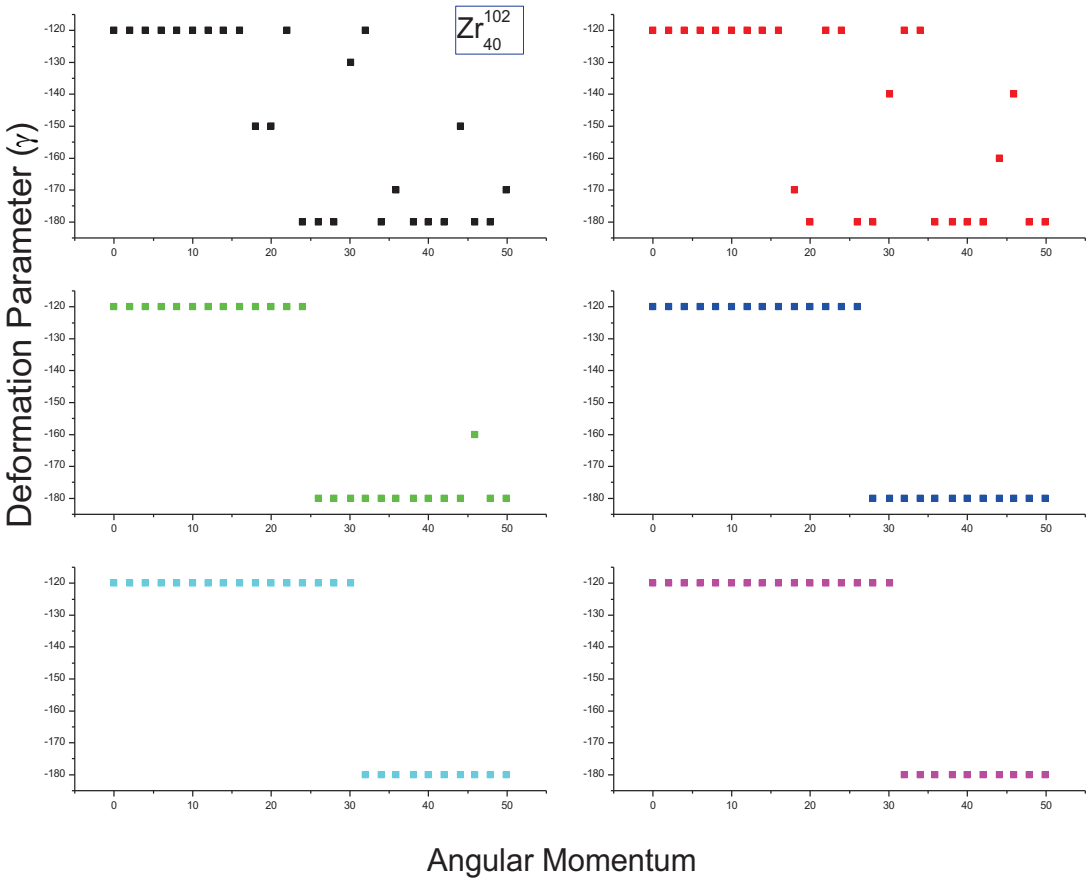


**FIG. 4.11: The deformation γ as a function of angular momentum I for the nuclei $^{102}$Zr**

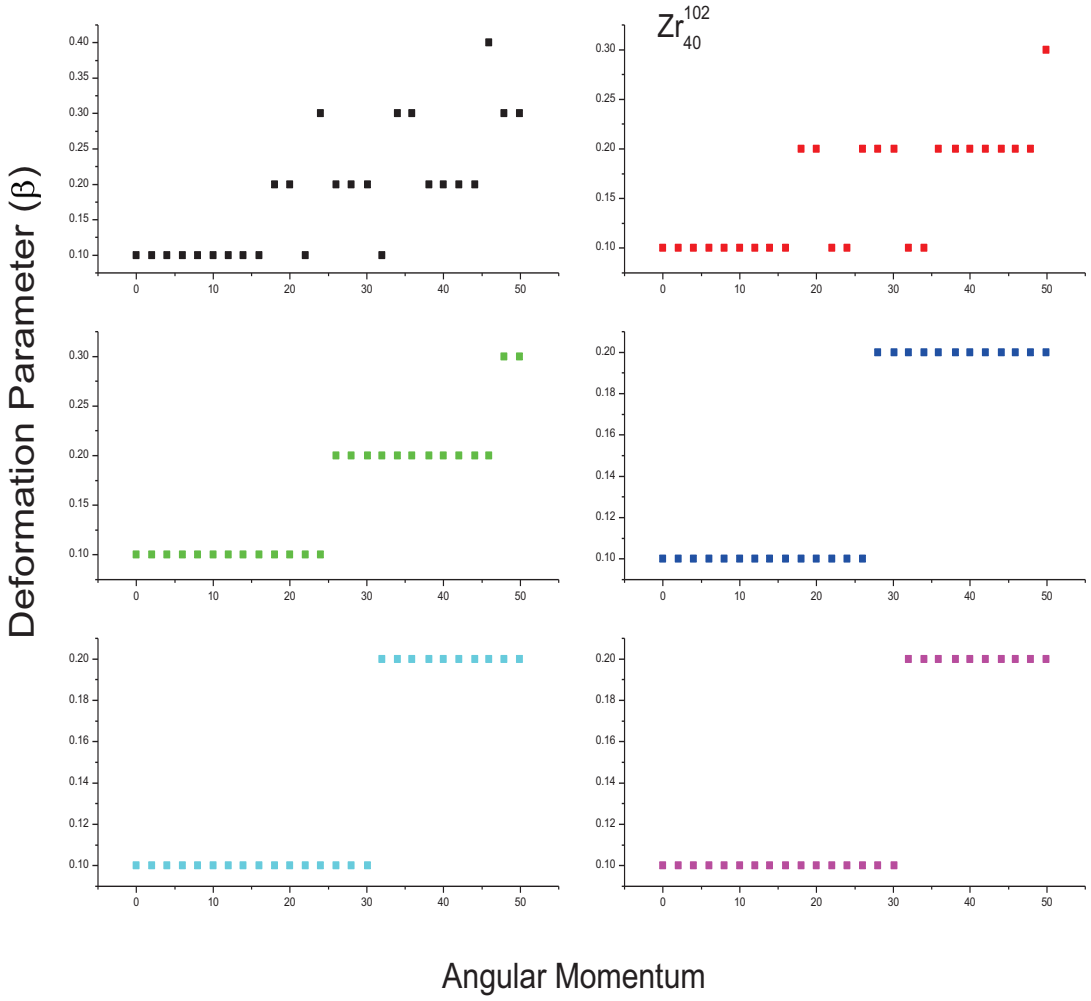


**FIG. 4.12: The deformation β as a function of angular momentum I for the nuclei $^{102}$Zr**

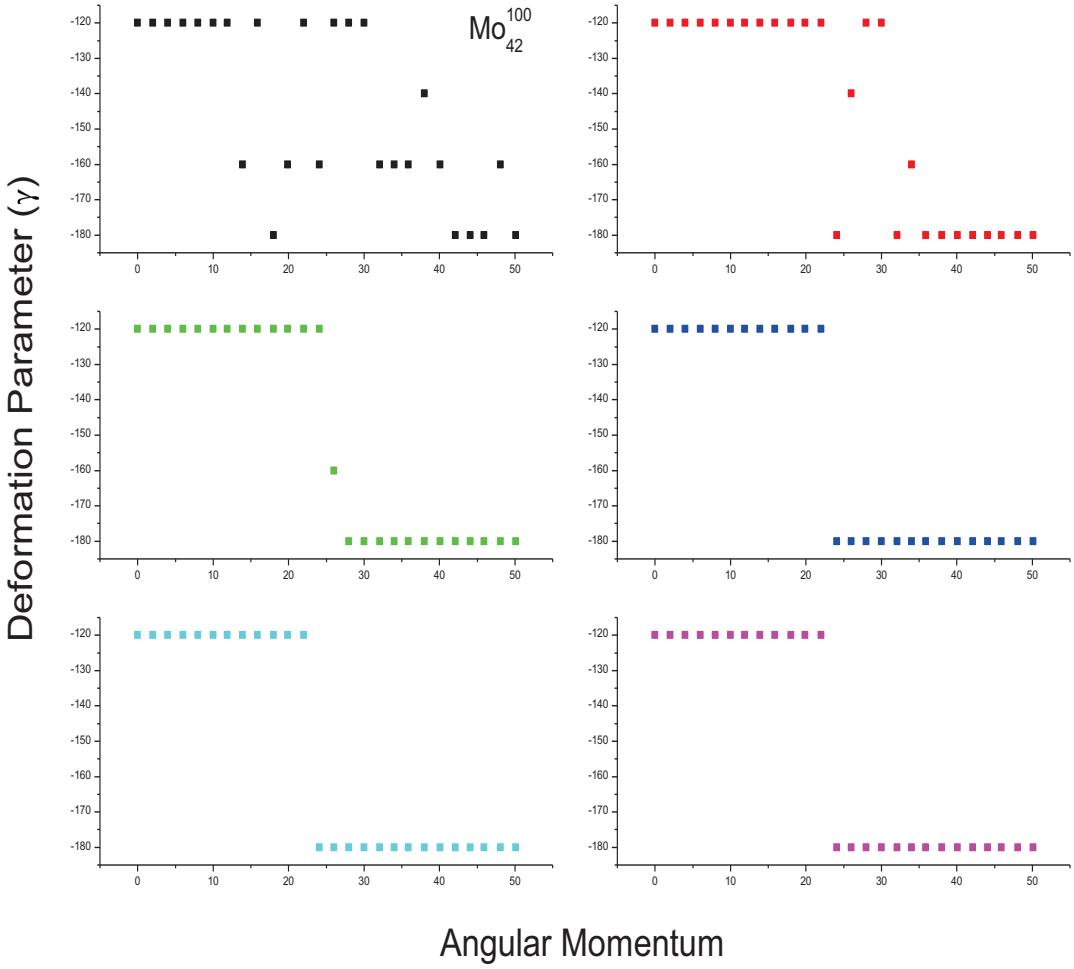


**FIG. 4.13: The deformation γ as a function of angular momentum I for the nuclei $^{100}$Mo**

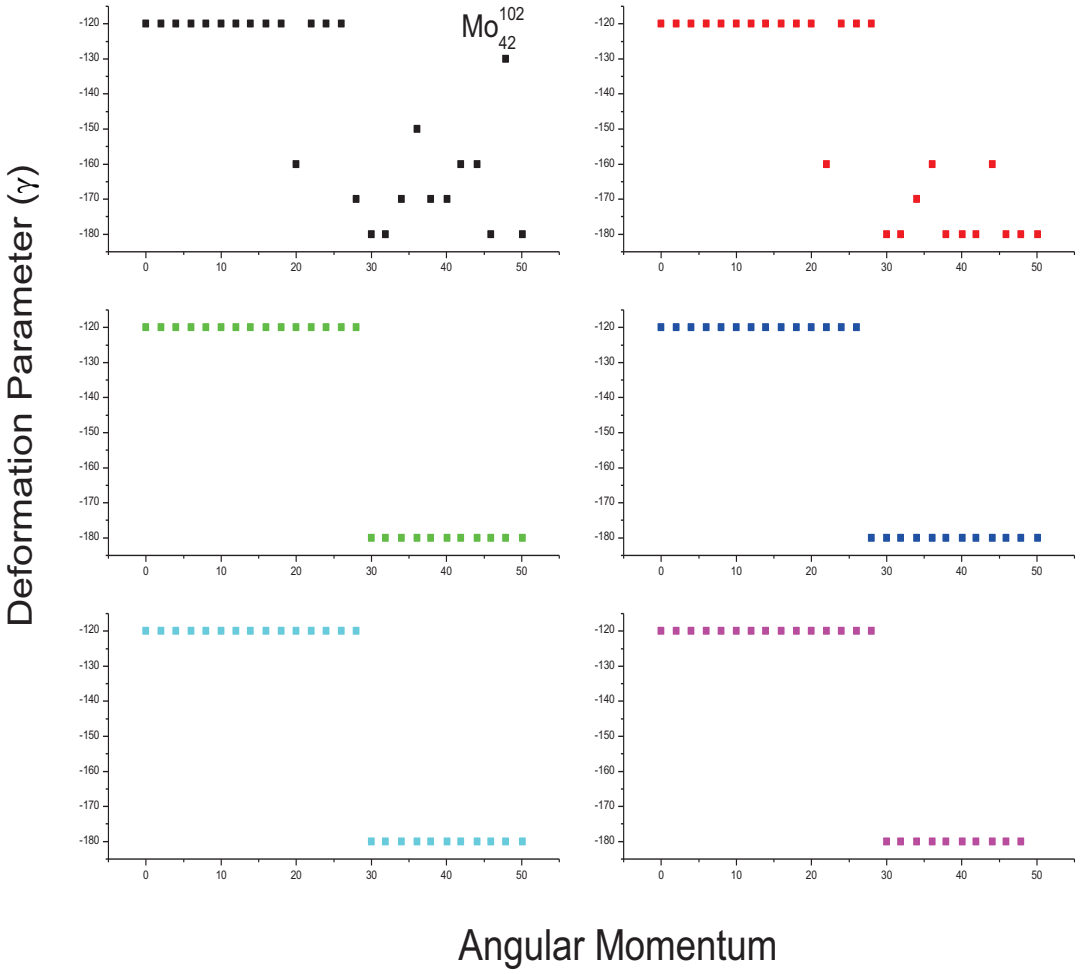


**FIG. 4.14: The deformation γ as a function of angular momentum I for the nuclei $^{102}$Mo**

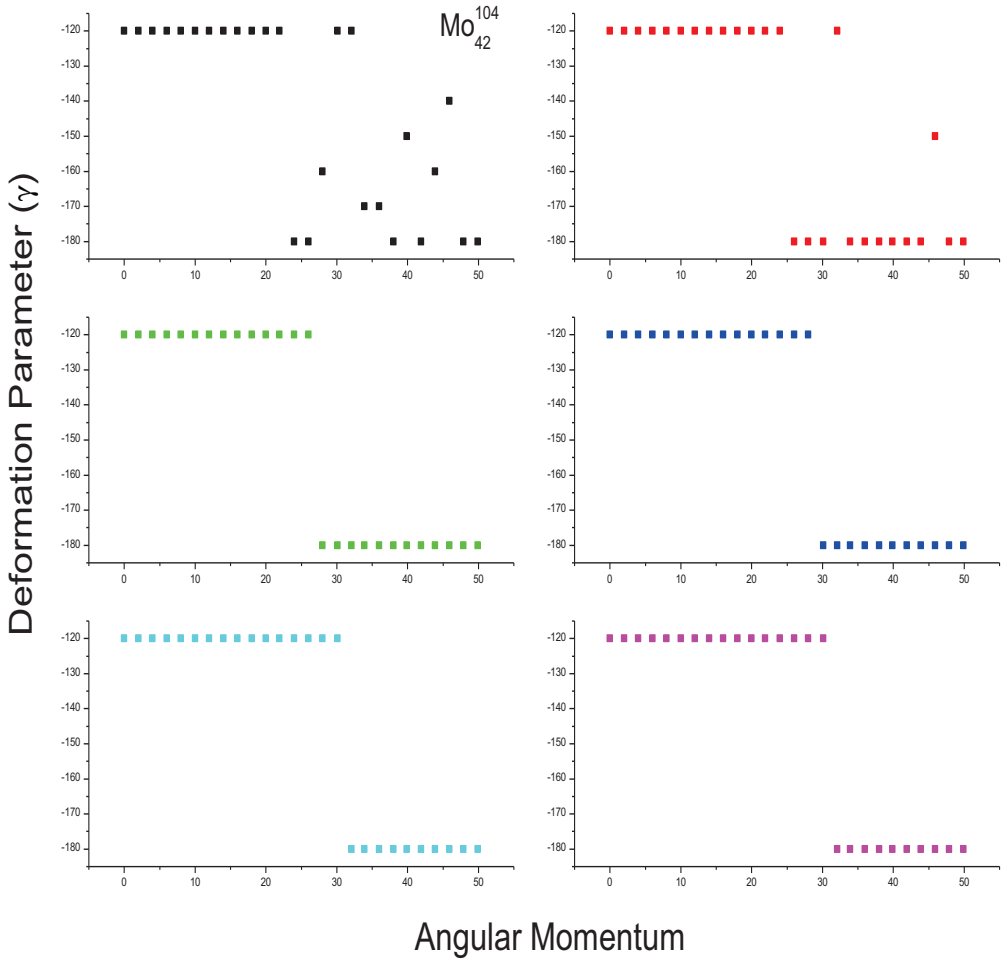


**FIG. 4.15: The deformation γ as a function of angular momentum I for the nuclei $^{104}$Mo**

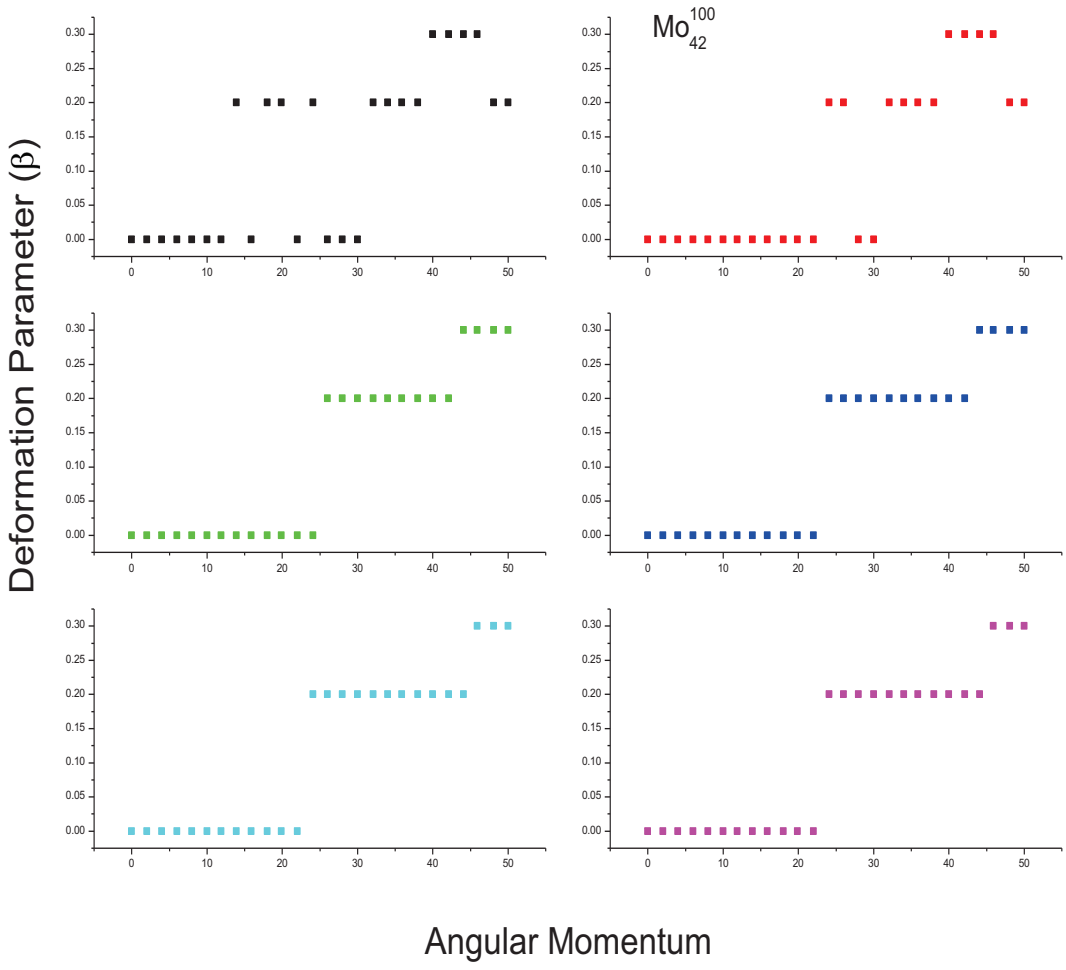


**FIG. 4.16: The deformation β as a function of angular momentum I for the nuclei $^{100}$Mo**

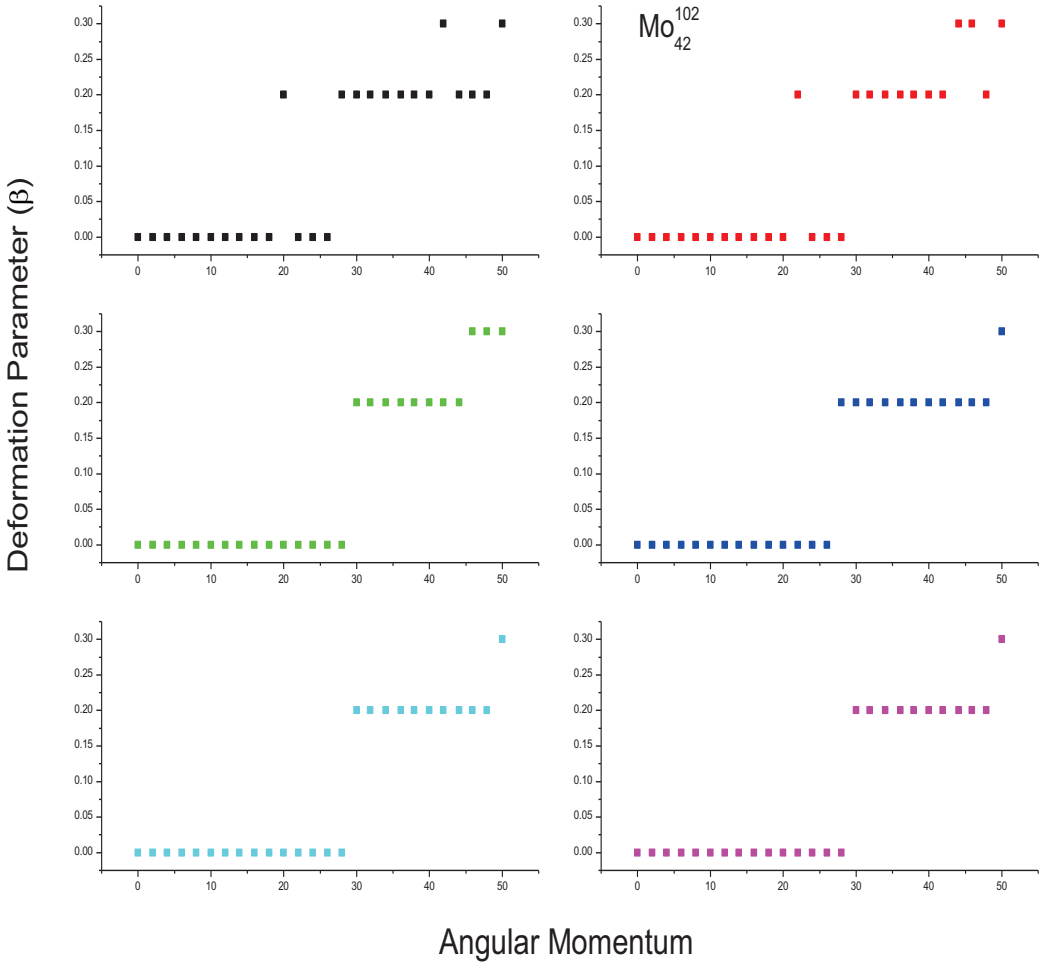


**FIG. 4.17: The deformation β as a function of angular momentum I for the nuclei $^{102}$Mo**

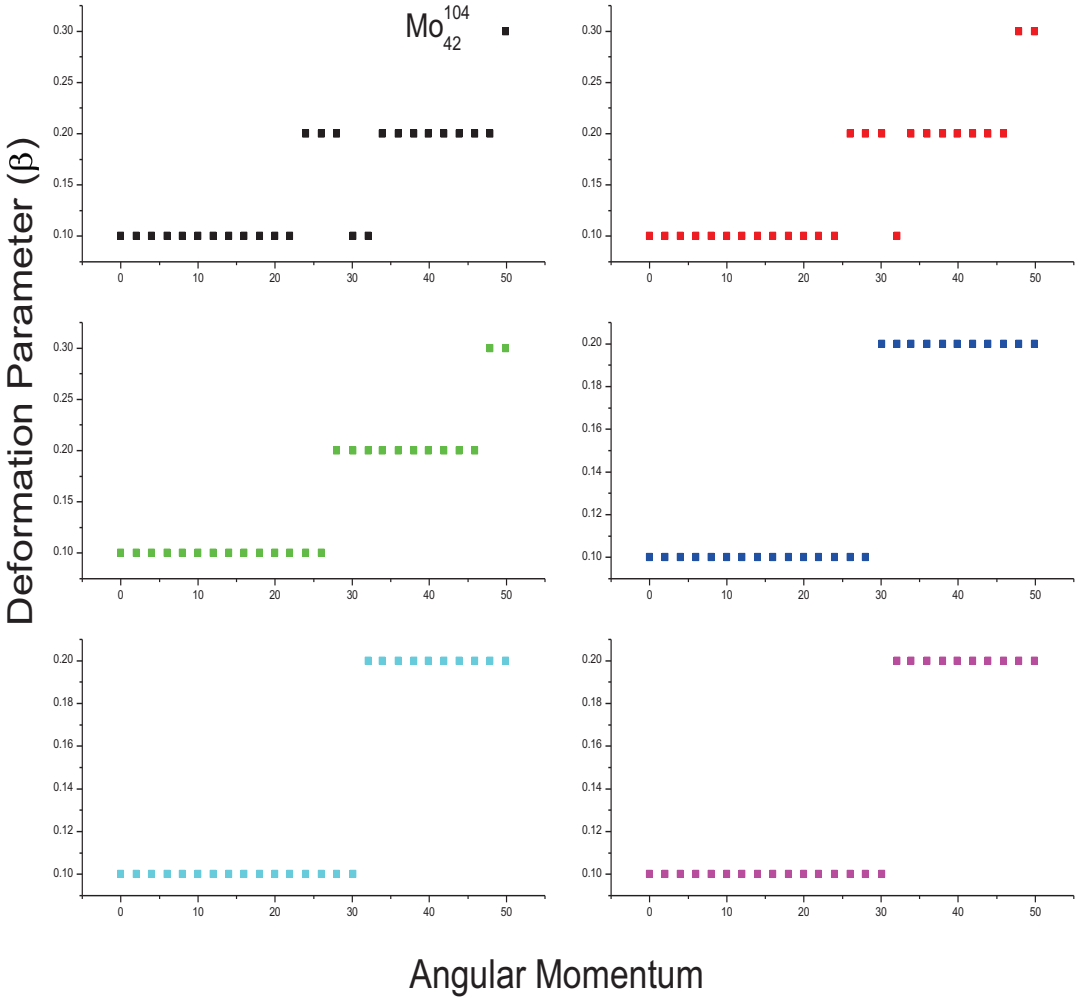


**FIG. 4.18:** **The deformation β as a function of angular momentum I for the nuclei $^{104}$Mo**

The numerical results of rotational energy as a function of angular momentum and temperature are shown in Figures 4.19(a-c) for the nuclei $^{94}$Kr, $^{96}$Kr and $^{98}$Kr. The fluctuations at low temperature and low angular momentum indicate the shape fluctuation from non collective prolate to triaxial and triaxial to non collective oblate. By increasing the angular momentum and at high temperature these shape fluctuation occur at low temperature were washed out and the nucleus uphold its deformed shape.

Figures 4.20(a-c), represents the rotational energy as a function of angular momentum at different temperatures for the nuclei $^{98}$Zr, $^{100}$Zr and $^{102}$Zr, respectively. The fluctuations at low temperature and low angular momentum indicate the shape fluctuation in these nuclei. At higher angular momentum these fluctuations were washed out and the nucleus maintains its deformed state.

Figures 4.21(a-c), represents the rotational energy as a function of angular momentum at different temperatures for the nuclei $^{100}$Mo, $^{102}$Mo and $^{104}$Mo, respectively. The fluctuations at low temperature and low angular momentum indicate the shape fluctuation in these nuclei. At elevated angular momentum and temperatures the fluctuation are washed out and the nucleus maintain its deformed state.

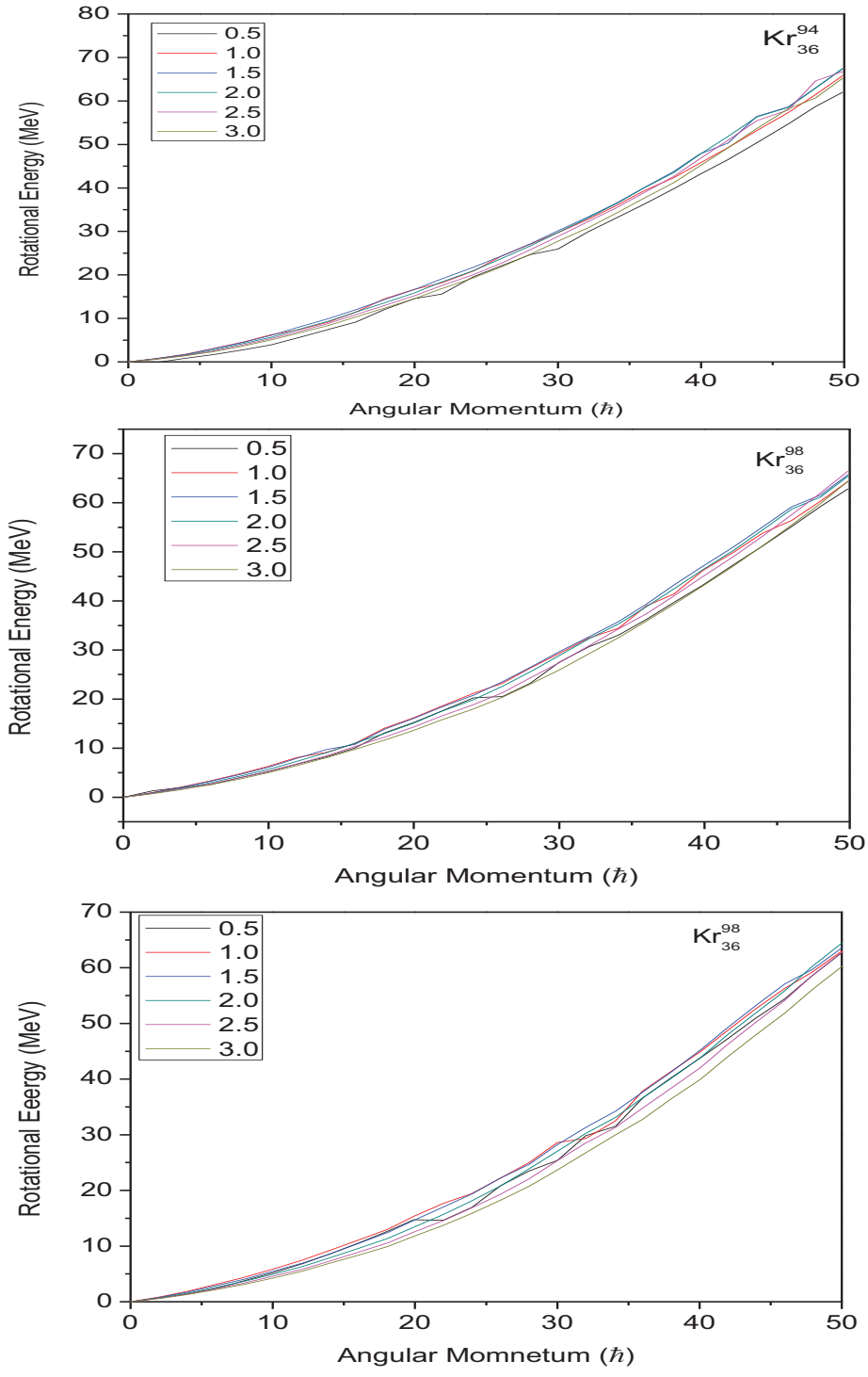


**Figure 4.19a-c: The rotational energy as a function of angular momentum for different temperature T for $^{94}$Kr, $^{96}$Kr and $^{98}$Kr**

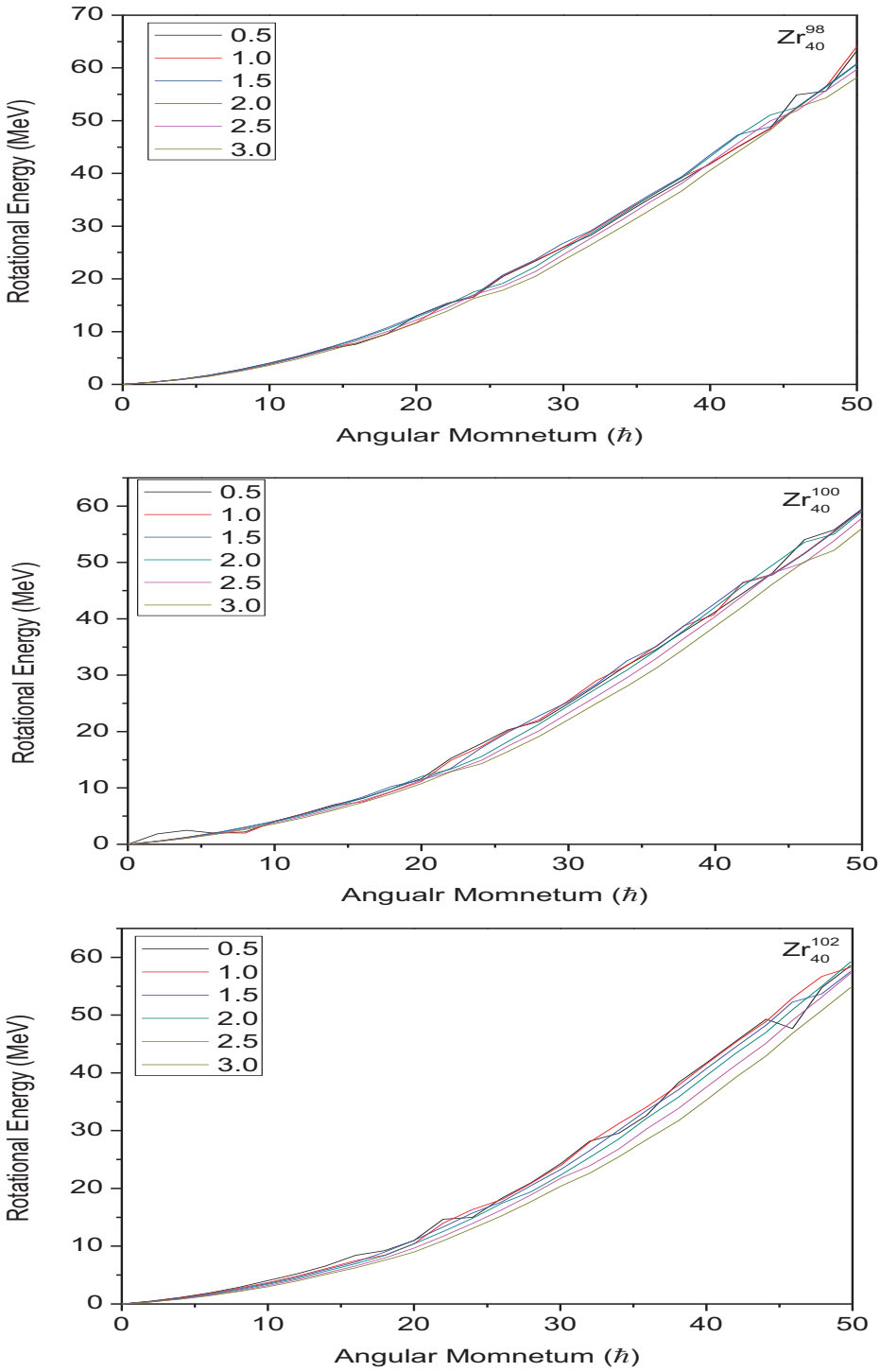


**Figure 4.20a-c: The rotational energy as a function of angular momentum for different temperature T for nuclei $^{98}$Zr, $^{100}$Zr, $^{102}$Zr**

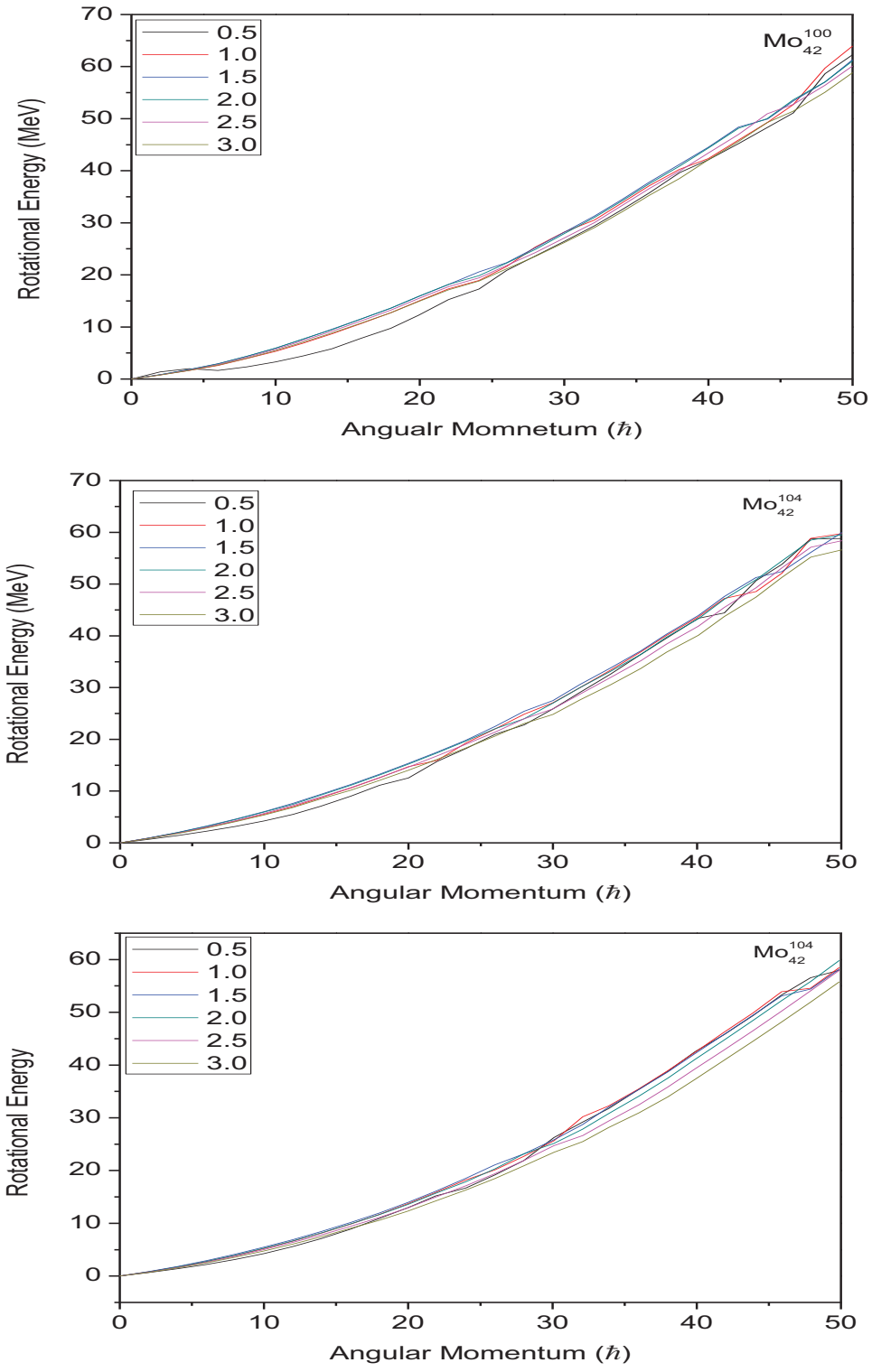


**Figure 4.21a-c: The rotational energy as a function of angular momentum for different temperature T for nuclei $^{100}$Mo, $^{102}$Mo and $^{104}$Mo**

The proton separation energy (SZ) and neutron separation energy (SN) is shown as a function of angular momentum in Fig. 4.22 (a-c) for the nuclei $^{94}$Kr, $^{96}$Kr and $^{98}$Kr for different temperatures. There is a general tendency the system to experience an abrupt change in the separation indicates the shape and phase transition. This abrupt change in SN at low temperature indicates the shape changes in system. At higher temperatures these fluctuations are get rid of.

The neutron separation energy (SN) and neutron separation energy (SN) is shown as a function of angular momentum in Fig. 4.22 (d-f) for the nuclei $^{94}$Kr, $^{96}$Kr and $^{98}$Kr for different temperatures. There is a general tendency the system to experience an abrupt change in the separation indicates the shape and phase transition. This abrupt change in SN at low temperature indicates the shape changes in system. As the temperature increase the fluctuation takes place at low temperature was washed out in all system. The neutron separation energy is higher than the proton separation energy. Similar trends were observed for the nuclei $^{98}$Zr, $^{100}$Zr, $^{102}$Zr $^{100}$Mo, $^{102}$Mo and $^{104}$Mo. But for these nuclei spherical to deformed phase transition occur (fig. 4.23 and 4.24).

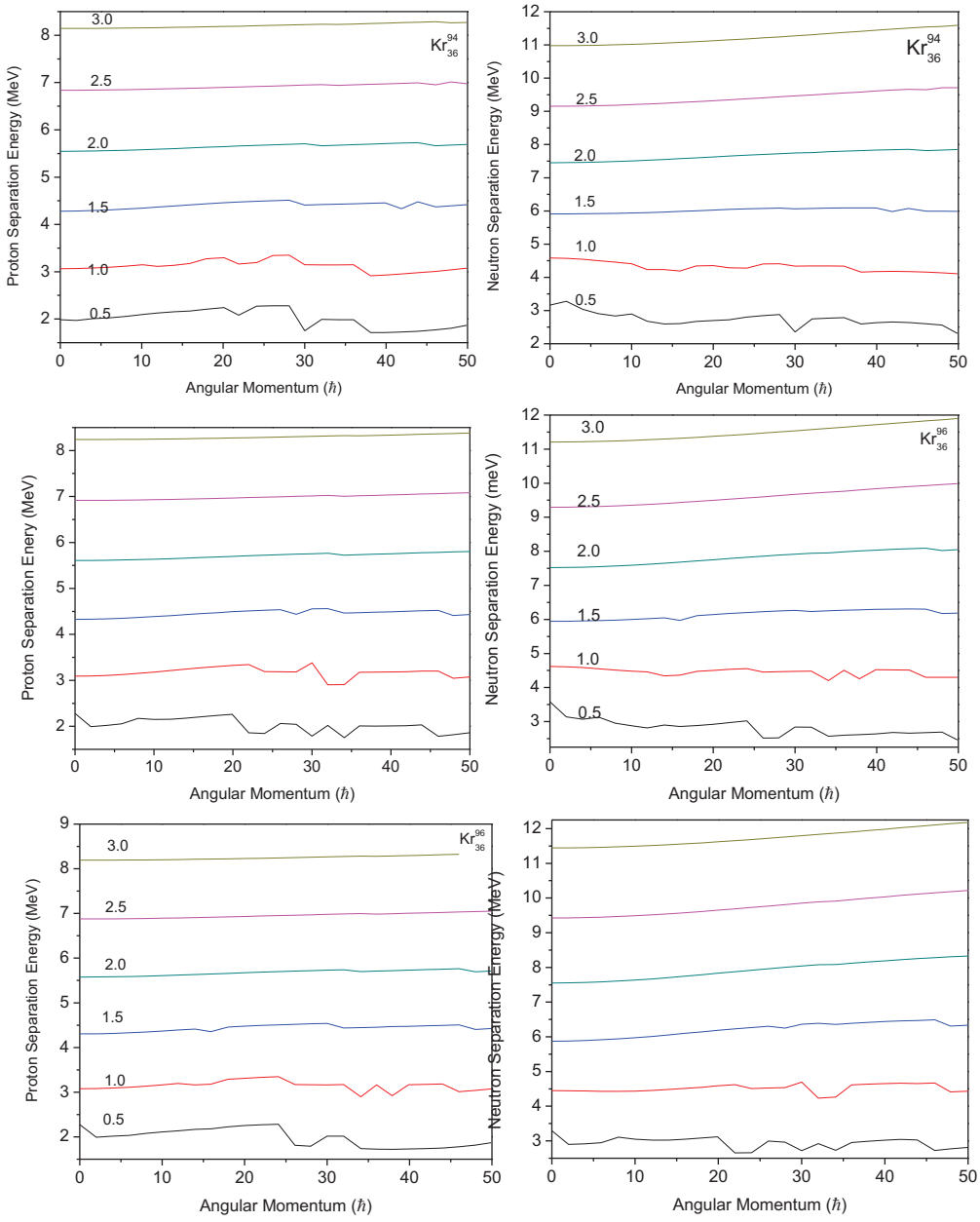


**Figure 4.22a-c: The proton and neutron separation energy as a function of angular momentum for different temperature T for $^{94}$Kr, $^{96}$Kr and $^{98}$Kr**

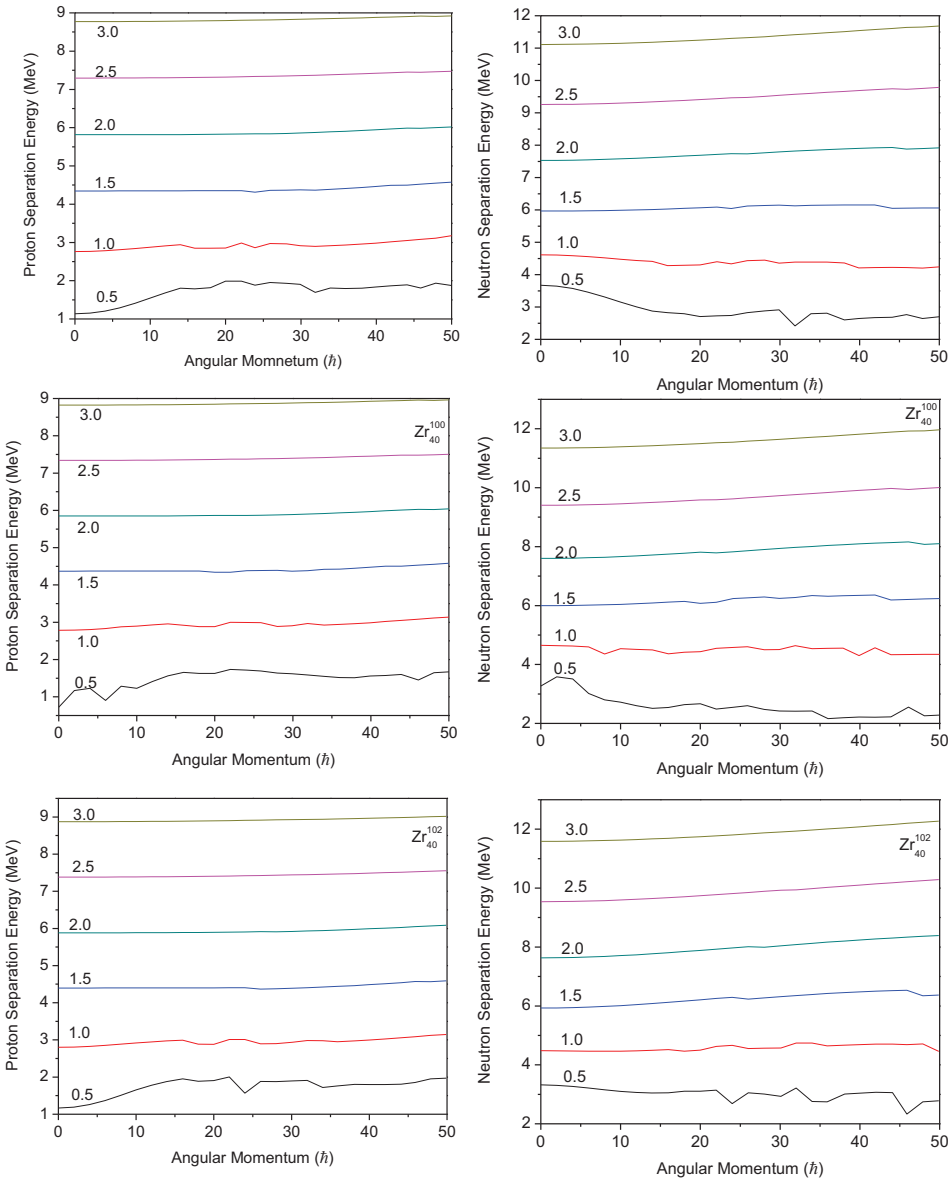


**Figure 4.23a-c: The proton and neutron separation energy as a function of angular momentum for different temperature T for $^{98}$Zr, $^{100}$Zr, $^{102}$Zr**

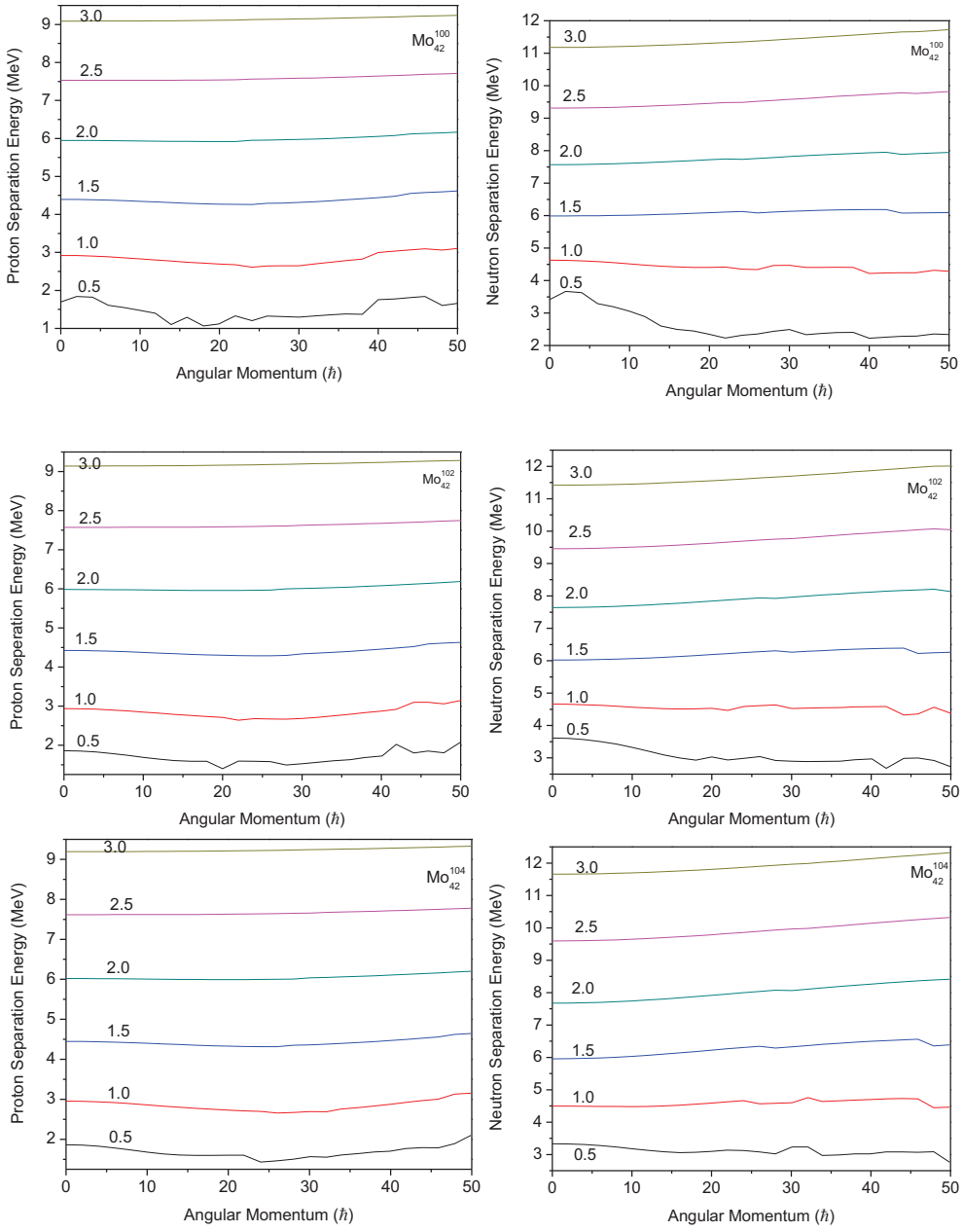


**Figure 4.24a-c: The proton and neutron separation energy as a function of angular momentum for different temperature T for $^{100}$Mo, $^{102}$Mo and $^{104}$Mo**

The single particle level density parameter 'a' as a function of temperature T and angular momentum are presented in Figs. 4.25(a-c) for the nuclei $^{94}$Kr, $^{96}$Kr and $^{98}$Kr, respectively. The effect of rotation on the single particle level density parameter is very pronounced at low temperatures. At low temperatures the shell structure plays a major role in the determination of the level density parameter. From the shell correction point of view a lower value of 'a' indicates relatively greater stability of the system. The single particle level density parameter 'a' shows a linear behaviour for the spin greater than 10. The value of level density parameter, for high spins there is a general tendency for 'a' to have a value lower than the ones for lower spins. Another important aspect of these curves is that they have been drawn after minimizing the free energy of the system with respect to the deformation parameter. Similar trends were observed for the nuclei $^{98}$Zr, $^{100}$Zr, $^{102}$Zr $^{100}$Mo, $^{102}$Mo and $^{104}$Mo (Figs. 4.26(a-c) and Figs. 4.27(a-c)).

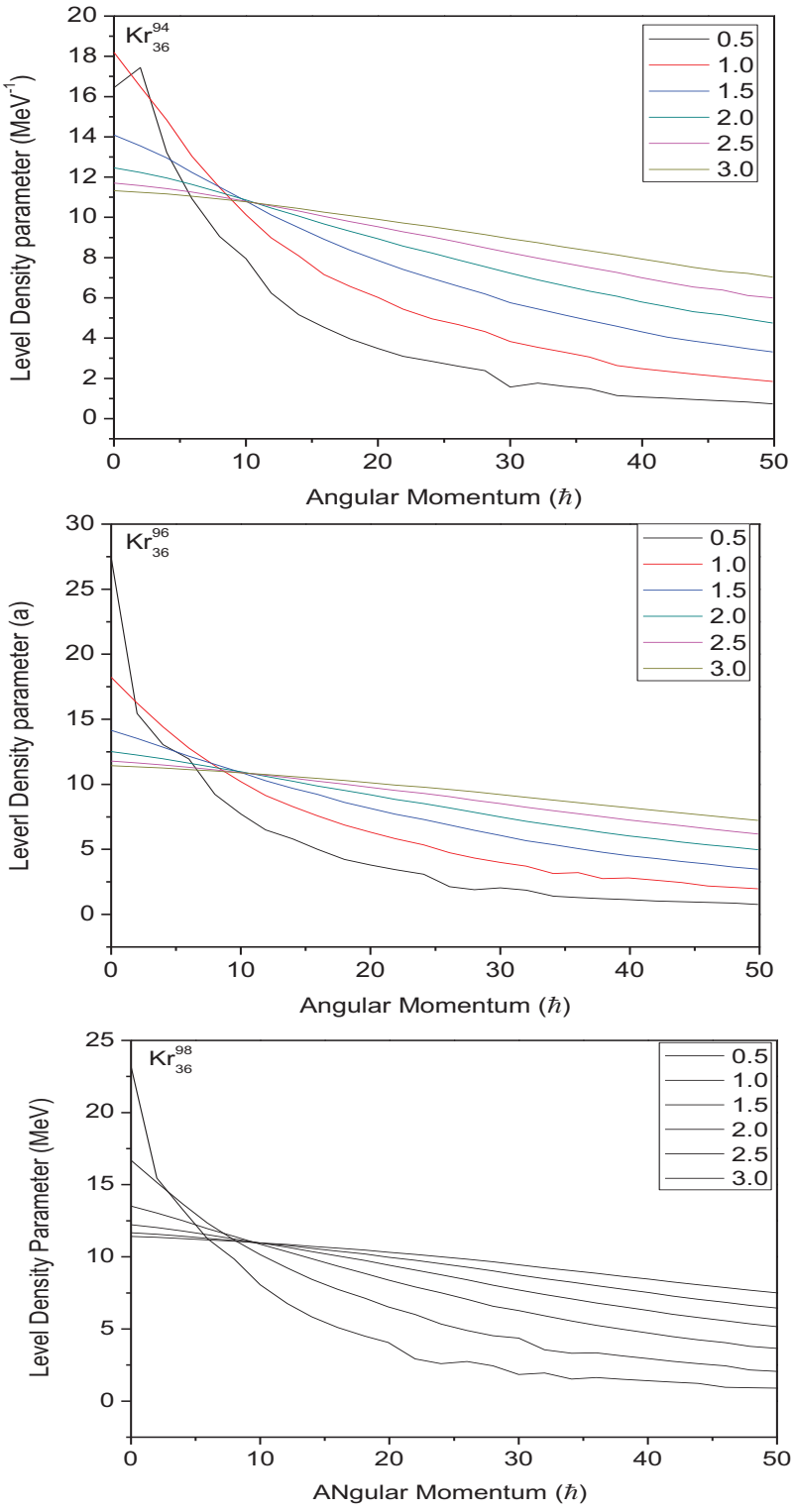


**Figure 4.25a-c: The level density parameter as a function of angular momentum for different temperature T for $^{94}$Kr, $^{96}$Kr and $^{98}$Kr**

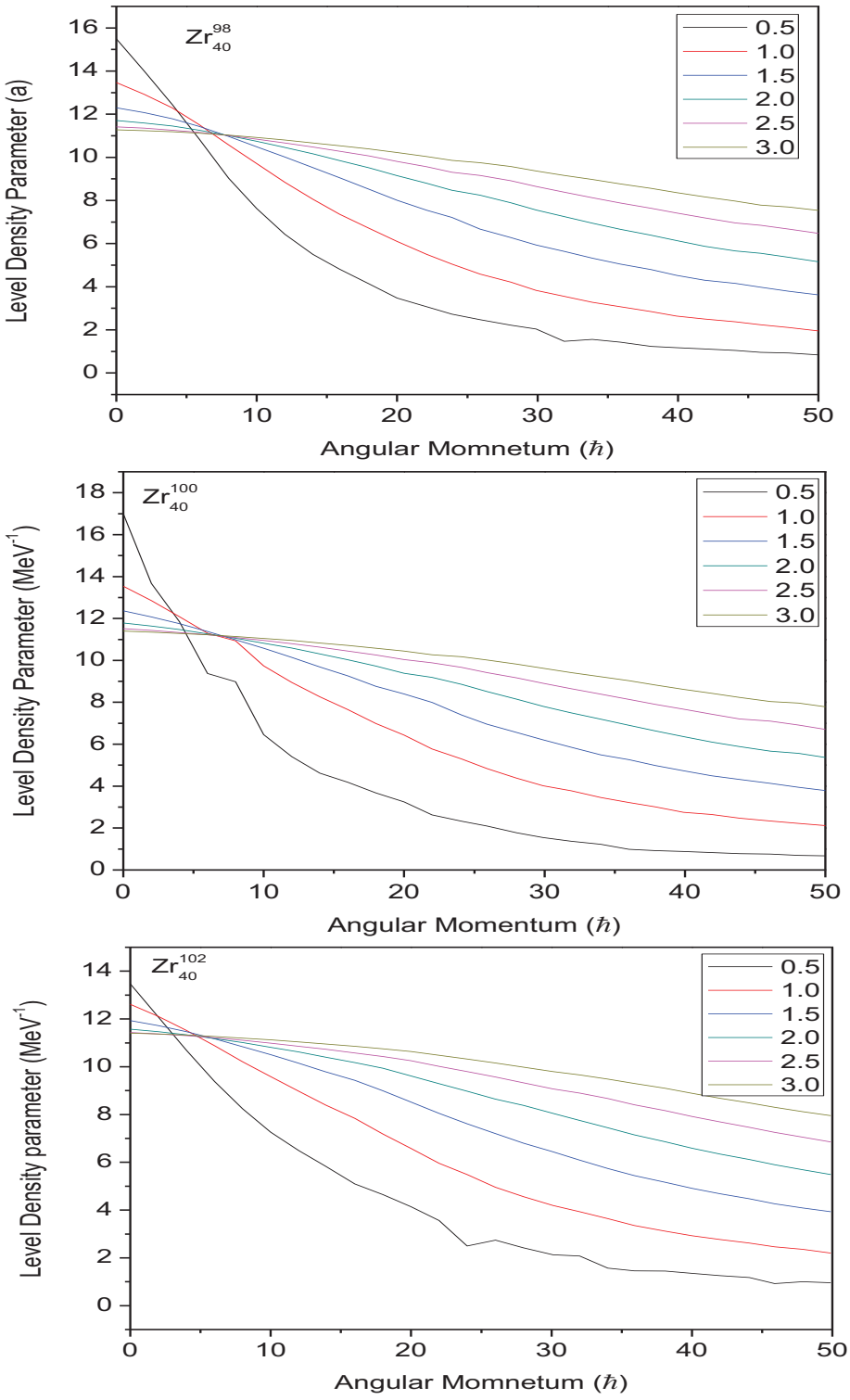


**Figure 4.26a-c: The level density parameter as a function of angular momentum for different temperature T for $^{98}$Zr, $^{100}$Zr, $^{102}$Zr**

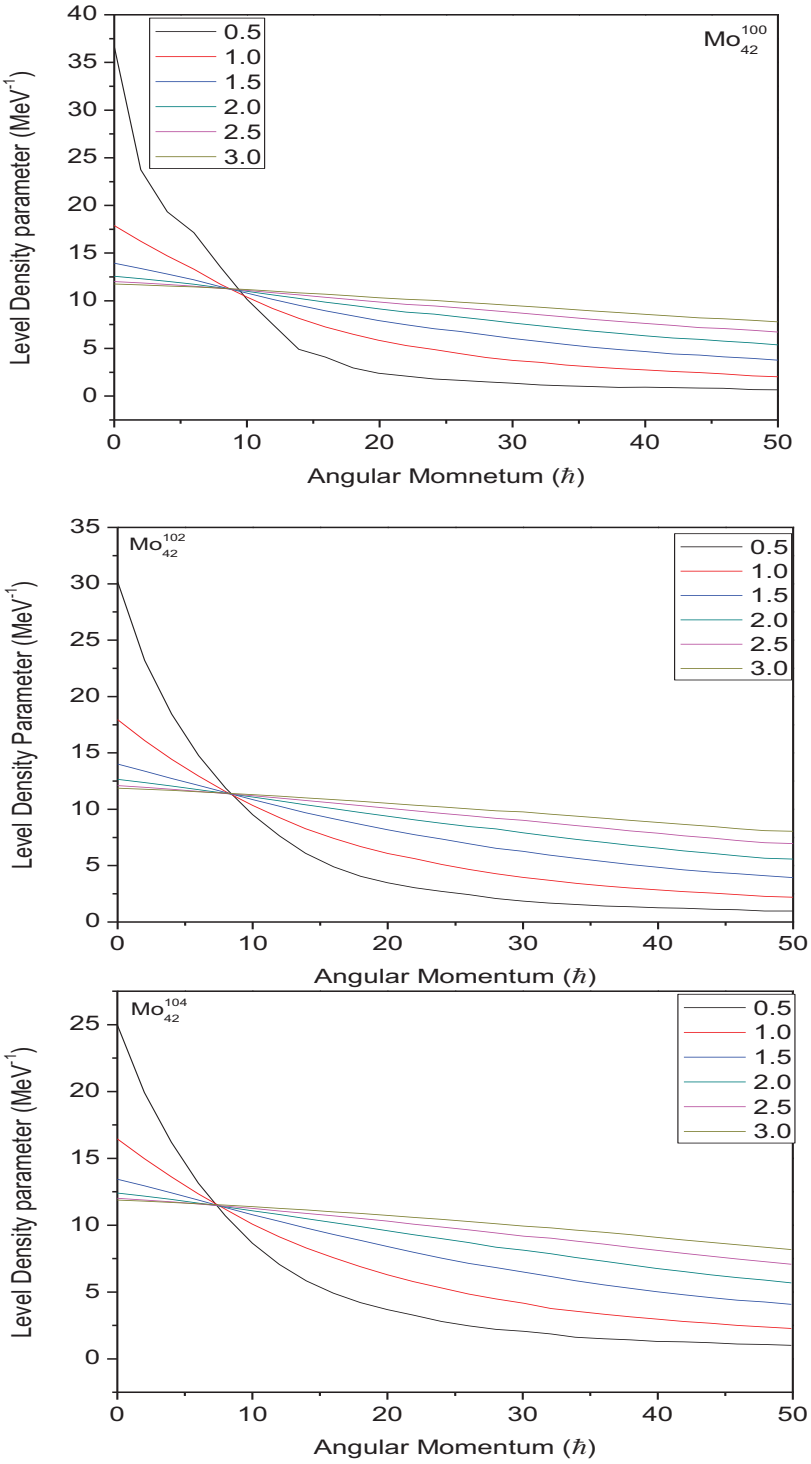


**Figure 4.27a-c: The level density parameter as a function of angular momentum for different temperature T for $^{100}$Mo, $^{102}$Mo and $^{104}$Mo**

### 4.3 Conclusion

In the present work we have made an attempt to study the shape evolutions of hot rotating $^{94,96,98}$Kr, $^{98,100,102}$Zr and $^{100,102,104}$Mo isotopes using the Statistical Theory. Focus is made mainly on the temperature T and angular momentum I induced shape transition from prolate collective to oblate non-collective. The sample results of shape transitions obtained as a function of angular momentum at temperatures 0.5, 1.0, 1.5, 2.0, 2.5 and 3.0 MeV. It is noted that at T = 0.5 MeV, the nuclei undergo a shape transition from nearly triaxial to nearly oblate as a function of angular momentum and. In the transition, the deformation increases with spin. Almost the same trend, but increased deformations are obtained as a function of spin at other temperatures also for all nuclei. The influence of temperature dependent effect, i.e., collapse of shell corrections has been observed around a temperature T > 1.5 MeV as is evident from the values of level density parameter. Single neutron and proton separation energies are very sensitive to the structural transitions.

# CHAPTER V
# STRUCTURAL CHANGES IN STRONTIUM ISOTOPES

## 5.1. Introduction

The studies of nuclear structure at high excitation energies, the so called hot nuclei [Cheifetz 1970, Arseniev1969, Sheline 1972, Clement 2016, Clement 2016 Regis 2017] identify today an important field of investigation in nuclear physics. During the last few decade considerable interests has been shown to the investigation of structural transitions as a function of both angular momentum and temperature of highly excited nuclei. A heavy ion fusion reaction produces a hot and rapidly rotating compound nucleus. Hot nuclei are formed in heavy ion fusion reactions where the relative kinetic energy of the colliding nuclei is converted into internal excitation energy and high angular momentum of the compound nuclei. After emission of neutrons has cooled down the system, the compound nucleus still keeps high angular momenta and moderate heat energy. Hot and rotating nuclei are expected to exhibit a rich variety of different shapes.

There is considerable interest in the study of the structure of nuclei in the mass region A≈100 due to the onset of deformation in the neutron rich nuclei [Schussler 1980, Park 2016 Urban 2001]. These neutron rich nuclei are of special interest because they are just at the border between a rather spherical and a well deformed shape. Theoretically, the region has been studied using interacting boson model [Sirag 2015], Nilsson Strutinsky Cranking method [Mamta Aggarwal 2016], statistical theory [Mamta Aggarwal 2016] and Hartree-Fock-Bogolyubov [Sotty 2015].

The experimental and theoretical aspects of transitional nuclei in the neutron rich A∼100 [Campbell 2002, Petrovici 2011, de Roubin 2017] has been under intensive and extensive investigations, in the last a few decades. In this part of the nuclear chart, the most rapid development of deformation has been observed. By adding just few neutrons/protons, a rapid shape transition occurs from spherical to well deformed ground state shape around N∼60. Most of these methods correspond to cold nuclei and are applicable strictly speaking only to yrast spectroscopy. In these investigations of the nuclear shape at high excitation energies are absent, and the statistical properties of fast rotating nuclei have not been given proper consideration.

The study of neutron rich Strontium isotopes helps one to understand the nature of collective motion occurring in these nuclei. This collective motion is susceptible to modulation by shell structure. The development of deformation in $^{100-102}$Sr has been analysed experimentally [Chabanat 1998] and also using self consistent mean-field Hartree-Fock-Bogoliubov (HFB) approximation [Pinston 2005]

To understand the structure of neutron-rich nuclei and to validate the existing theoretical model for the exotic mass region, we study systematically strongly-deformed, neutron-rich even–even Sr isotopes with neutron number 52,54,56,58,60 &62. For this purpose statistical theory proposed by Moretto [Moretto 1975] and developed by [Rajasekaran Rajasekaran 19888, Rajasekaran 1981, Rajasekaran 1987, Rajasekaran 1988, Rajasekaran 1988] is used. The triaxial deformation is introduced into the picture by using the single particle levels generated by diagonalizing the triaxially deformed Nilsson Hamiltonian in the cylindrical representations. The observed oblate and prolate minima are related to the low single-particle energy level density around the Fermi surfaces of neutron and proton respectively.

## 5.2 Result and Discussion

The effect of angular momentum and temperature on the shape of Strontium isotopes has been systematically analyzed. The free energy minimum of Sr as functions of angular momentum and deformation parameters $\beta$ and $\gamma$ calculated at different temperatures were shown in Figs. 5.1 – 5.12. From Fig. 5.1, for $^{90}$sr, we find that the nucleus in prolate shape at low angular momentum, triaxial at moderate angular momentum and achieve oblate shape at higher angular momentum. These deformation fluctuations vanish at high temperature of about 1.5 MeV, because of vanishing shell effects at these temperatures. Similar behaviour is observed for $^{90,92,94,96,98,100}$Sr, as evident from Fig. 5.2 - 5.12. These changes in the shape of the nuclei suggest an impression that interplays among angular momentum, temperature and deformation is responsible for the observed behaviour of the nuclei.

The rotational energy for the Strontium isotopes (N = 52, 54, 56, 58, 60 &62) against temperature is plotted in Fig.5.13-5.18, and which is increasing with temperature. Figure 5.13 shows the rotational energy for low temperature is higher than the high temperature at low angular momentum. However at high angular momentum the rotational energy for high temperature is higher than the lower temperature. The shape of the nucleus is found to be collective prolate and triaxoial and unaltered till the spin I = 30ħ. Above I = 30ħ the shape of the nucleus found to be non collective oblate. The rotational energy increases with angular momentum and temperature and the occurrence of shape transition beyond temperature T = 1.5MeV is almost at a particular spin (J ≈ 26h) (Fig.5.14-5.18) and hence the role of temperature in the shape transition beyond T = 1.5MeV is relatively negligible.

The calculated single-neutron separation energy SN versus temperature T is plotted for various angular momentum I in Fig. 5.15a and 5.16a and proton separation energy SZ in Fig. 5.15b and 5.16b. The proton and neutron separation energies have its own importance in the isotopic transition. Our calculations show that the proton separation energy almost constant with increasing spin. Figure shows fluctuation at low temperatures, it may be due to effect of rotation at low temperatures where shell effects play a very important role. At higher temperatures for T >1.0MeV, these fluctuations disappear and the energy values become almost constant due to the absence of shell effects. At high temperature the proton and the neutron separation energy becomes almost constant, shown in Fig. 5.15-5.16, i.e., the particle emission get saturated even if the temperature is increased, and the shape evolution get started slowly.

Nuclear reaction calculations based on standard nuclear reaction models play an important role in determining the accuracy of various parameters of theoretical models and experimental measurements. Especially, the calculations of nuclear level density parameters (ldp) for the isotopes can be helpful in the investigation of reaction cross-sections. For Strontium isotopes (N=52,54,56,58,60&62) the level density parameter "a" calculated at different temperatures are plotted against angular momentum, (Fig. 5.15). Fig. 5.15 shows the variation of level density parameter as function of temperature and angular momentum. The single particle level density parameter has maximum values at angular momentum $0\hbar$ for all temperatures though these maximum values are reduced with increase in temperature as seen from Figs. These figures indicate that the single particle level density parameter approaches constant values at higher angular momentum for all temperatures. A significant effect

of rotation on the level density parameter is observed at very low temperatures. At these temperatures where the contribution of shell structure dominates, the level density parameter varies for different angular momentum states of the nucleus. The nucleons start to behave like a degenerate system at T = 1.5MeV when the shell corrections vanish. In the present case the temperature T = 1.5MeV, at which the shell correction collapses, may be treated as a critical temperature $T_C$, where the system behaves like a degenerate Fermi gas represented by a constant level density parameter of the order of A/8. For T > 1.5MeV the level density parameter 'a' shows a linear behaviour for all the angular momentum considered.

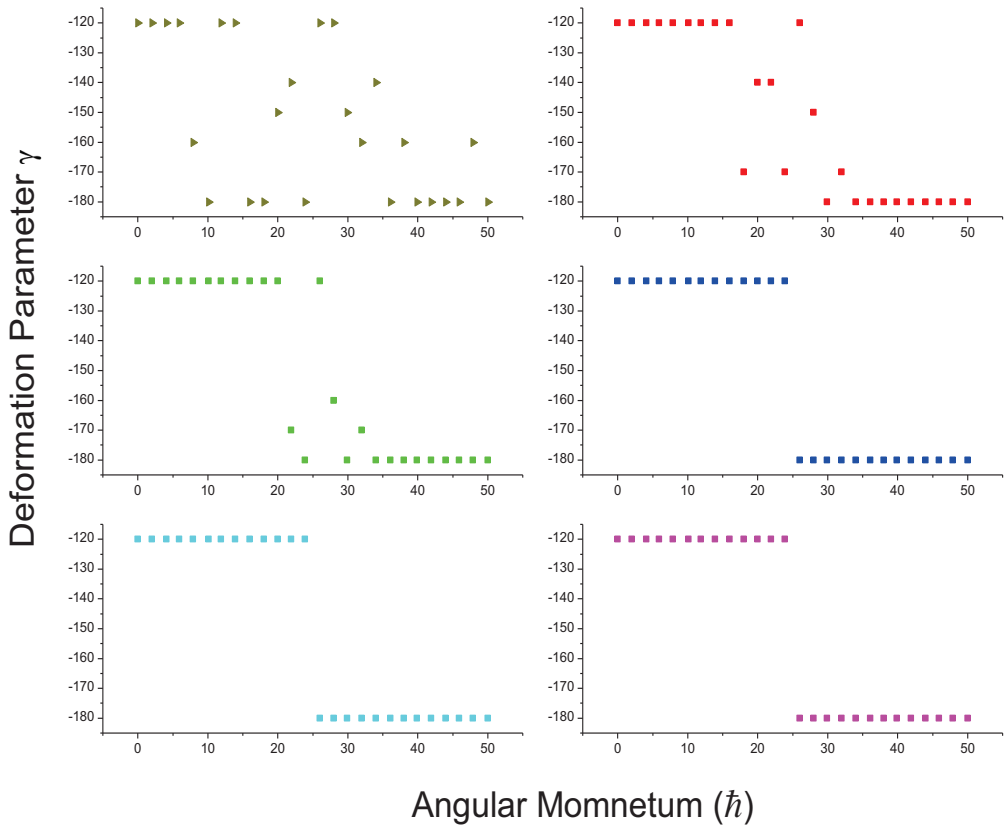


**FIG. 5.1: The deformation γ as a function of angular momentum I for the nuclei $^{90}$Sr**

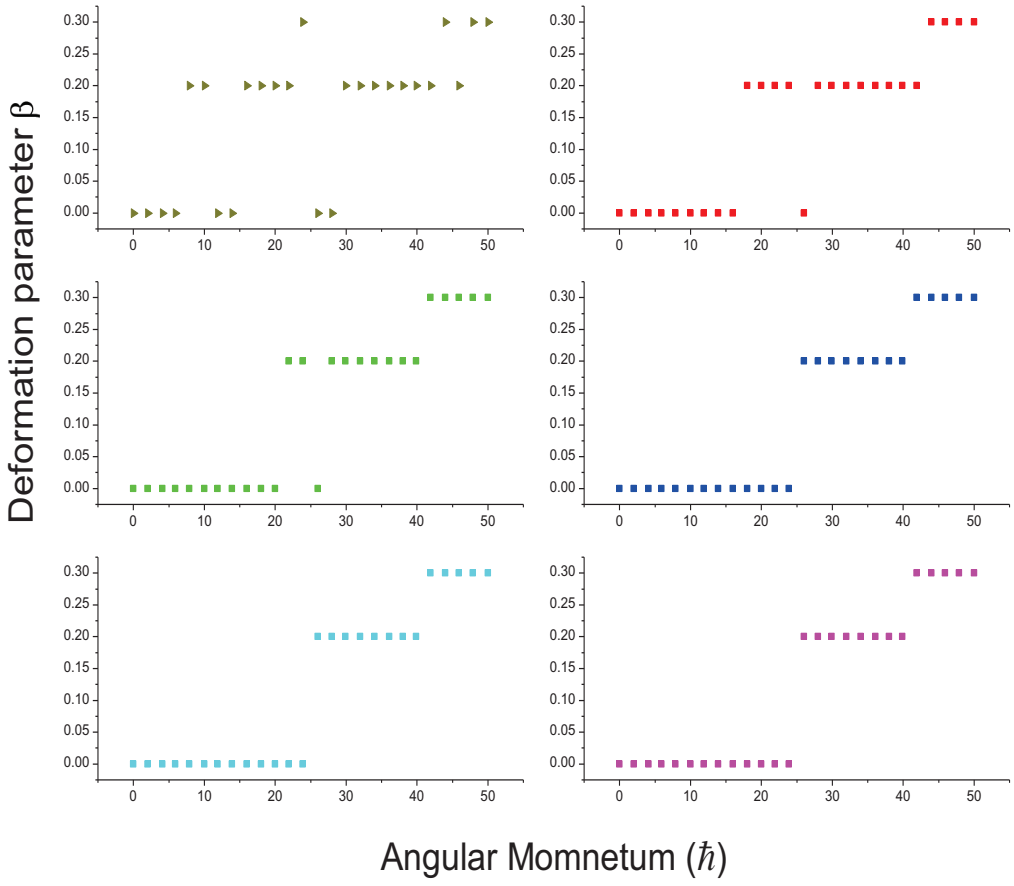


**FIG. 5.2: The deformation β as a function of angular momentum I for the nuclei $^{90}$Sr**

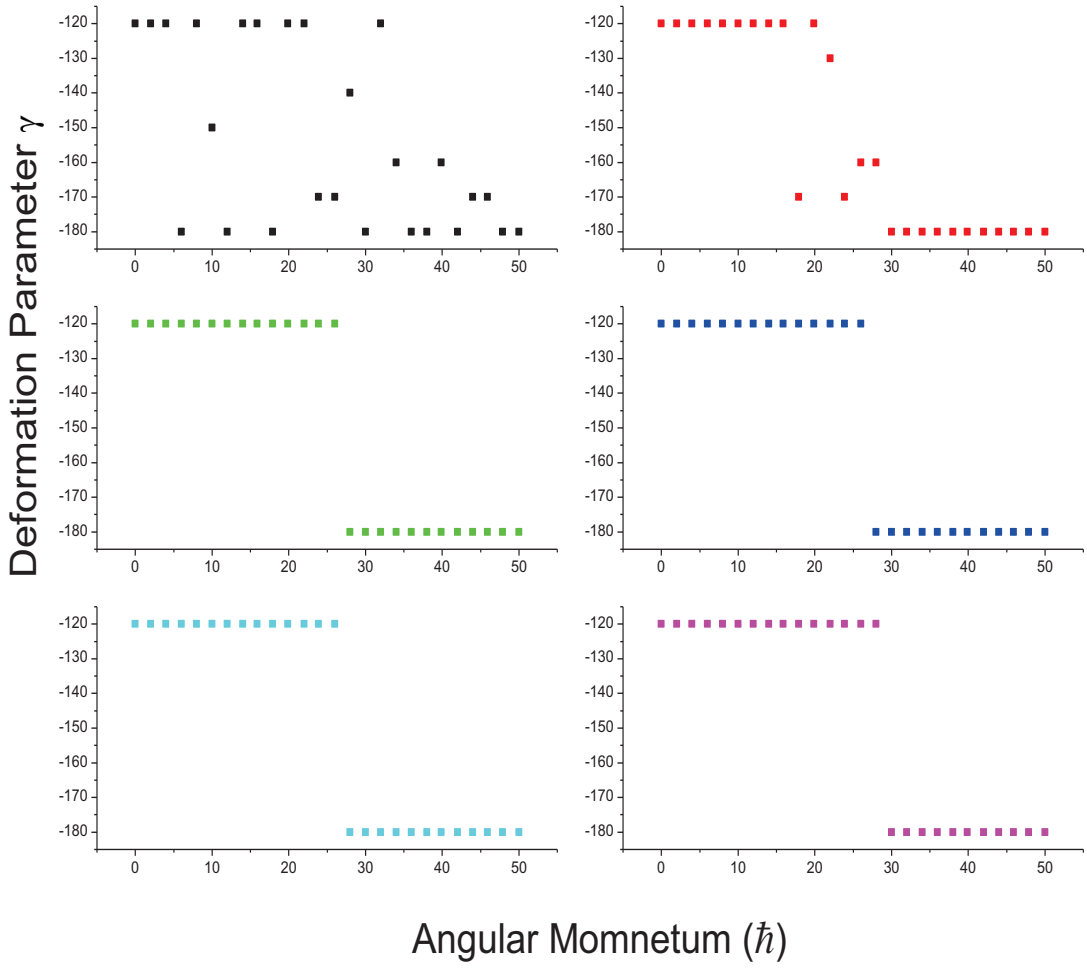


**FIG. 5.3: The deformation γ as a function of angular momentum I for the nuclei $^{92}$Sr**

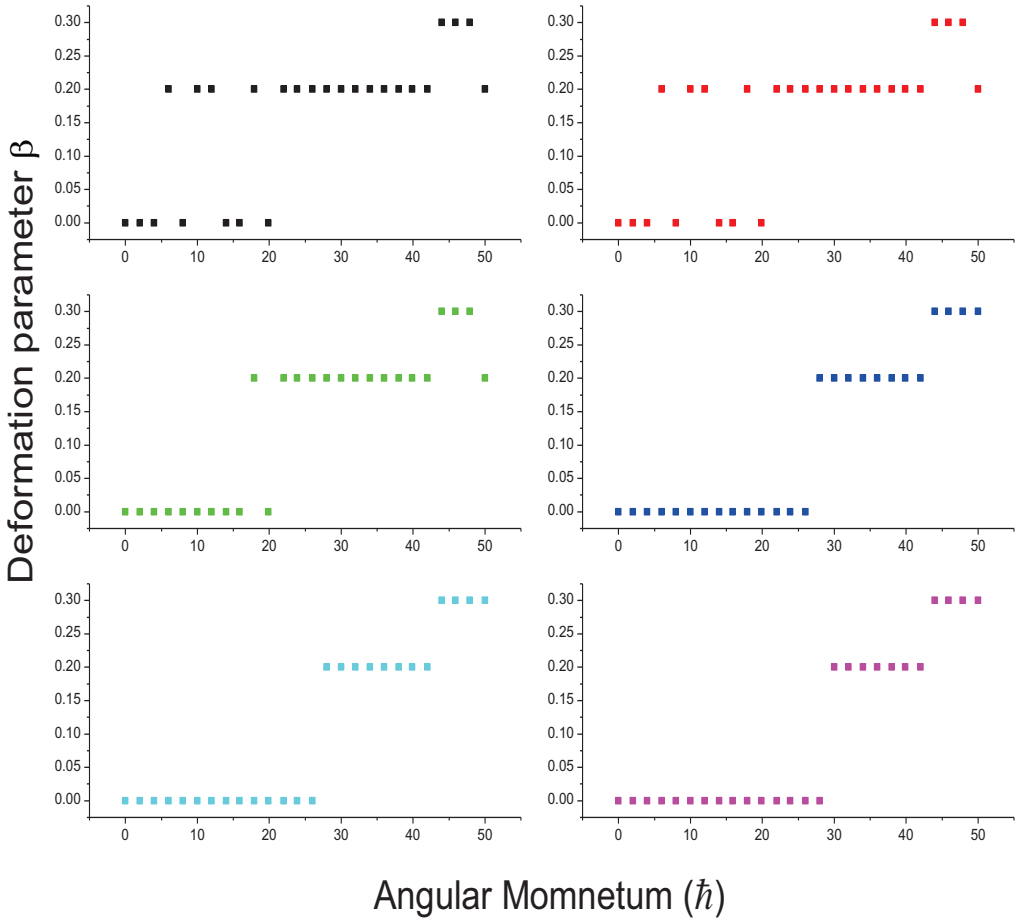


**FIG. 5.4: The deformation β as a function of angular momentum I for the nuclei $^{92}$Sr**

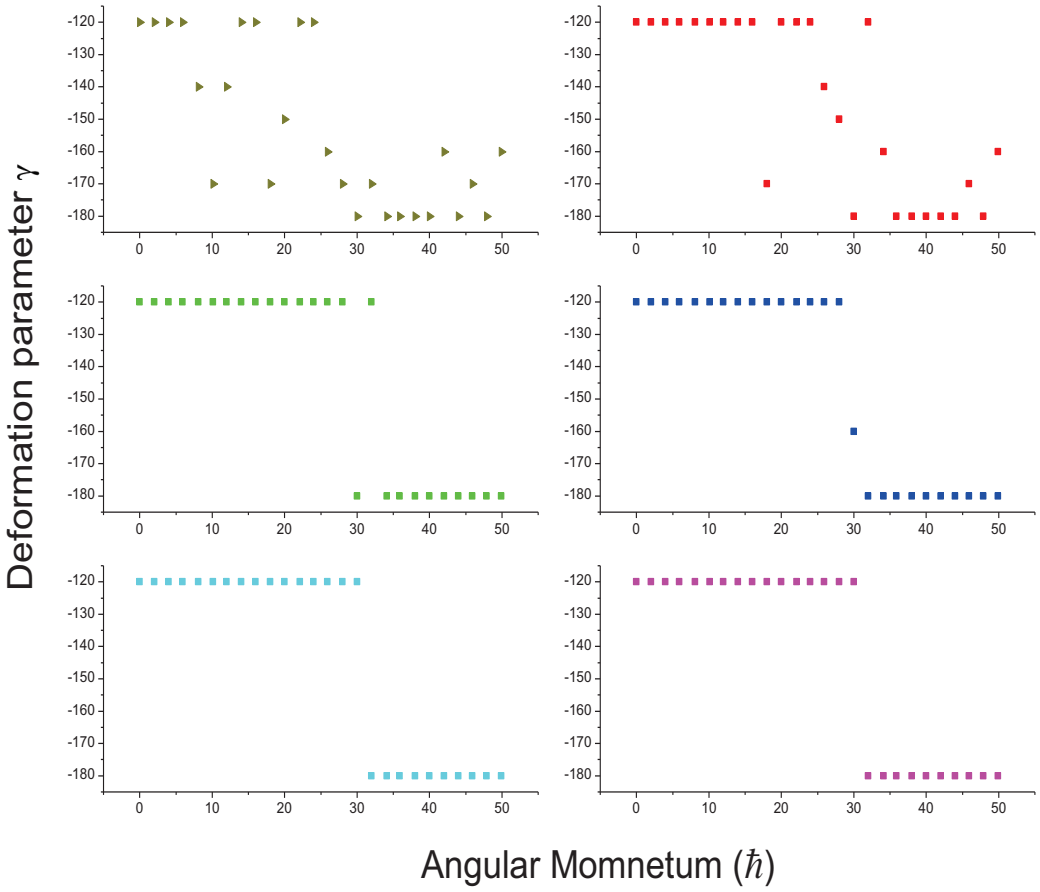


**FIG. 5.5: The deformation γ as a function of angular momentum I for the nuclei $^{94}$Sr**

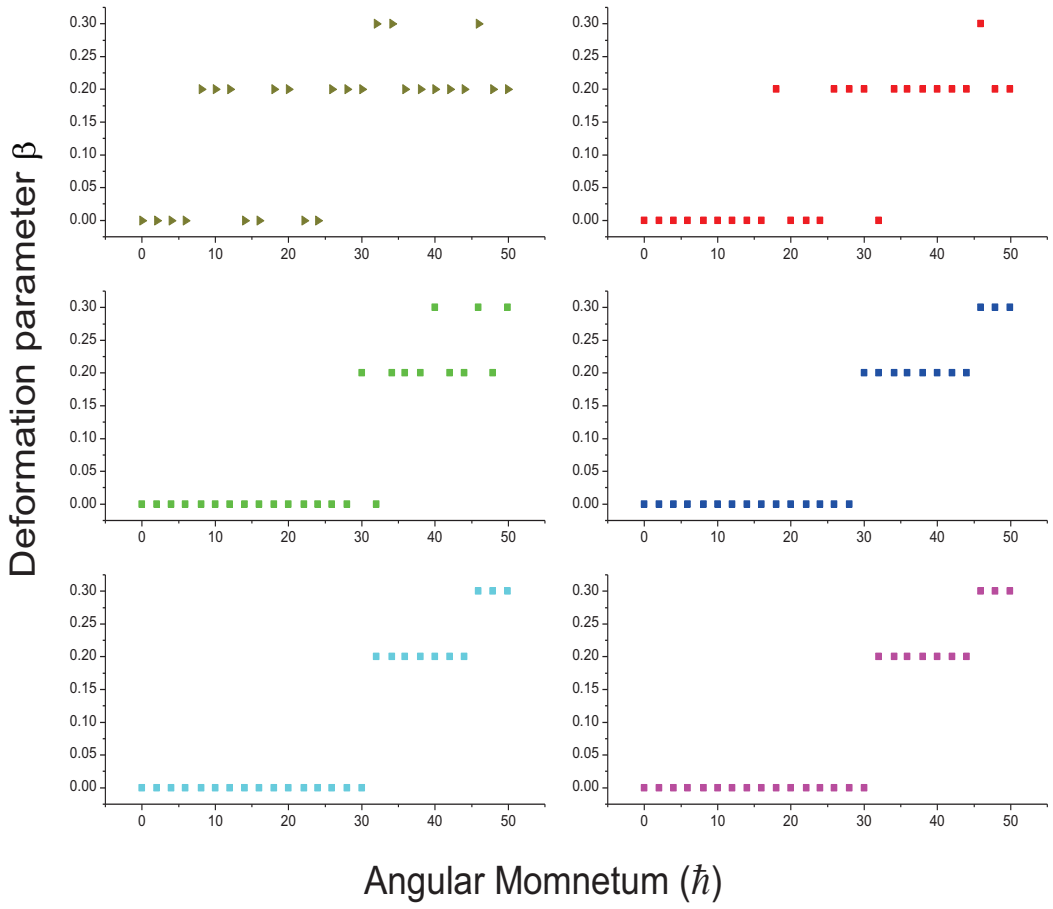


**FIG. 5.6: The deformation β as a function of angular momentum I for the nuclei $^{94}$Sr**

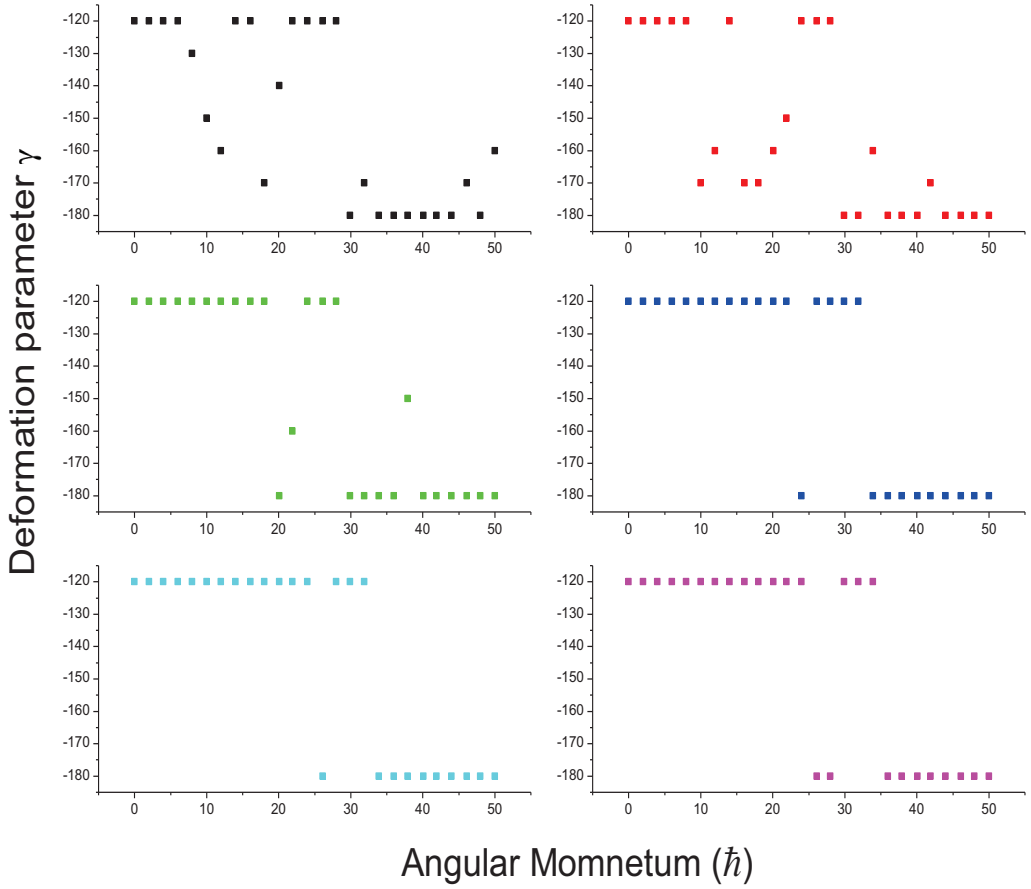


**FIG. 5.7: The deformation γ as a function of angular momentum I for the nuclei $^{96}$Sr**

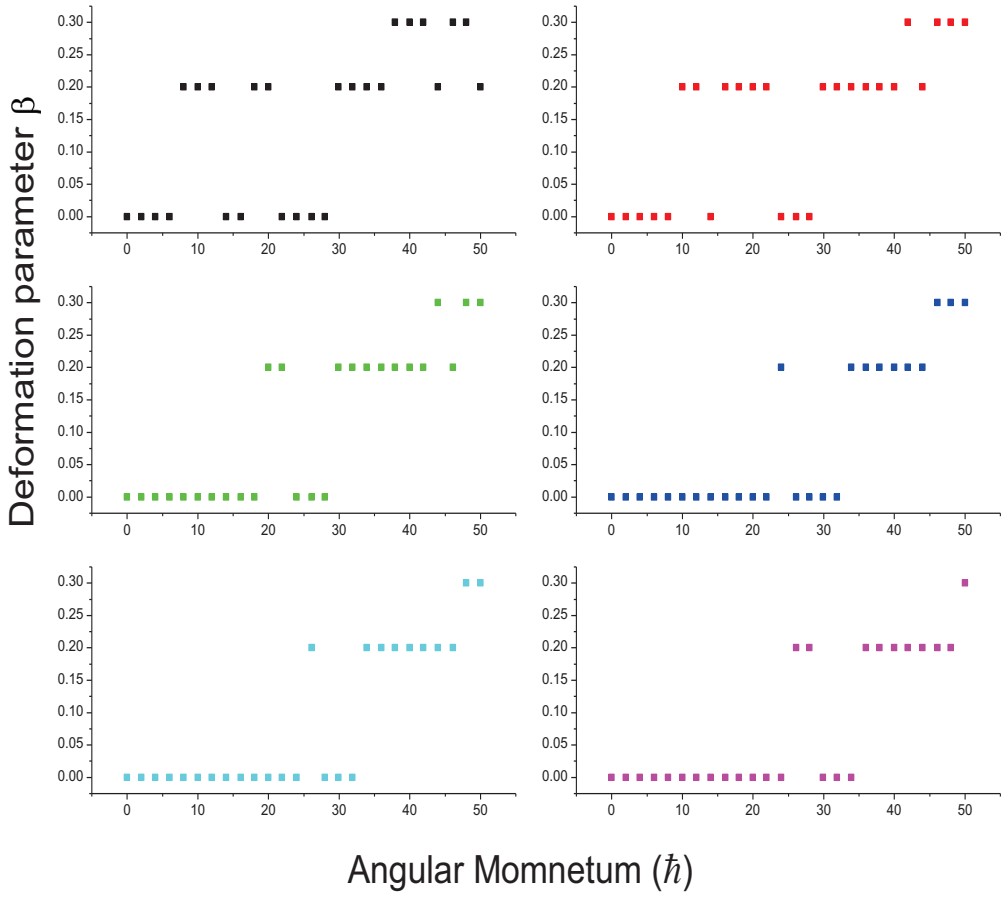


**FIG. 5.8: The deformation β as a function of angular momentum I for the nuclei $^{96}$Sr**

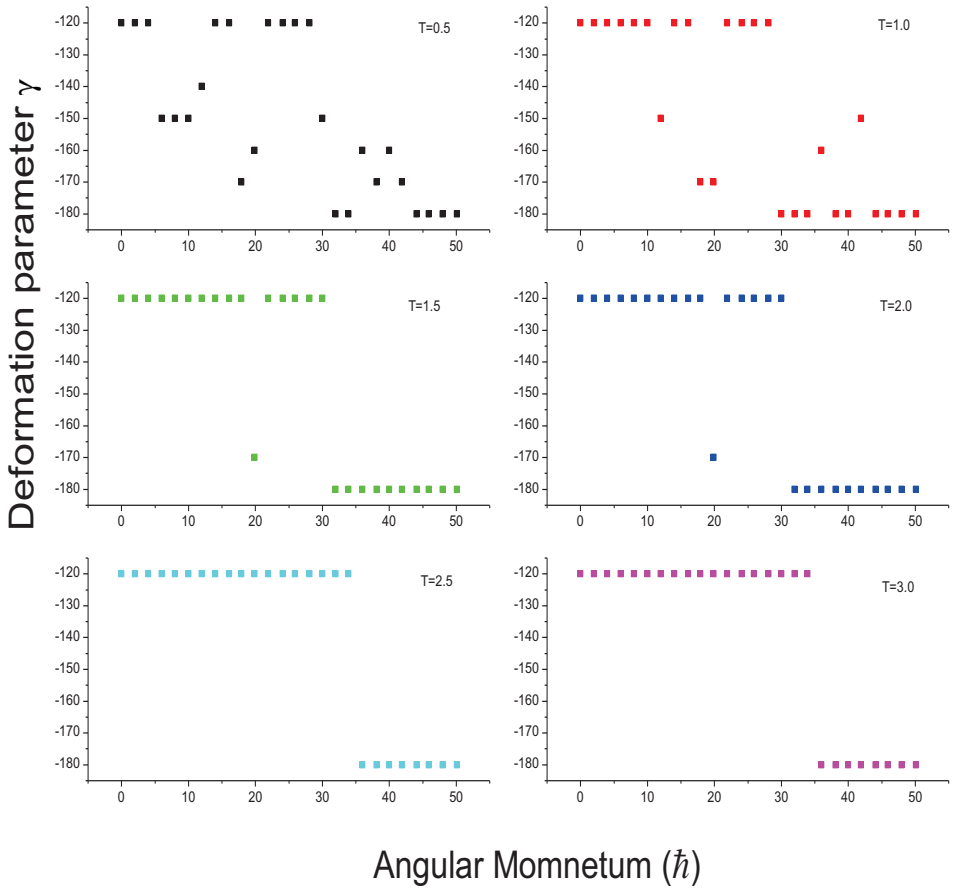


**FIG. 5.9: The deformation γ as a function of angular momentum I for the nuclei $^{98}$Sr**

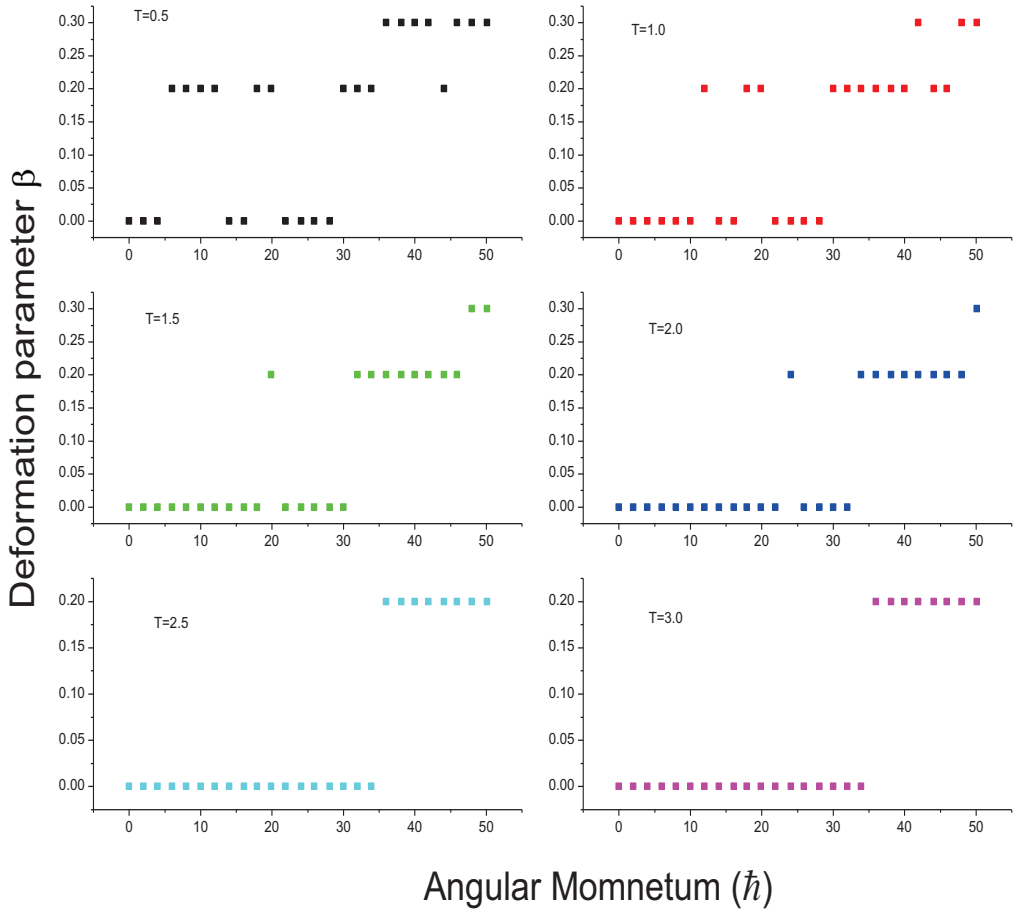


**FIG. 5.10: The deformation β as a function of angular momentum I for the nuclei $^{98}$Sr**

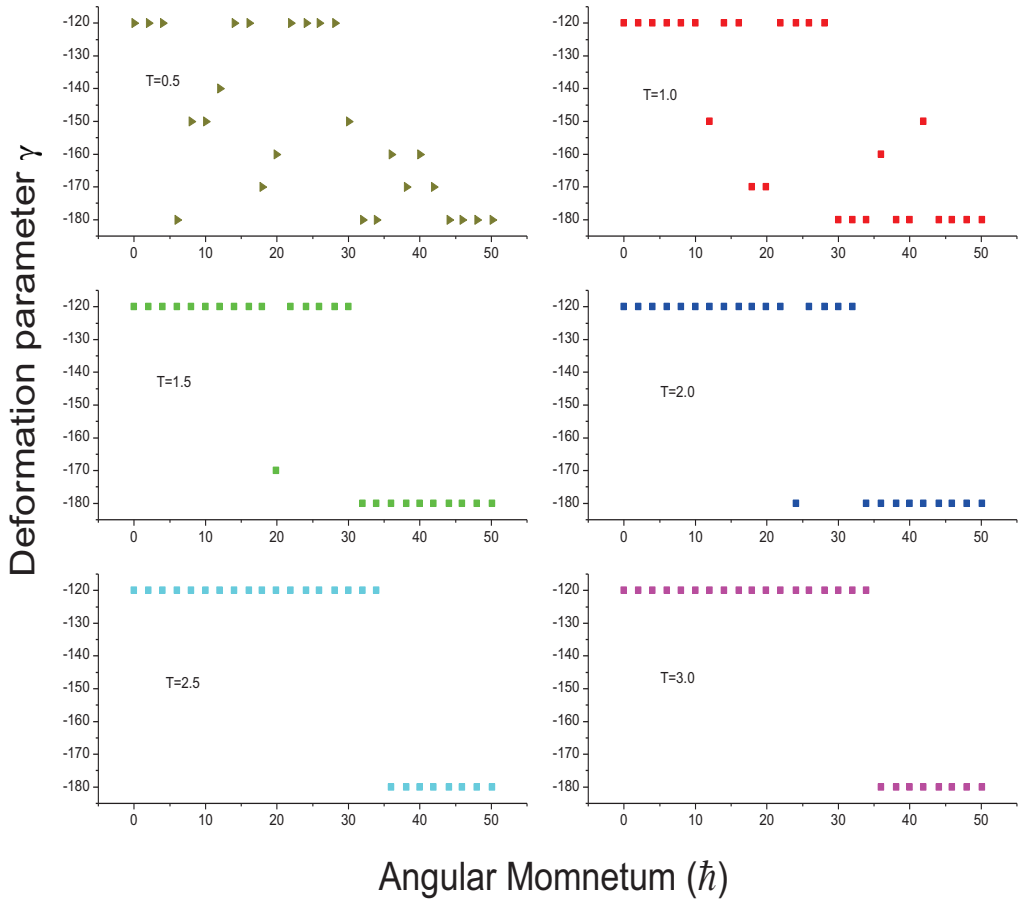


**FIG. 5.11: The deformation γ as a function of angular momentum I for the nuclei $^{100}$Sr**

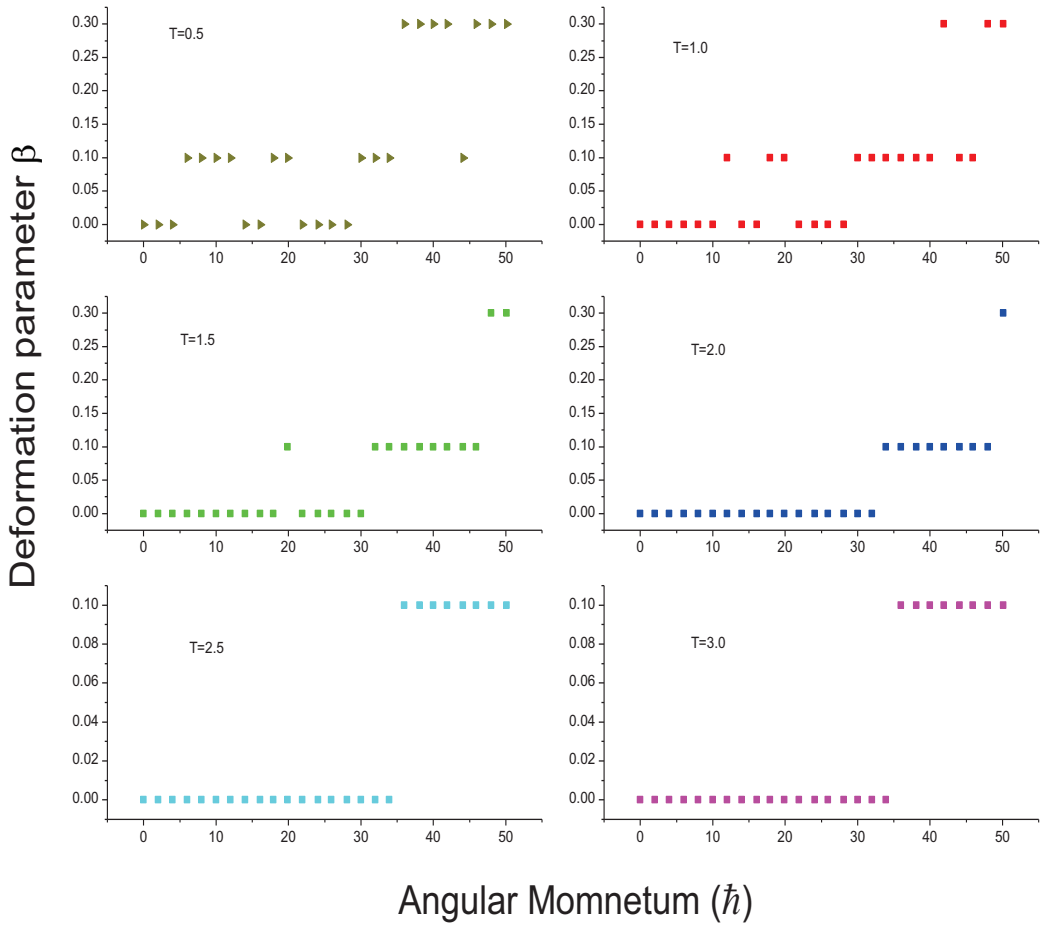


**FIG. 5.12: The deformation β as a function of angular momentum I for the nuclei $^{100}$Sr**

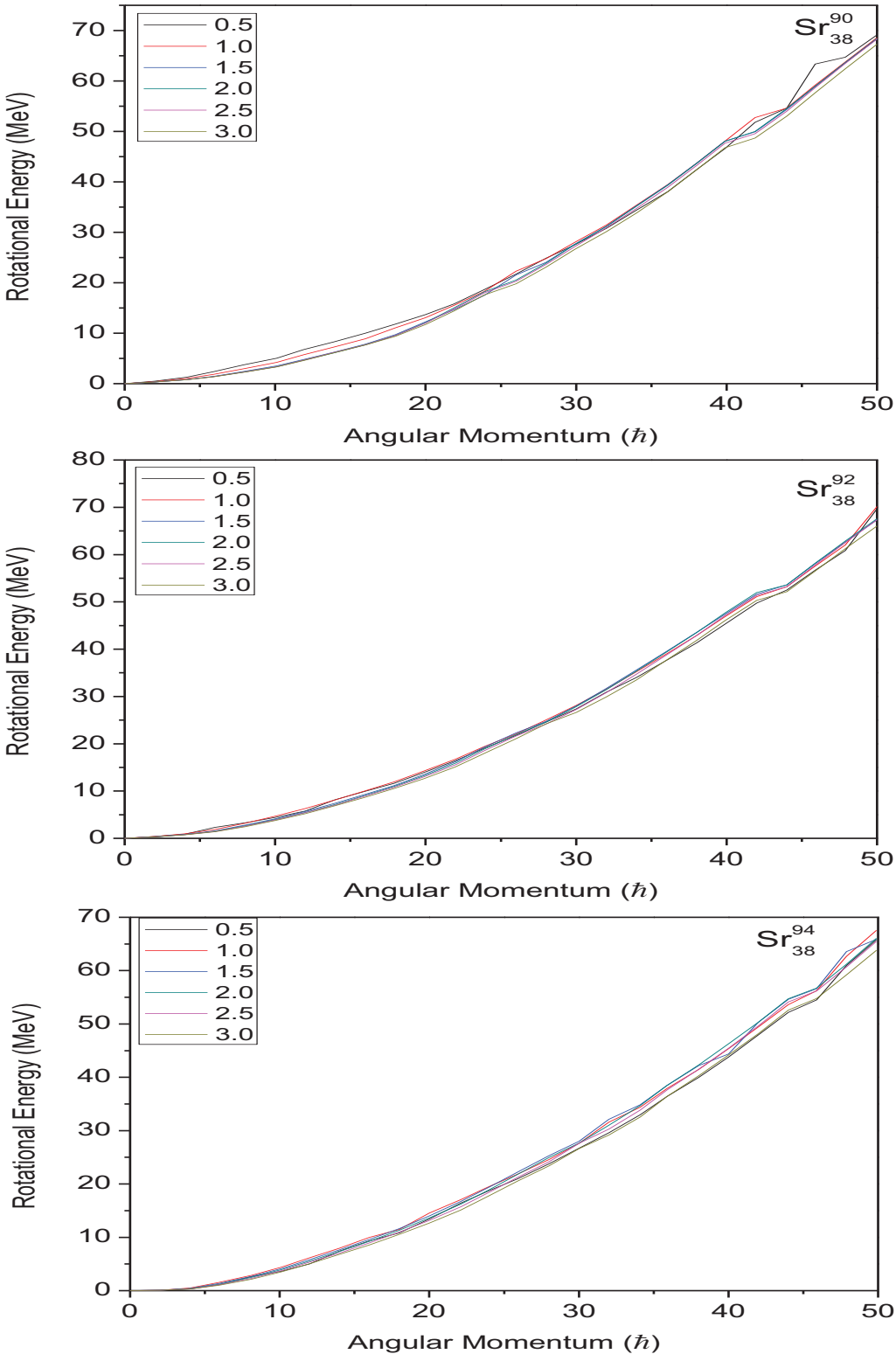


**Figure 5.13a-c:** **The rotational energy as a function of angular momentum for different temperature T for nuclei $^{90}$Sr, $^{92}$Sr and $^{94}$Sr**

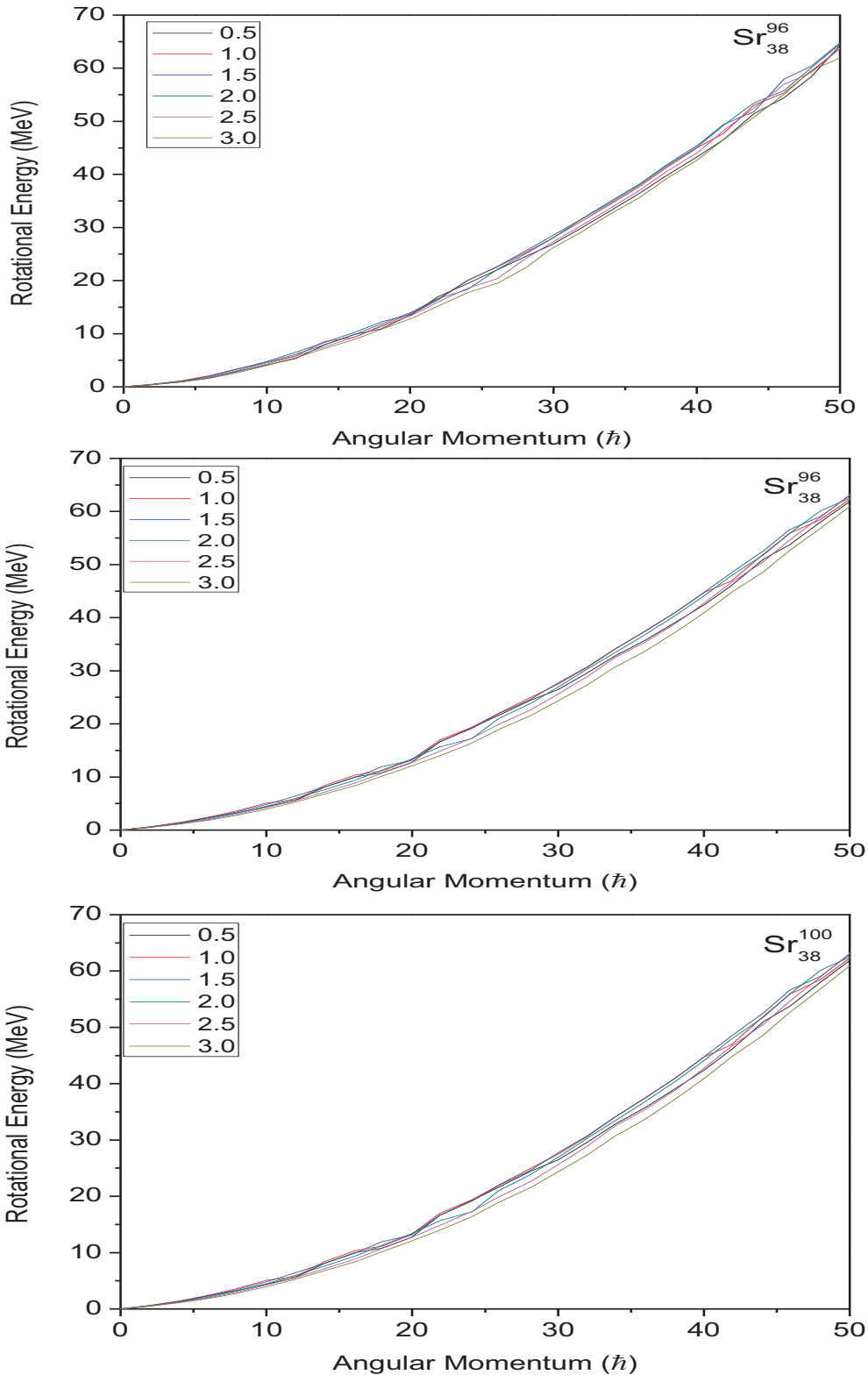


**Figure 5.14a-c: The rotational energy as a function of angular momentum for different temperature T for nuclei $^{96}$Sr, $^{98}$Sr and $^{100}$Sr**

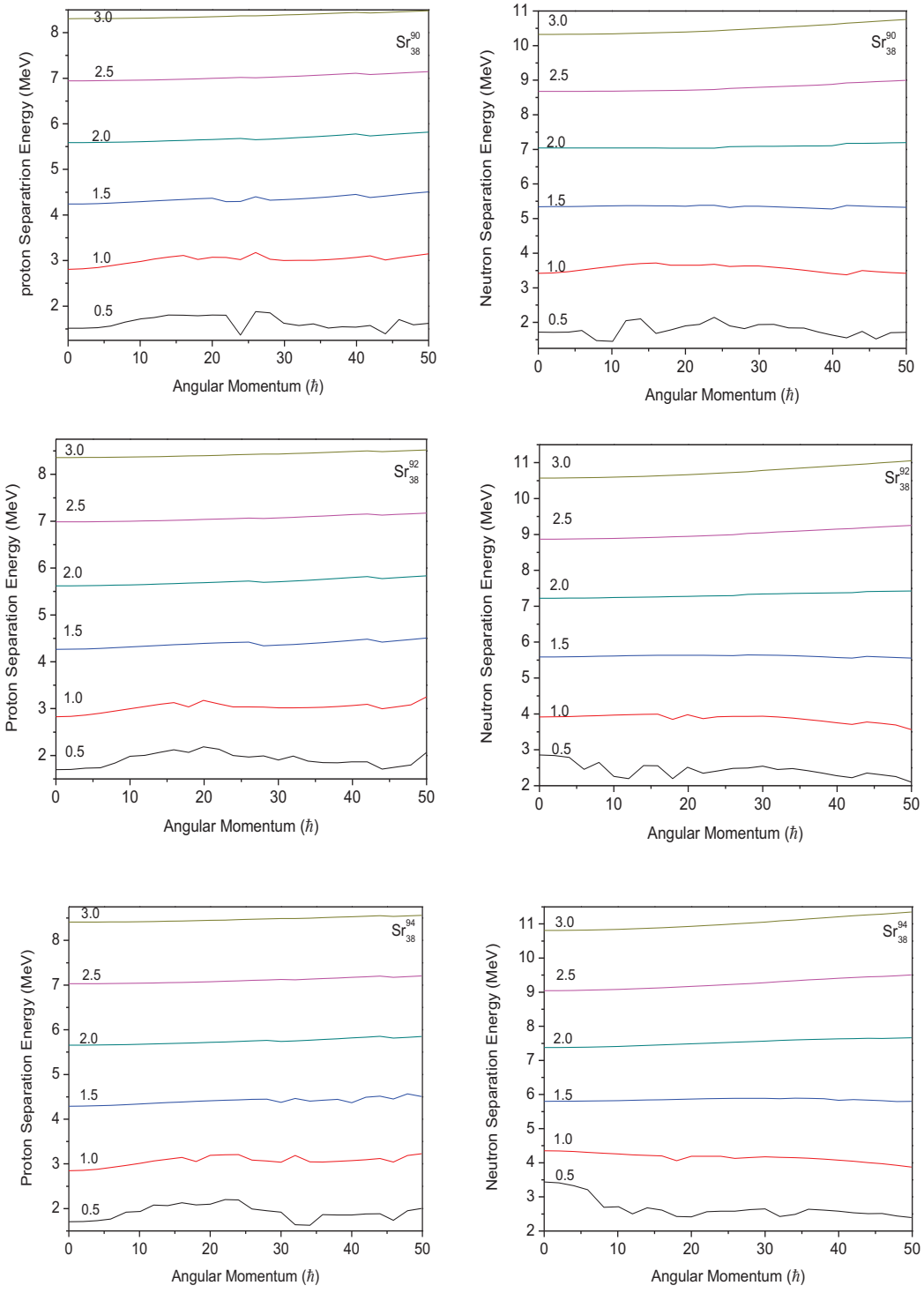


**Figure 5.15a-c: The proton and neutron separation energy as a function of angular momentum for different temperature T for $^{90}$Sr, $^{92}$Sr and $^{94}$Sr**

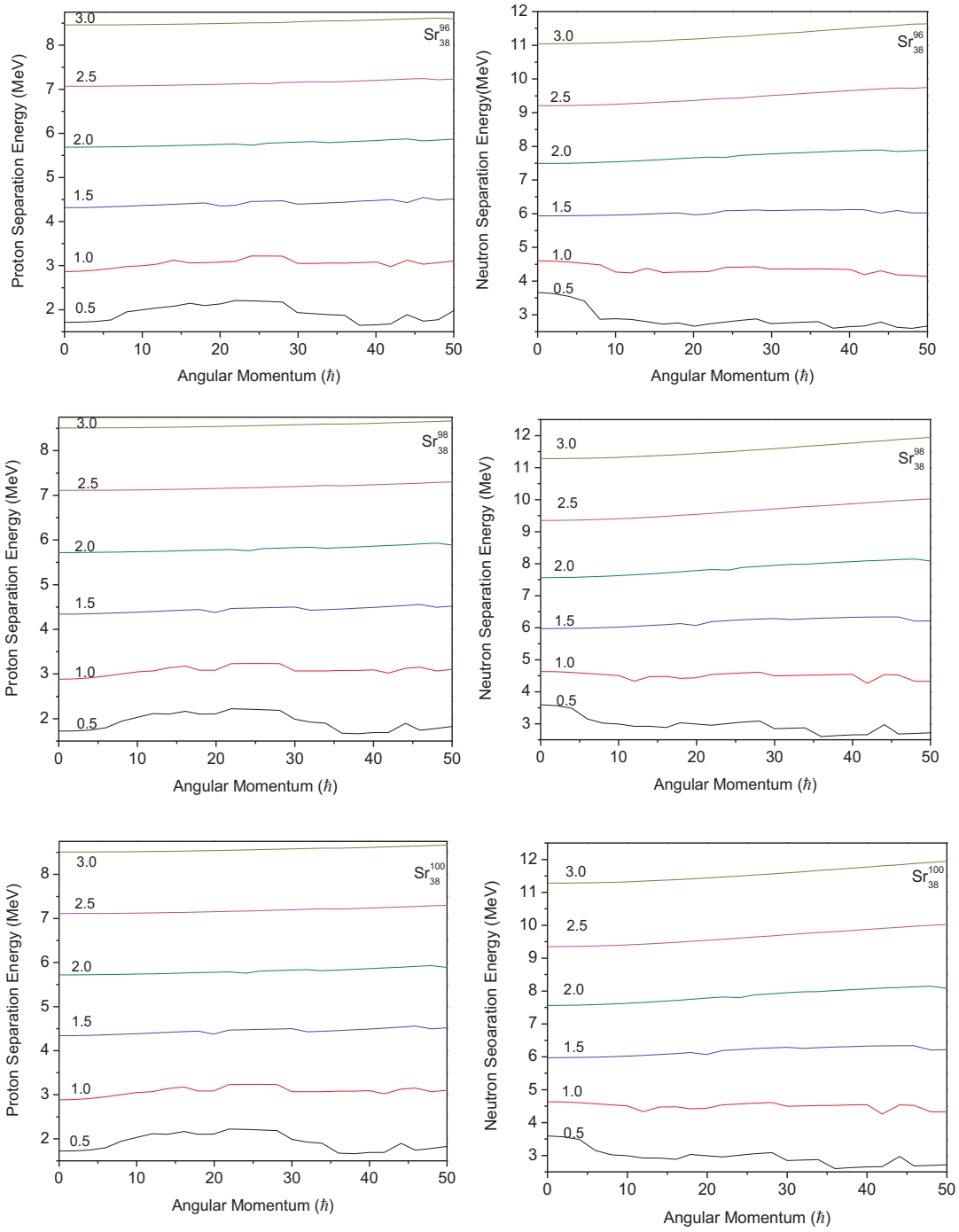


**Figure 5.16a-c: The proton and neutron separation energy as a function of angular momentum for different temperature T for $^{96}$Sr, $^{98}$Sr and $^{100}$Sr**

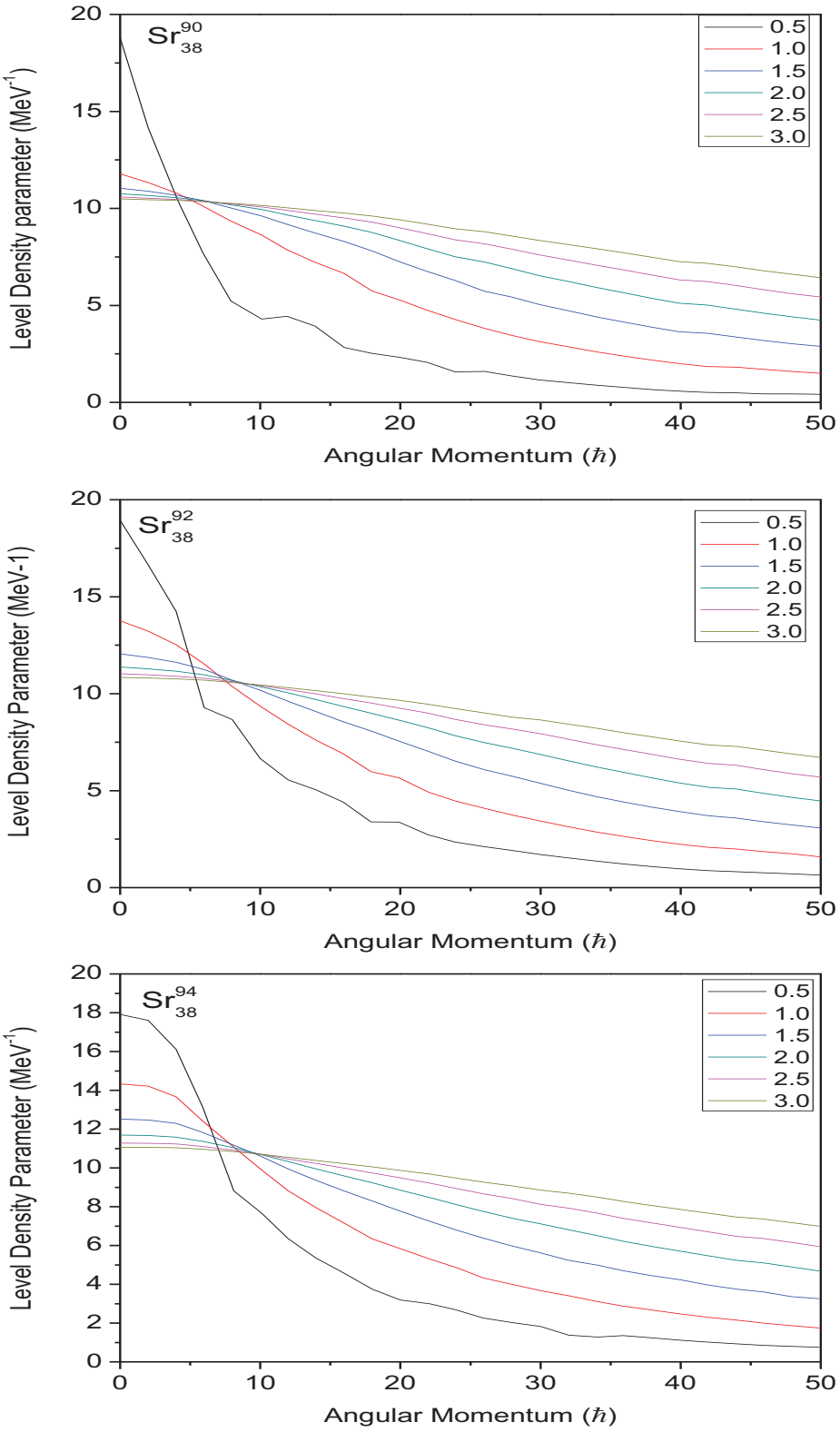


**Figure 5.17a-c: The level density parameter as a function of angular momentum for different temperature T for $^{90}$Sr, $^{92}$Sr and $^{94}$Sr**

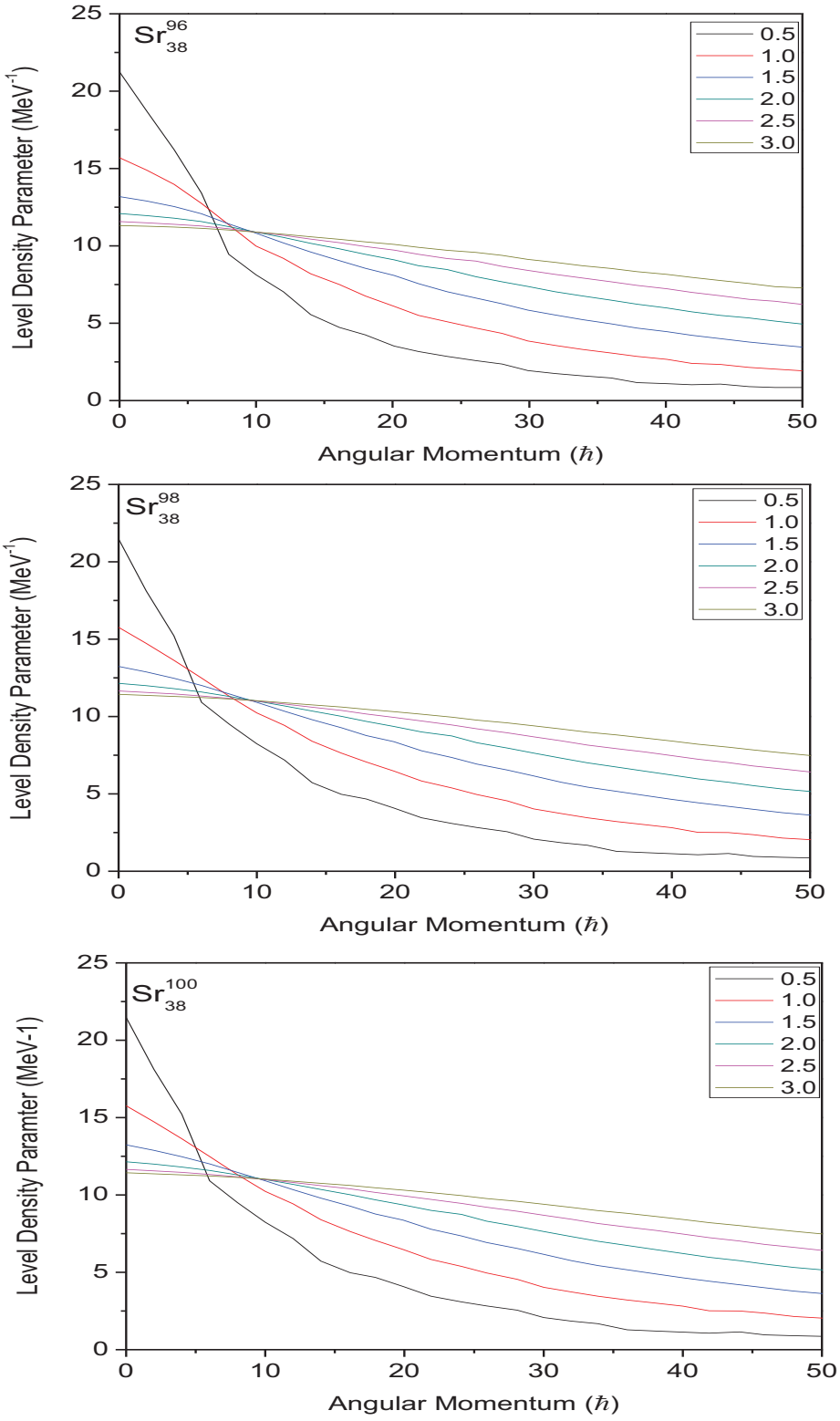


**Figure 5.18a-c: The level density parameter as a function of angular momentum for different temperature T for $^{96}$Sr, $^{98}$Sr and $^{100}$Sr**

## 5.3 Conclusion

In this chapter the structural properties of $^{90, 92, 94, 96, 98, 100}$Sr are investigated using statistical theory. The effect of interplay and competition between different degrees of freedom such as temperature, angular momentum and deformation on the structural properties are analyzed. The empirical relation a = A/8 could be reproduced by the investigation on the level density parameter. The shape transition from prolate collective to oblate at I = 30 and temperature T > 0.6 MeV is also observed. The influence of the temperature dependent effect such as the collapse of the shell correction has been observed at a critical temperature (≈ 1.5MeV) as is evident from the values of the level density parameter.

# CHAPTER VI

# STRUCTURAL STUDY ON SOME ODD –EVEN AND ODD-ODD NUCLEI AROUND A ~ 100 MASS REGION

## 6.1 Introduction

The atomic nucleus is an exceedingly convoluted quantum mechanical system comprising of many nucleons. It can embrace distinctive configurations according to the interacting forces between the nucleons. The most significant forces are the short-ranged attractive nuclear force between nucleons and the long-ranged repulsive Coulomb force between protons. The shell effects and pairing correlation also contribute to the determination of nucleonic configuration. Depending on the configurations, the atomic nuclei exhibit spherical, quadrupole, and higher order multipole deformed shapes. The major interest in this field of nuclear physics is the study of evolution of nuclear shape under extreme conditions of spin and temperature. The shape of an atomic nucleus determines the allowed excited energy levels of a nucleus and other nuclear properties. Current and future developments of more sophisticated nuclear models to explain the behavior of nuclear matter inside a nucleus depend on knowing nuclear shapes. Nuclear shapes can be determined by measuring the properties of the excited states in a nucleus. Most atomic nuclei have either spherical shapes or prolate for their ground states. In a few regions on the chart of the nuclides, for a given atomic number ($Z$), nuclei are found to change their ground-state shapes in a complex way from prolate shapes to oblate shapes (like a discus or thick pancake), or vice versa, as their neutron number increases. Both prolate and oblate shapes are axially symmetric, with two axes being equal.

The influence of the unpaired nucleon on the location and nature of shape transitions in odd-mass nuclei is an interesting issue. To study this, one needs to find adequate choice of the control and order parameters, empirical signatures of the phase transition, and possible candidates for critical point nuclei. The variety of shapes and structures, observed in A ~ 100 nuclei, have been discussed in view of different angular momentum coupling schemes and their interplay that comes into effect at high spin.

Shape transition in odd nuclei are much less studied in comparison with the even-even ones, the main reason being the large diversity of the low-energy excitations, which makes it impossible to follow the evolution of the same quantity in many nuclei. It is a very interesting issue to determine how the unpaired fermion influences on the nature and the location of the phase transition. In the present study the Shape transitions in odd-even and odd-odd nuclei around A ~ 100 are investigated within the framework of the statistical model [Pinston 2005, Shizuma 1984, Dara 2015 Wadsworth 2009].

**6.2 Result and Discussion**

The Fig. 6.1 and 6.2 shows the equilibrium shape of the system is determined by minimizing the free energy with respect to the deformation parameters $\beta$and$\gamma$, as a function of angular momentum for different temperature for the nuclei $^{98}Rb_{37}$. It is observed from Fig. 6.1 and 6.2 (T = 0.5MeV) that the nucleus is found to be deformed ($\beta$ = 0.2 and $\gamma = -180°$) for the angular-momentum range M = 0 ħ to 2ħ, above 2ħ the nucleus is in triaxial shape up to 12ħ, 14-22ħ the nucleus reaches the spherical shape. For the angular momentum 24 & 26ħ the nucleus again found to be deformed and

non-collective oblate shape ($\beta = 0.2$ and $\gamma = -180°$). At the angular momentum 30 and 32ħ, the nucleus reaches the spherical shape. Above 34ħ the nucleus found to be deformed and non-collective oblate shape. For T = 1.0MeV the nucleus remains at spherical shape with $\beta = 0.0$ and $\gamma = -120°$ for the angular- momentum range M = 0 to 8ħ, triaxial ($\beta = 0.2$ and$\gamma = -180°$ for M = 10 and $\beta = 0.0$ and$\gamma = -120°$ for M = 12 &14ħ,$\beta = 0.0$ and $\gamma = -120°$ for M = 18-24ħ, $\beta = 0.2$ and $\gamma = -180°$ for M = 26&28ħ and $\beta = 0.0$ and$\gamma = -120°$ for M = 30&32ħ, it reaches the oblate shape for M = 34 to 50ħ ($\beta = 0.3$ and$\gamma = -180°$). Above T = 1.0 MeV the nuclei undergoes a shape transition from collective prolate to oblate shape(M= 34ħ for T=1.5MeV, M= 34ħ for T=2.0MeV, M= 34ħ for T=2.5MeV and M= 34ħ for T=3.4MeV)

Figure 6.3 and 6.4 shows minimized free energies as a function of deformation variable $\beta$ and $\gamma$ for different angular momentum and temperatures $^{99}Rb_{37}$. The evolution of the different minima as a function of deformation and spin is detailed below:

At angular momentum 0-4ħ, it is found that in $^{99}Rb_{37}$ takes a deformed non-collective oblate shape with $\varepsilon = 0.2$ and $\gamma = -180°$. The fluctuation around the angular momentum 6ħ corresponds to the deformation change $\gamma$= -180° to -140°. For the angular-momentum range M = 8ħ to 10ħ, the nucleus is in non-collective oblate shape with $\beta$= 0.2. Beyond 10ħ the total energy minima moved to spherical shape with $\beta$ = 0.0 up to angular momentum value 20ħ. From 22 to 20ħ the nucleus moves to deformed shape with $\beta$= 0.3 and 0.2. At angular momentum 30, again attains the spherical shape and above 30ħ it reaches deformed shape with $\beta$= 0.3 and 0.2. As the

temperature increases (above 1.5MeV) and at low angular momentum (below 30ħ) the nucleus move from deformed to spherical shape. Above the critical angular momentum (around 30ħ) the spherical minimum moves gradually to deformed shape.

Similar behavior is observed for $^{100}Rb_{37}$ and $^{99}Y_{39}$, as evident from Fig. 6.5 – 6.8. These changes in the shape of the nuclei suggest an impression that interplays among angular momentum, temperature and deformation is responsible for the observed behavior of the nuclei.

The rotational energy of the nucleus $^{98}Rb_{37,}$ $^{99}Rb_{37.}$ $^{100}Rb_{37}$ and $^{99}Y_{39}$ as a function of angular momentum for different temperature was plotted in Fig.6.9-6.10. Figure 6.9 shows the rotational energy at low temperature is higher than the high temperature at low angular momentum. However at high angular momentum the rotational energy for high temperature is higher than the low temperature. The rotational energy increases with angular momentum and temperature. The fluctuation in rotational energy at low temperatures is due to the shape transition takes place in the nucleus. The occurrence of shape transition beyond temperature T = 1.5MeV is almost at a particular spin (J ≈ 30h) and hence the role of temperature in the shape transition beyond T = 1.5MeV is relatively negligible.

The single particle level density parameter 'a' as a function of temperature T and angular momentum are presented in Figs. 6.11 and 6.12 for the nuclei $^{98}Rb_{37,}$ $^{99}Rb_{37.}$ $^{100}Rb_{37}$ and $^{99}Y_{39}$. The effect of rotation on the single particle level density parameter is very pronounced at low temperatures. At low temperatures the shell structure plays a major role in the determination of the level density parameter. From the shell correction point of view a lower value of 'a' indicates relatively greater

stability of the system. The single particle level density parameter 'a' shows a linear behaviour for the temperature greater than 0.5 MeV [28]. At higher temperature (T > 0.5MeV), our results reproduce usual empirical value of the single particle level density parameter i.e., one tenth or one eighth of the mass number (A/8 or A/10). In Fig. 6.11, the single particle level density parameter 'a' is plotted versus angular momentum for temperatures ranging from 0.5 to 3.5 MeV. However, for high spins there is a general tendency for 'a' to have a value lower than the ones for lower spins. Another important aspect of these curves is that they have been drawn after minimizing the free energy of the system with respect to the deformation parameter.

The calculated single-neutron separation energy SN versus temperature T is plotted for various angular momenta I in fig. 6.13a and proton separation energy SZ in fig. 6.13b for the nucleus $^{98}Rb_{37,}$ $^{99}Rb_{37.}$ Fig. 6.14a shows the neutron separation energy SN and fig. 6.14b shows the proton separation energy SZ for the nucleus $^{100}Rb_{37}$ and $^{99}Y_{39}$. Figures shows fluctuation in proton and neutron separation energies at low temperatures, it may be due to effect of rotation at low temperatures where shell effects play a very important role. At higher temperatures for T >1.0MeV, these fluctuations disappear and the energy values become almost constant due to the absence of shell effects. At high temperature the proton and the neutron separation energy becomes almost constant, the particle emission get saturated even if the temperature is increased, and the shape evolution get started slowly. Our calculations show that the proton separation energy almost constant with increasing spin.

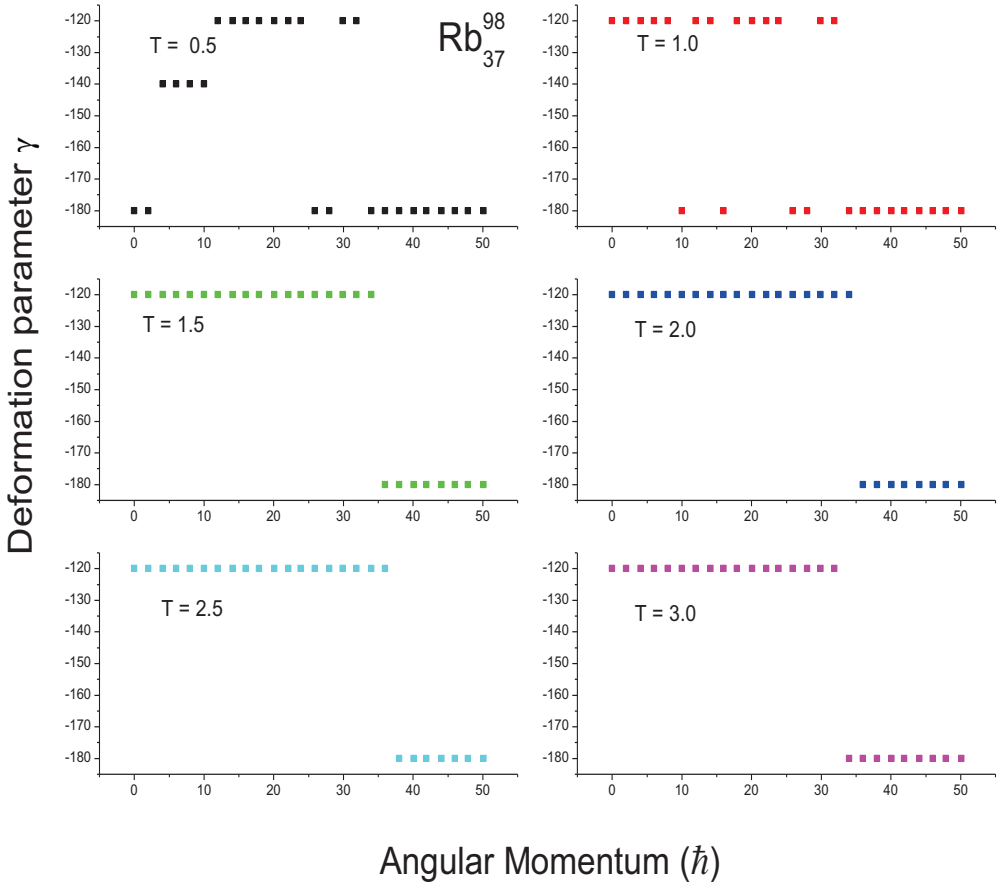


**FIG. 6.1: The deformation γ as a function of angular momentum I for the nuclei $^{98}Rb_{37}$**

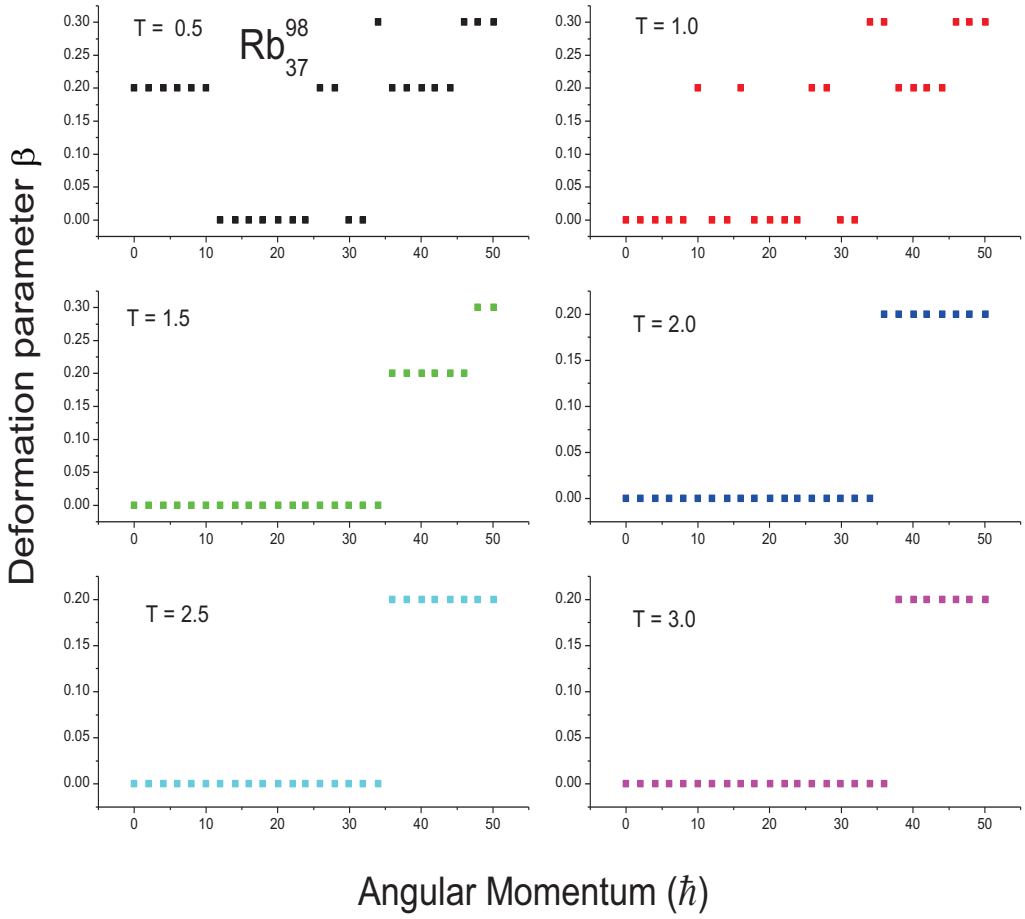


**FIG. 6.2: The deformation β as a function of angular momentum I for the nuclei $^{98}Rb_{37}$**

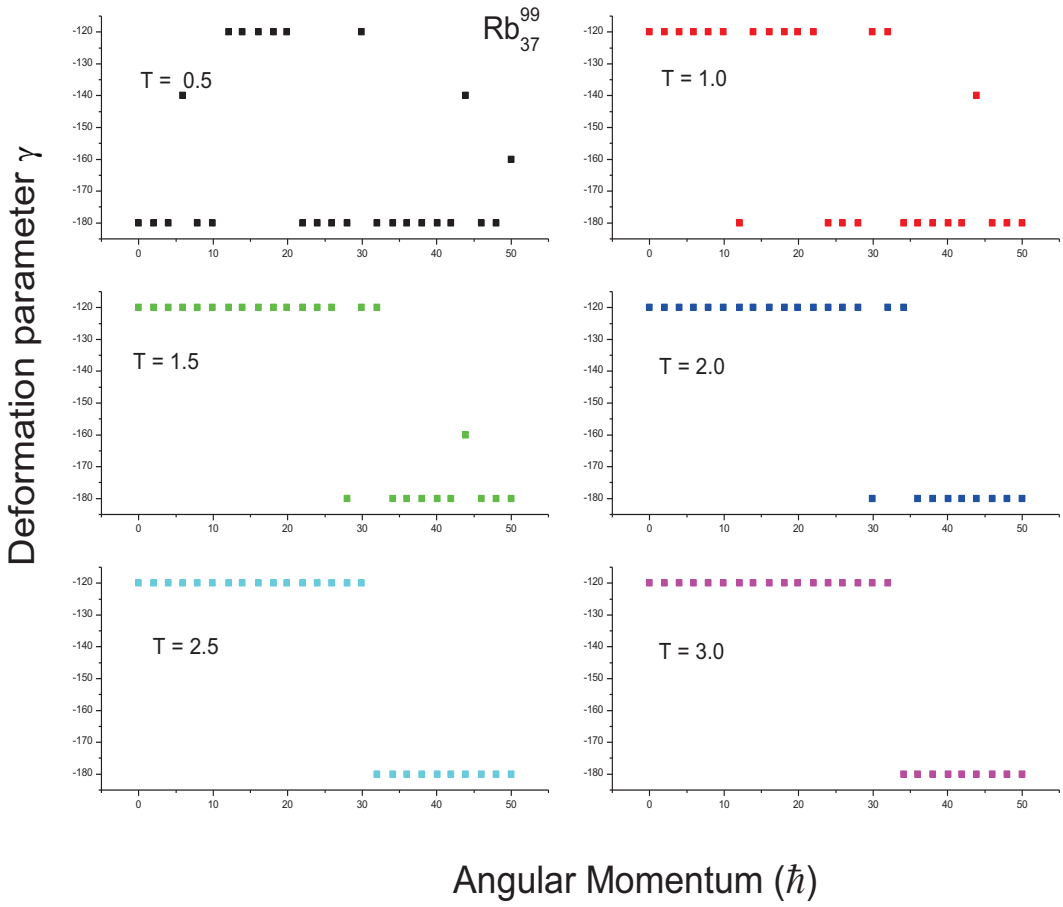


**FIG. 6.3: The deformation γ as a function of angular momentum I for the nuclei $^{99}Rb_{37}$**

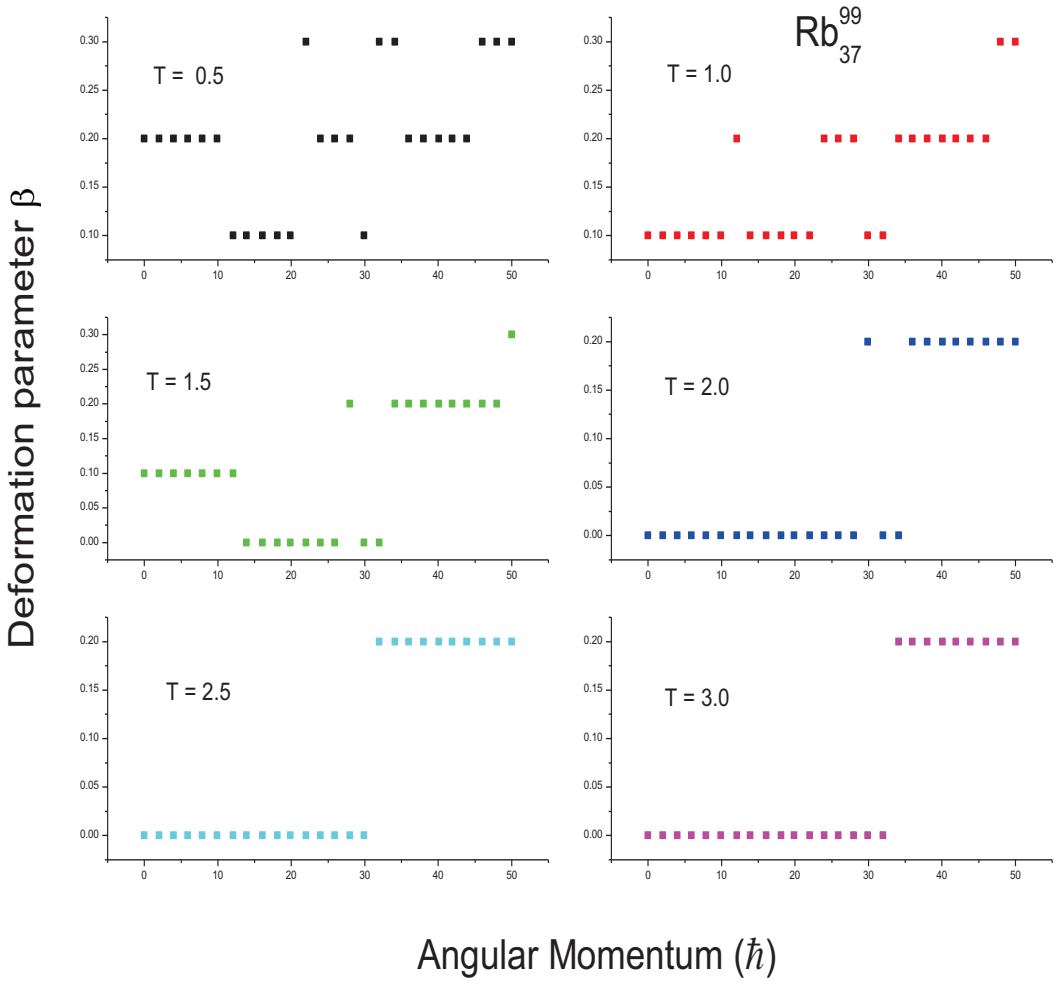


**FIG. 6.4: The deformation β as a function of angular momentum I for the nuclei $^{99}Rb_{37}$**

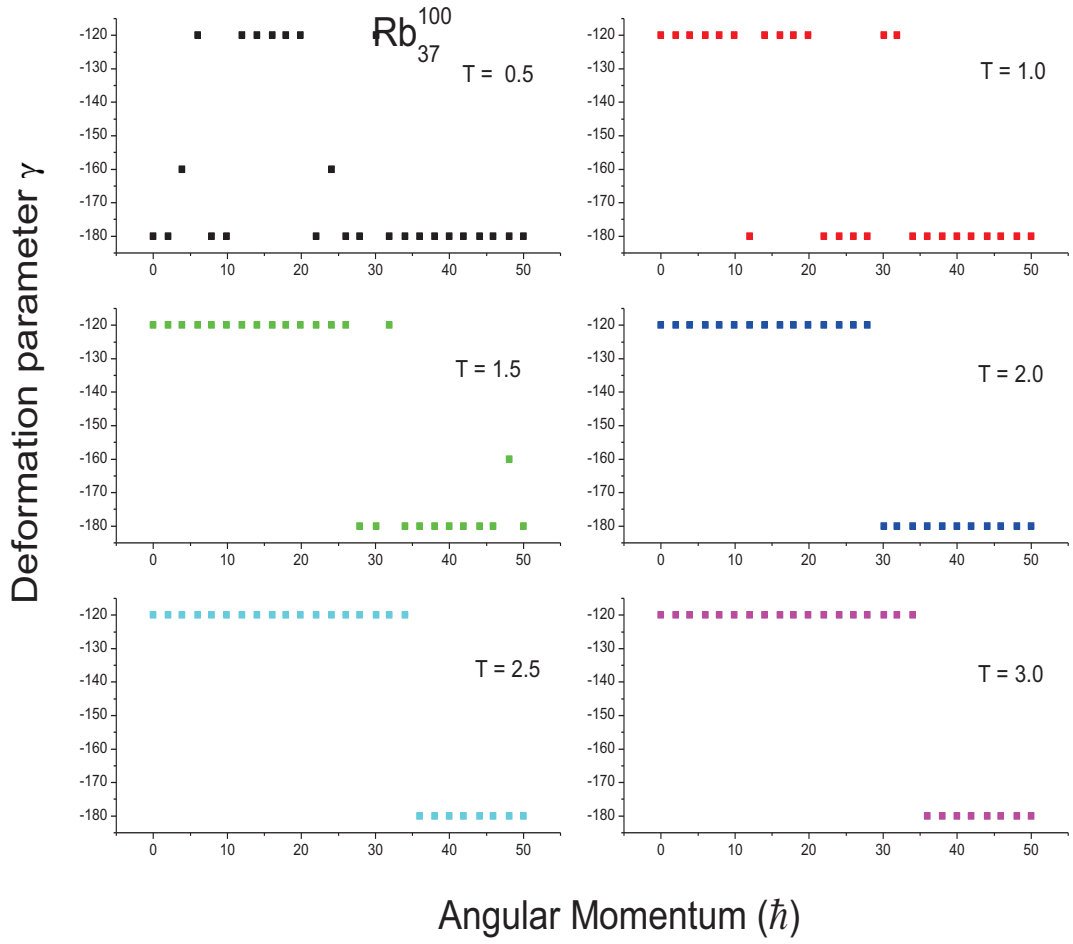


**FIG. 6.5:** **The deformation γ as a function of angular momentum I for the nuclei $^{100}Rb_{37}$**

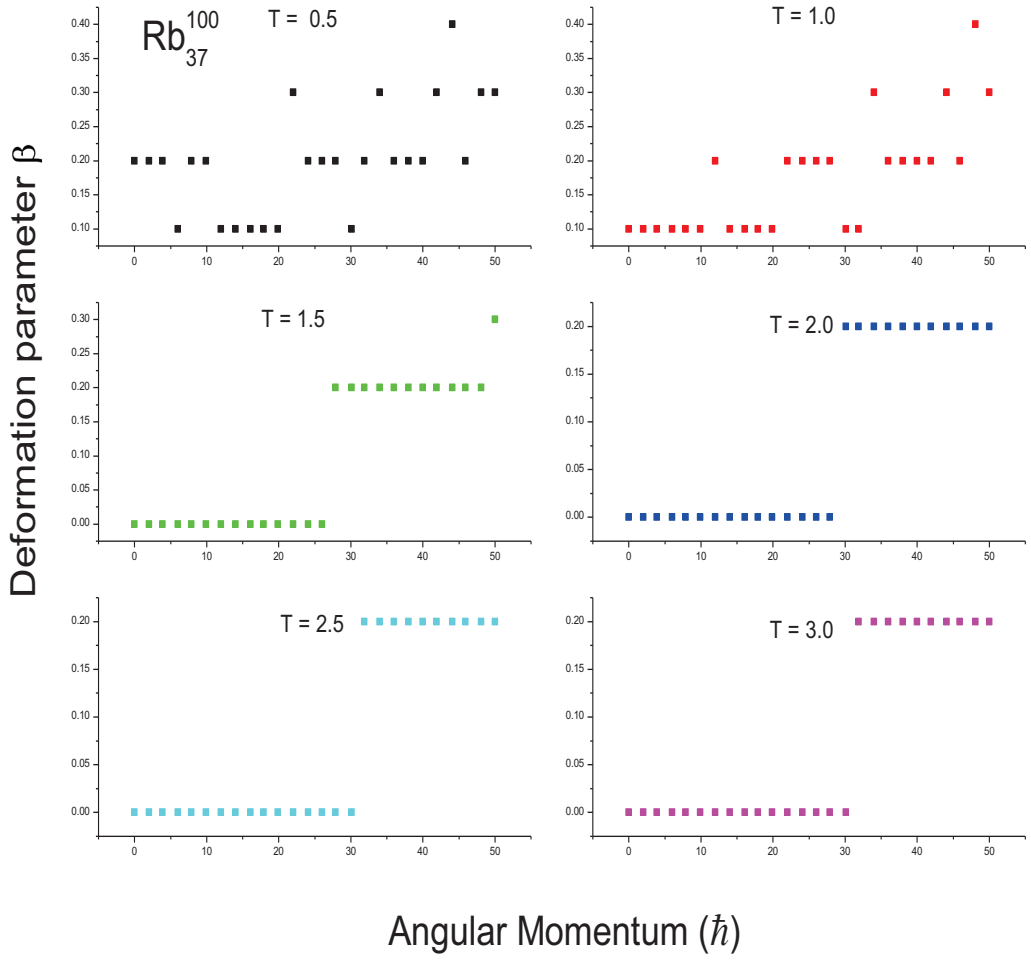


**FIG. 6.6: The deformation β as a function of angular momentum I for the nuclei $^{100}Rb_{37}$**

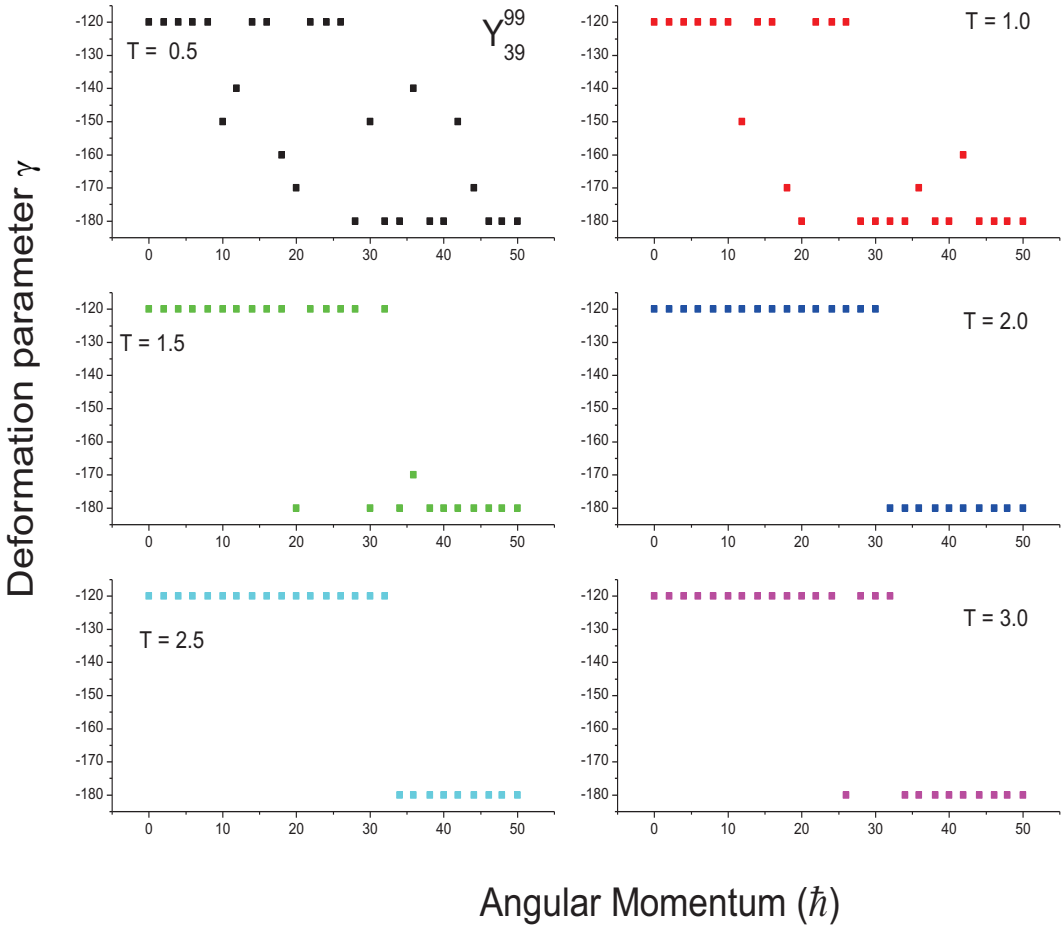


**FIG. 6.7: The deformation γ as a function of angular momentum I for the nuclei $^{99}Y_{39}$**

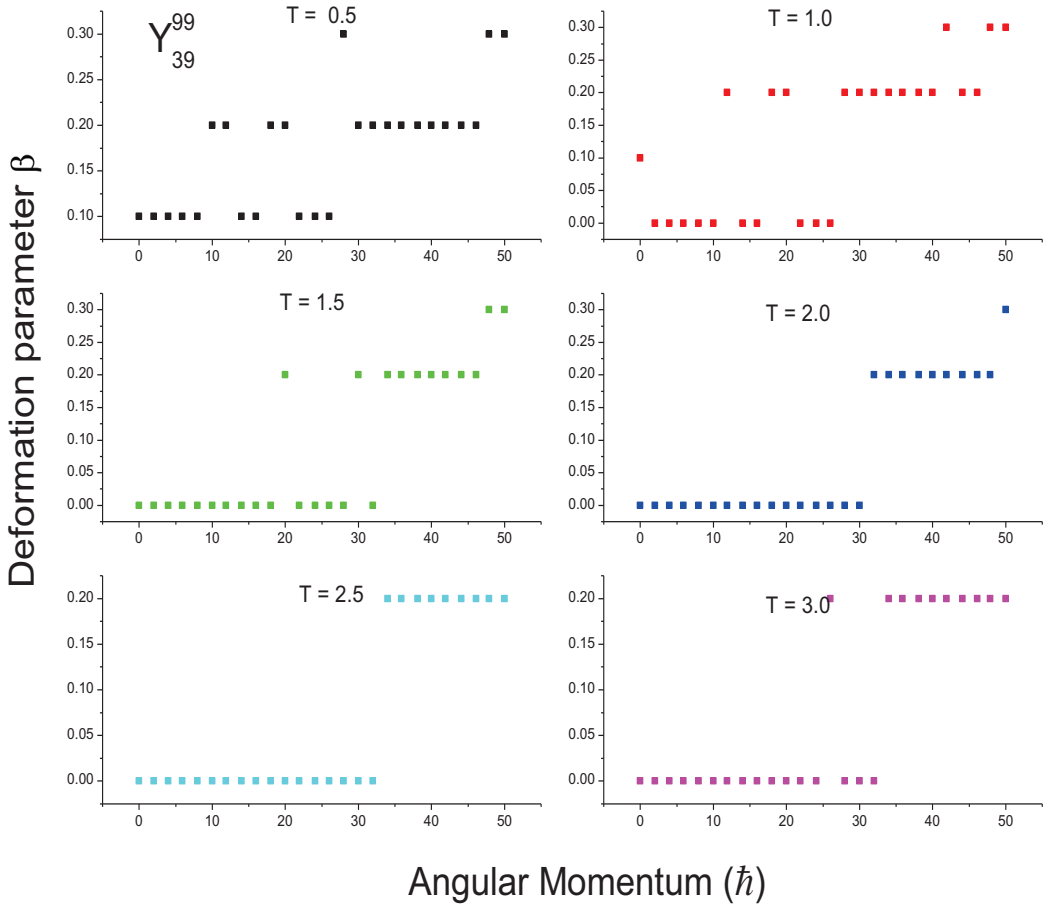


**FIG. 6.8: The deformation β as a function of angular momentum I for the nuclei $^{99}Y_{39}$**

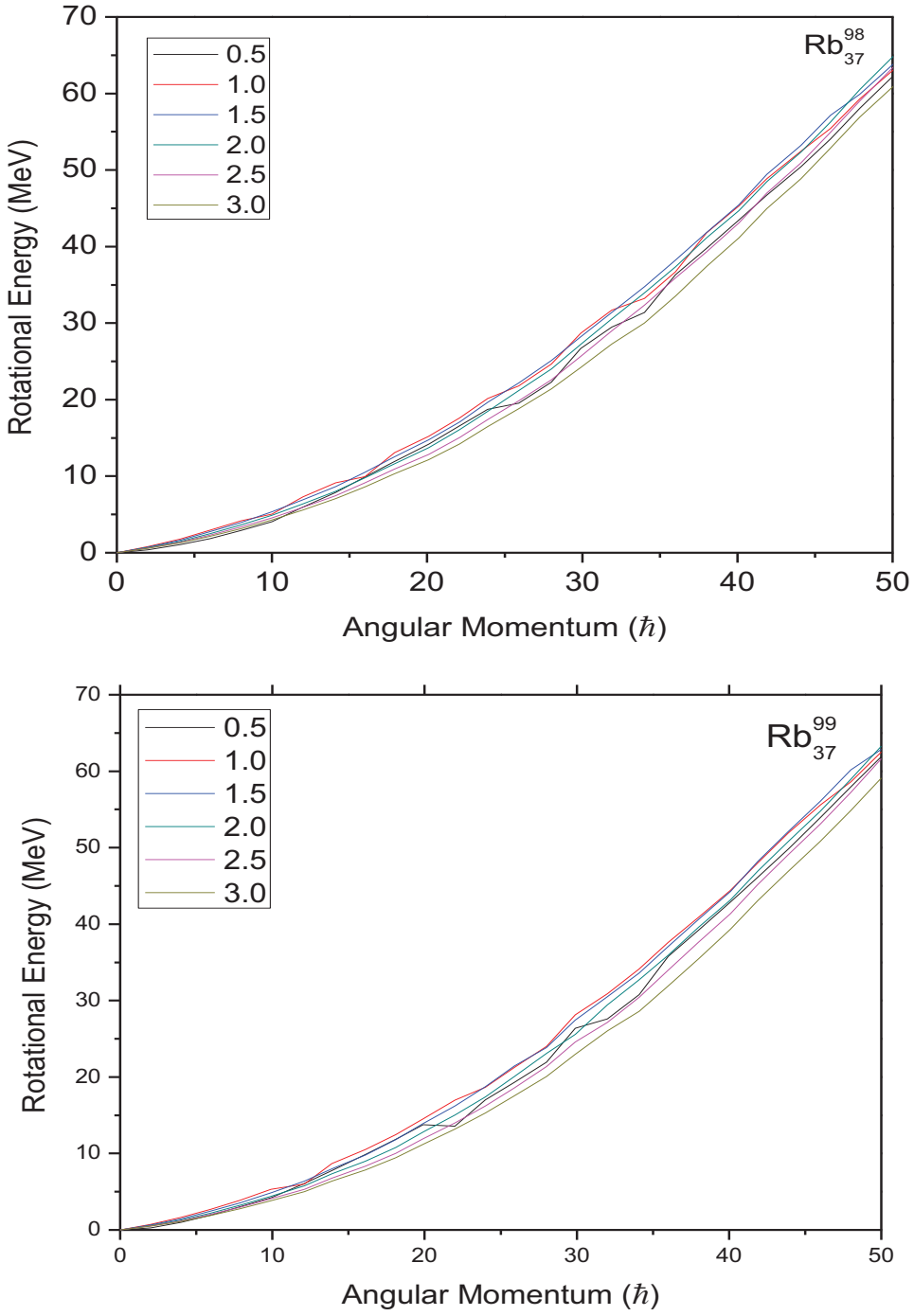


**Figure 6.9: The rotational energy as a function of angular momentum for different temperature T for $^{98}Rb_{37}$and $^{99}Rb_{37}$**

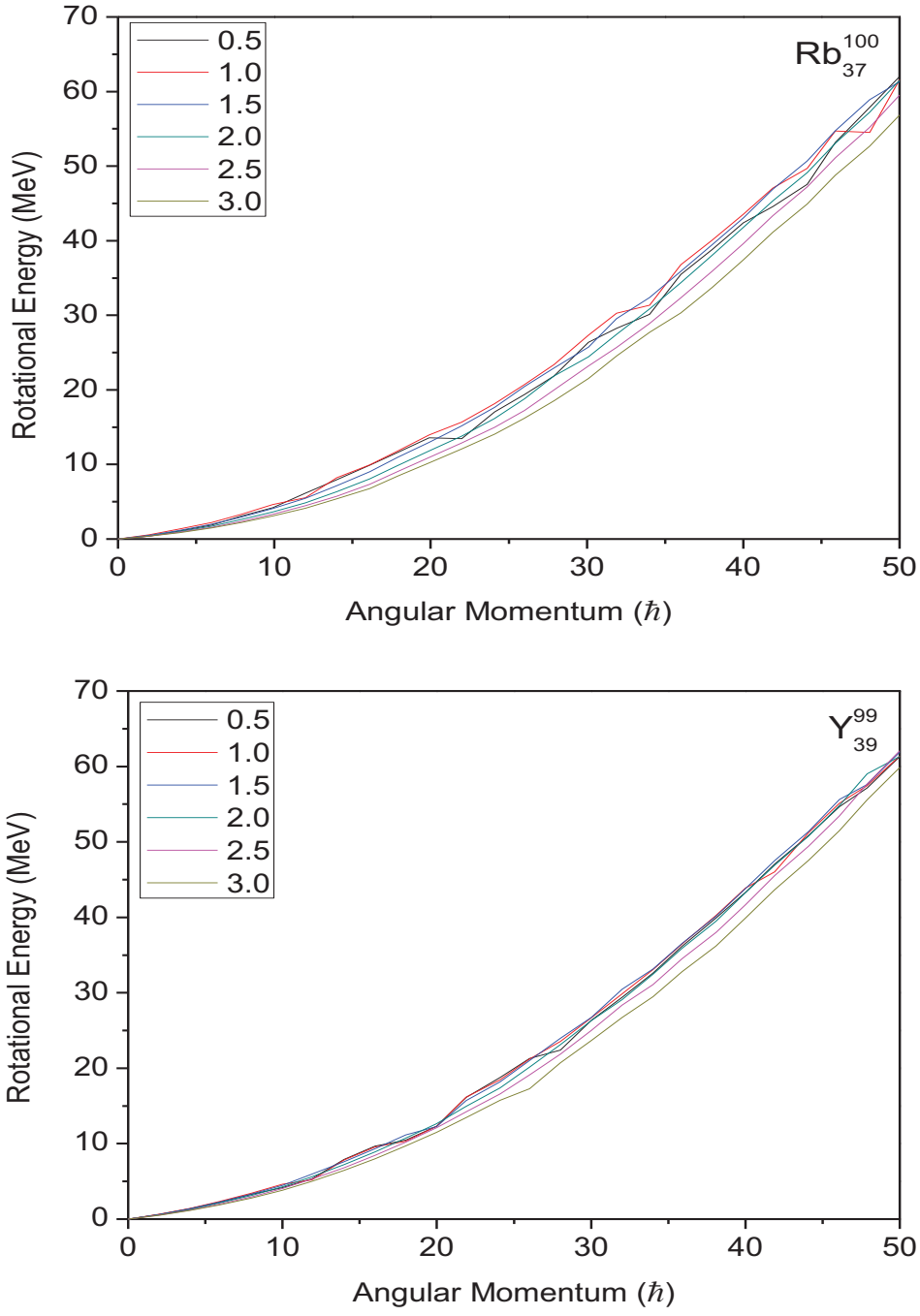


**Figure 6.10: The rotational energy as a function of angular momentum for different temperature T for $^{100}Rb_{37}$and$^{99}Y_{39}$**

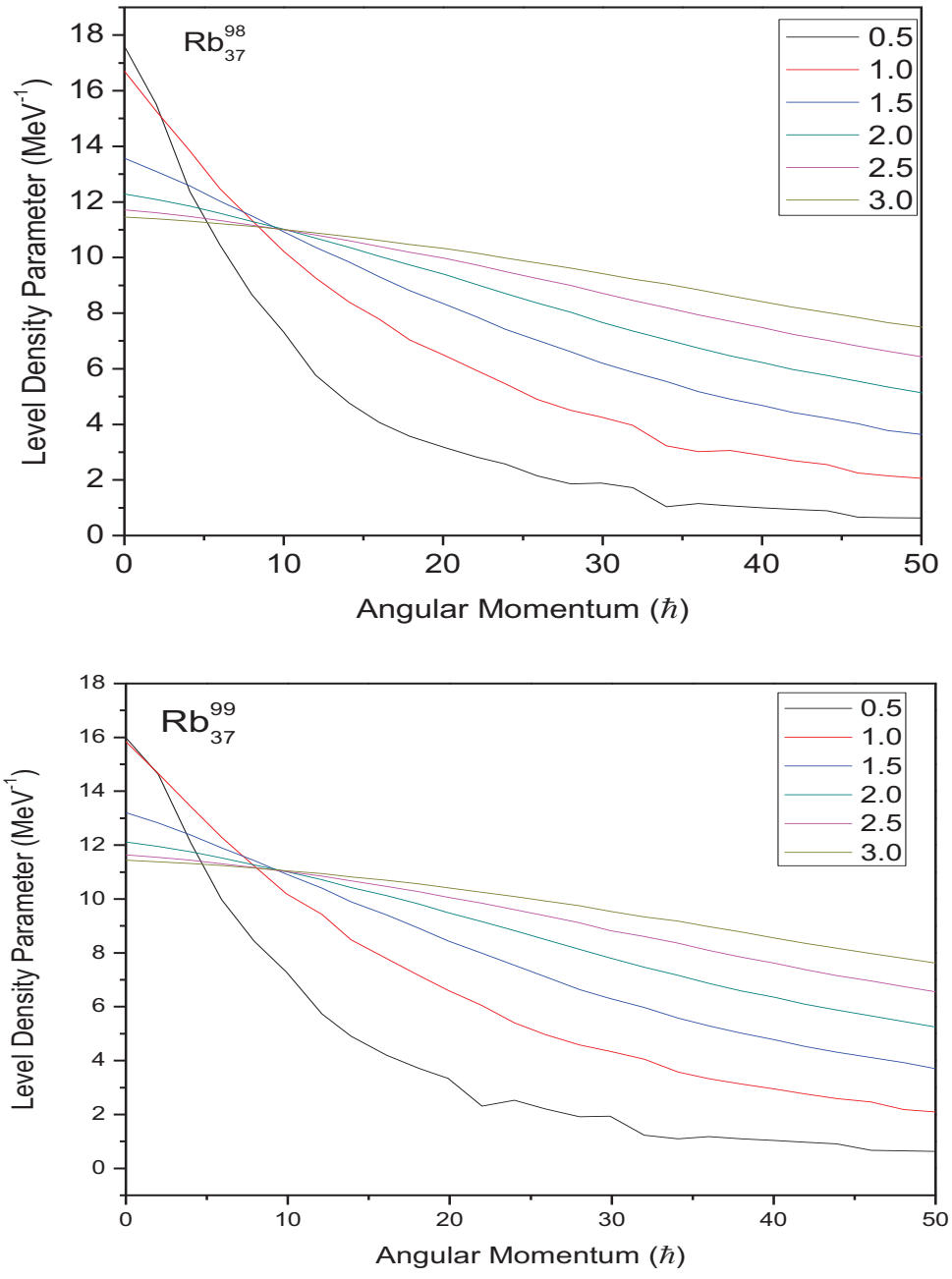


**Figure 6.11: The level density parameter as a function of angular momentum for different temperature T for $^{98}Rb_{37}$ and $^{99}Rb_{37}$**

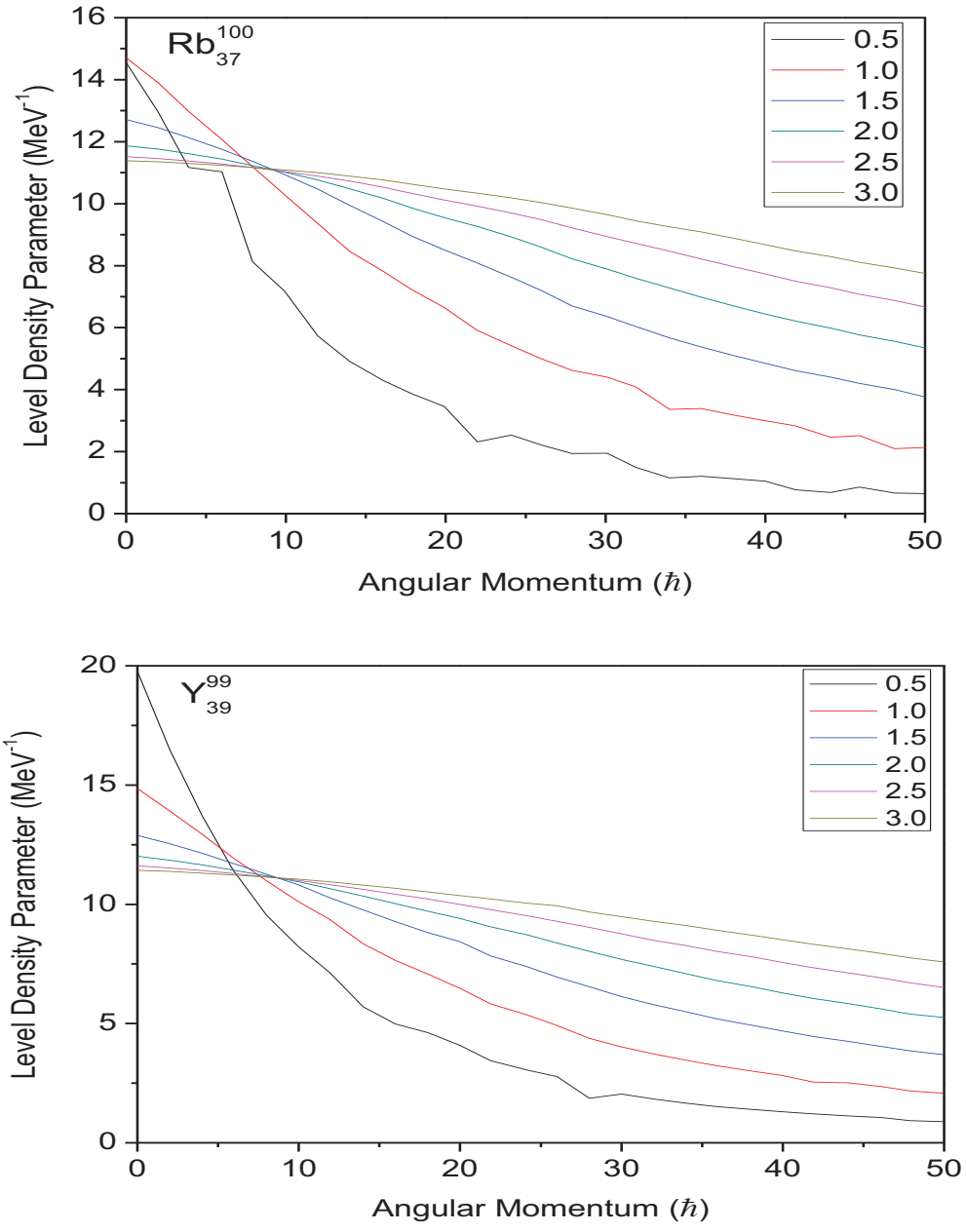


**Figure 6.12: The level density parameter as a function of angular momentum for different temperature T for $^{100}Rb_{37}$and $^{99}Y_{39}$**

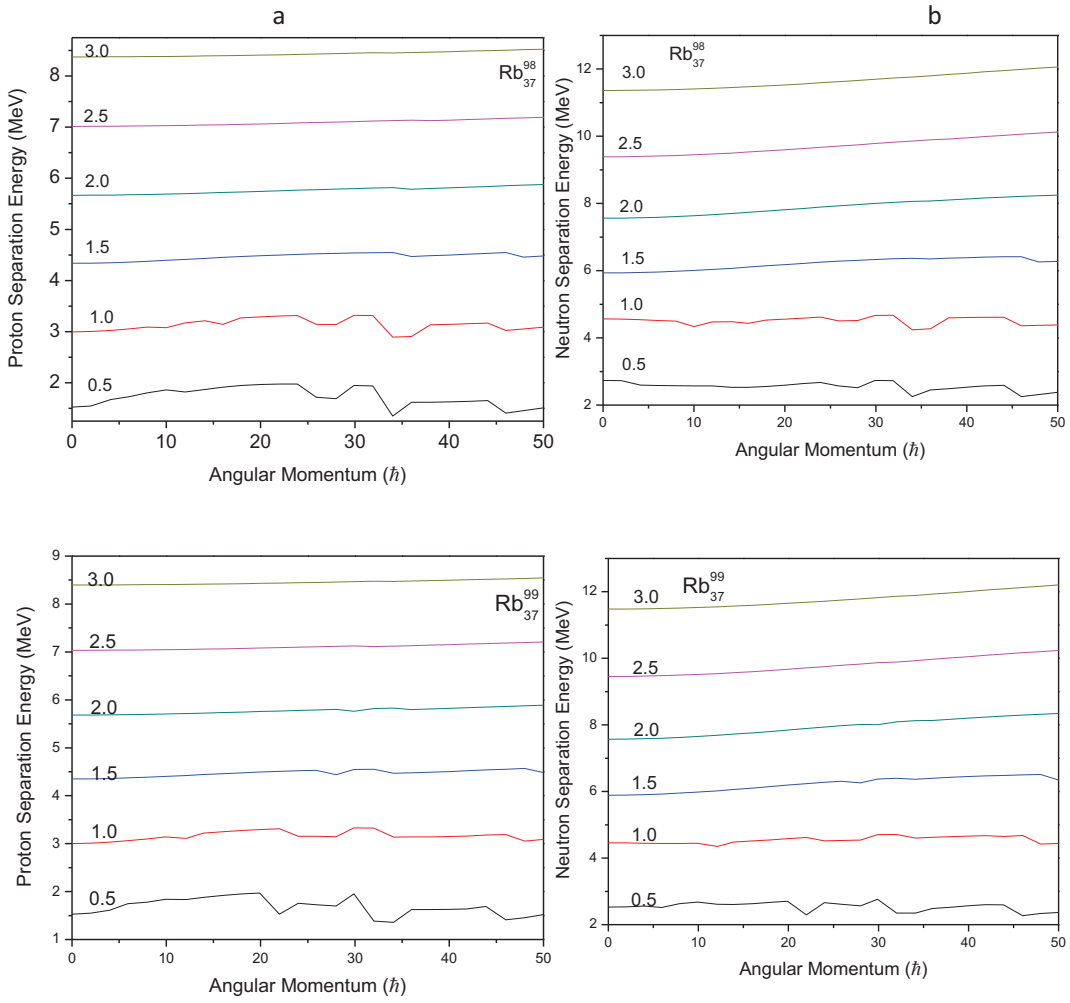


**Figure 6.13: The proton and neutron separation energy as a function of angular momentum for different temperature T for $^{98}Rb_{37}$ and $^{99}Rb_{37}$**

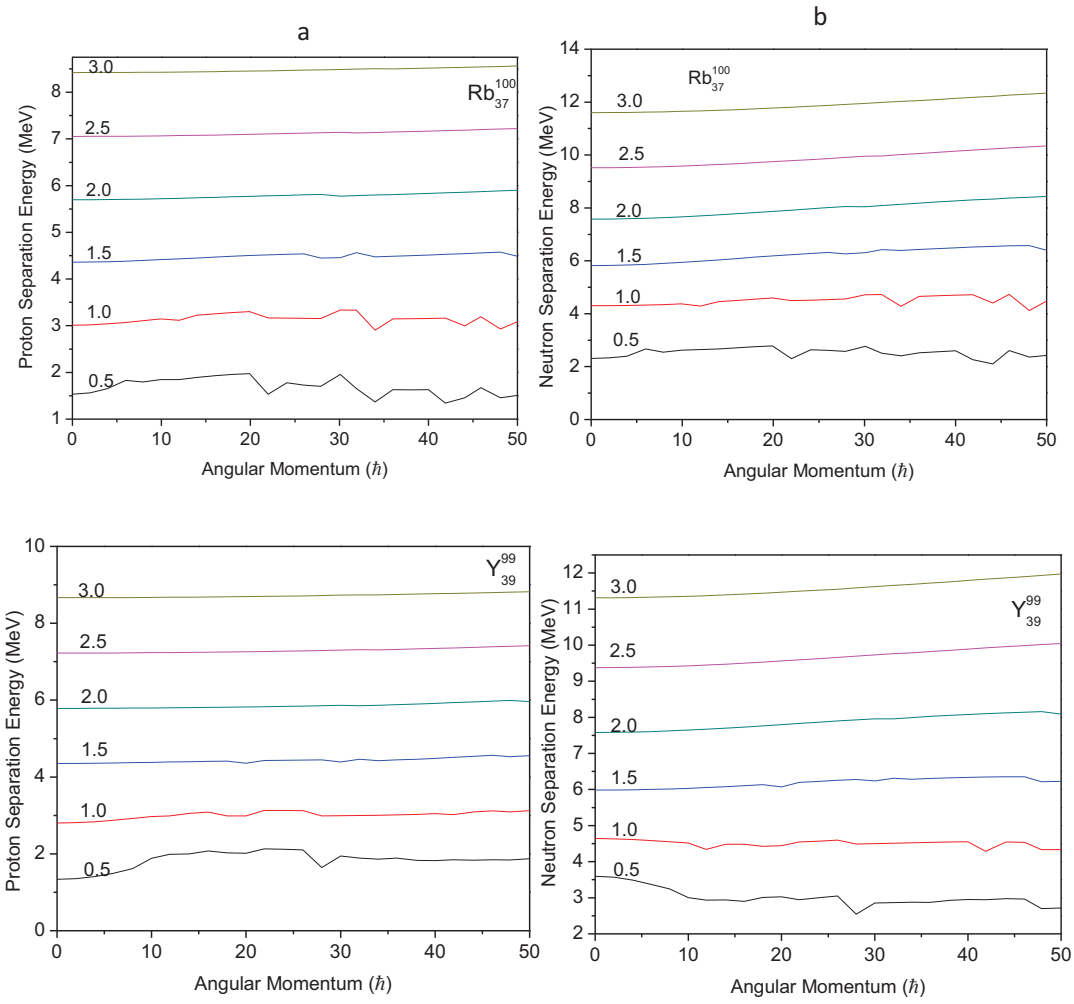


**Figure 6.14: The proton and neutron separation energy as a function of angular momentum for different temperature T for $^{100}Rb_{37}$and $^{99}Y_{39}$**

## 6.3 Conclusion

In this chapter the structural properties of some odd –even and odd-odd nuclei around A ~ 100 Mass region were investigated using statistical theory. The effect of interplay and competition between different degrees of freedom such as temperature, angular momentum and deformation on the structural properties are analyzed. The empirical relation a= A/10 could be reproduced by the investigation on the level density parameter. The shape transition from prolate collective to oblate non-collective at M = 30 and temperature T >0.6MeV is also observed. The influence of the temperature-dependent effect such as the collapse of the shell correction has been observed at a critical temperature (≈ 1.5MeV) as is evident from the values of the level density parameter.

# CHAPTER VII
# SUMMARY AND CONCLUSION

In this chapter, we presents conclusions that were made from the results that have been presented in the preceding chapters and what it has contributed to our understanding of the structural changes and shape transition in the light A~100 region.

We have investigated the structure of nuclei, A~100 region by means of the statistical theory. Shape changes for different values of angular momentum were investigated for $^{94}$Kr, $^{96}$Kr, $^{98}$Kr, $^{98}$Zr$^{100}$Zr,$^{102}$Zr, $^{100}$Mo, $^{102}$Mo and $^{104}$Mo. It is observed that at low spin, the nucleus in an oblate non-collective shape. As spin is increased, it changes smoothly to triaxial shape. A similar behavior is exhibited by the nucleus for the temperature T = 1.0MeV. It is interesting to note that with increasing temperature the presence of triaxial shape vanish, the nuclei undergoes a shape transition from collective prolate to oblate shape.

.

Further, the effect of angular momentum and temperature on the shape of Strontium isotopes has been systematically analyzed. The free energy minimum of Sr as functions of angular momentum and deformation parameters $\beta$ and $\gamma$ calculated at different temperatures. We find that the nucleus in prolate shape for low angular momentum and achieve oblate shape at higher angular momentum. These deformation fluctuations vanish at high temperature of about 1.5 MeV, because of vanishing shell effects at these temperatures. Similar behaviour is observed for $^{92,94,96,98,100}$Sr.

Furthermore, the shape transitions in odd-even and odd-odd nuclei around A ~ 100 are investigated within the framework of the statistical model. The shape transition from prolate collective to oblate non-collective at M = 30 and temperature T > 0.6MeV is also observed. The influence of the temperature-dependent effect such as the collapse of the shell correction has been observed at a critical temperature (≈ 1.5MeV) as is evident from the values of the level density parameter

In conclusion, effects of temperature, angular momentum and Shell Effects on certain parameters evaluated using statistical theory, have been brought out in this thesis.

The scope for the future work is to include the effects of thermal and orientation fluctuations and pairing that may have its influence on the properties of nuclei.

# REFERENCE


[1] Agrawal B. K. and A. Ansari, 1994, ' Calculation of realistic level densities with Bethe's formula', Phys. Lett. B339, pp. 7.

[2] Albers M., K. Nomura, N. Warr, A. Blazhev, J. Jolie, D. Mcher, B. Bastin, C. Bauer, C. Bernards, L. Bettermann, et al., 2013, 'Shape dynamics in neutron-rich Kr isotopes: Coulomb excitation of $^{92}$Kr, $^{94}$Kr and $^{96}$Kr' Nucl. Phys. A 899, pp. 1.

[3] Albers M., N. Warr, K. Nomura, A. Blazhev, J. Jolie, D. Mucher, B. Bastin, C. Bauer, C. Bernards, L. Bettermann, et al., 2012, ' Evidence for a Smooth Onset of Deformation in the Neutron-Rich Kr Isotopes', Phys. Rev. Lett. 108, pp. 062701.

[4] Albers, M. K. Nomura, N. Warr, A. Blazhev, J. Jolie, D. Mcher, B. Bastin, C. Bauer, C. Bernards, L. Bettermann, et al. 2013, 'Shape dynamics in neutron-rich Kr isotopes: Coulomb excitation of Kr-92, Kr-94 and Kr-96`, Nucl. Phys. A 899, pp. 1-28.

[5] Albers, M. N. Warr, K. Nomura, A. Blazhev, J. Jolie,D. Mucher, B. Bastin, C. Bauer, C. Bernards, L. Bettermann, et al. 2012, 'Evidence for a Smooth Onset of Deformation in the Neutron-Rich Kr Isotopes' Phys. Rev. Lett. 109, pp. 209904.

[6] Andersson G., S.E. Larsson, G. Leander, P. Moller, S.G. Nilsson, I. Ragnarsson, S. Aberg, R. Bengtsson, J. Dudek, B. Nerlo-Pomrslo, K. Pomorski and Z. Szymanski 1978, 'Nuclear shell structure at very high angular momentum', Nucl. Phys. A268, pp. 205.

[7] Arseniev D., A. Sobiczewski, and V. Soloviev 1969, 'Equilibrium deformations of neutron-rich nuclei in the $A \approx 100$ region', Nuclear Physics A 139, pp.269.

[8] Arunachalam N., A. Alli Periaynayaki and K. Ilangovan 1997, 'Structural Properties of Hot Rotating $^{40}$Ca', Phys. Rev. C55, pp. 1826.

[9] Azuma R. E., G. L. Borchert, L. C. Carraz, P. G. Hansen, B. Jonson, S. Mattsson, O. B. Nielsen, G. Nyman, I. Ragnarsson, and H. L. Ravn 1979, 'The strongly deformed nucleus $^{100}$Sr', Phys. Lett. B 86, pp. 5.

[10] Baba H. 1970, 'A shell-model nuclear level density', Nucl. Phys. A159, pp. 625.

[11] Bardeen J., L. N. Cooper, and J. R. Schrieffer 1957, 'Theory of Superconductivity', Phys. Rev. 106, pp. 162; 108, pp.1175.

[12] Bengtsson R., S.E. Larsson, G. Leander, P. Moller, S.G. Nilsson, S. Abergand Z. Szymanski 1975, 'Yrast bands and high-spin potential-energy surfaces', Phys. Lett. 57B, pp. 301.

[13] Bethe H. 1936, 'An Attempt to Calculate the Number of Energy Levels of a Heavy Nucleus', Phys.Rev. 50, pp. 332.

[14] Bloch 1977, Proceedings of Statistical Properties of Nuclei, edited by J.B. Garg (Plenum, New York) pp. 379.

[15] Bogoliubov N.N. 1958, 'A New method in the theory of superconductivity'. Zh. Eksp. Teor. Fiz. 34, pp 41; pp. 34, (1958): [Sov.Phys.-JETP 7, (1958) pp. 4; 7, (1958) pp. 51]; Nuovo Cimento 7, (1958) pp. 794.

[16] Bohr and B.R. Mottelson 1961, 'Nuclear Structure', (Benjamin, New York,) Vol.I.

[17] Boyiiukata M., P. Van Isacker, and I. Uluer 2010, 'Description of nuclei in the $A \sim 100$ mass region with the interacting boson model', Phys. G: Nucl. Part. Phys. 37, pp.105102.

[18] Boyukata, M. P. Van Isacker, and I. Uluer 2010, 'Description of nuclei in the A ~ 100 mass region with the interacting boson model', J. Phys. G Nucl. Part. Phys. 37, 105102.

[19] Brack M., R.K. Bhaduri 1997, Semiclassical Physics, Frontiers in Physics Vol. 96, Addison-Wesley.

[20] Browne F., A. Bruce, T. Sumikama, I. Nishizuka, S. Nishimura, P. Doornenbal, G. Lorusso, P.-A. Sderstrm, H. Watanabe, R. Daido, et al. 2015, 'Lifetime measurements of the first 2+ states in $^{104,106}$Zr: Evolution of ground-state deformations', Phys. Lett. B 750, pp. 448.

[21] Campbell P., H. L. Thayer, J. Billowes, P. Dendooven, K. T. Flanagan, D. H. Forest, J. A. R. Griffith, J. Huikari, A. Jokinen, R. Moore, A. Nieminen, G. Tungate, S. Zemlyanoi, and J. Äystö 2002, 'Laser Spectroscopy of Cooled Zirconium Fission Fragments', Phys. Rev. Lett. 89, pp. 082501.

[22] Carjan N. 1979, A. Deloagrange and A. Fluery, 'Excitation energy dependence of the level density for fissionable nuclei', Phys. Rev. C19, pp. 2267.

[23] Chabanat E., P. Bonche, P. Haensel, J. Meyer, and R. Schaeffer 1998, 'A Skyrme parametrization from subnuclear to neutron star densities Part II. Nuclei far from stabilities', Nucl. Phys. A 635, pp. 23.

[24] Chakrabarty D. R., V. M. Datar, Suresh Kumar, T. Mirgule H. Oza and U.K. Pal 1995, 'Energy variation of nuclear level density in 104Pd and 114Sn in the excitation-energy region of 7 to 24 MeV', Phys. Rev. C 51, pp. 2942.

[25] Chan G. and J.R. Huizenga 1982, 'The significance of shell corrections in the parameterization of numerical state density calculations', Nucl. Phys. A187, pp. 225.

[26] Charlwood F. et al. 2009, 'Nuclear charge radii of molybdenum fission fragments', Phys. Lett. B 674, pp. 23.

[27] Cheal B. et al. 2007, The shape transition in the neutron-rich yttrium isotopes and isomer', Phys. Lett. B 645, pp. 133.

[28] Cheifetz E., R. C. Jared, S. G. Thompson, and J. B. Wilhelmy 1970, 'Experimental Information Concerning Deformation of Neutron Rich Nuclei in the A∼100 Region', Phys. Rev. Lett. 25, pp. 38.

[29] Civitarese O. and M. Schvellinger 1994, 'The nuclear level density parameter and nuclear structure effects at finite temperature', J. Phys. G, 20, pp. 1933.

[30] Clement E., M. Zieli_nska, A. Gorgen, W. Korten, S. Peru, J. Libert, H. Goutte, S. Hilaire, B. Bastin, C. Bauer, et al. 2016, 'Coexistence in Neutron-Rich Strontium Isotopes at N=60', Phys. Rev. Lett. Phys. Rev. Lett. 116, pp. 022701.

[31] Clement E., M. Zielinska, A. G¨orgen,W. Korten, S. P´eru, et al. 2016, 'Spectroscopic Quadrupole Moments in $^{96,98}$Sr: Evidence for Shape Coexistence in Neutron-Rich Strontium Isotopes at N=60', Phys. Rev. Lett. 116, pp. 022701.

[32] Clement E., M. Zielinska, et al. 2016, 'Low-energy Coulomb excitation of $^{96,98}$Sr beams', Phys. Rev. C 94, pp. 054326.

[33] Clement, E. M. Zielinska, A. Gorgen, W. Korten, S. Peru, J. Libert, H. Goutte, S. Hilaire, B. Bastin, C. Bauer, et al. 2016, 'Nuclear deformation in the A ≈ 100 region: Comparison between new masses and mean-field predictions', Phys. Rev. Lett. 116, 02270.

[34] Dara W.A., J.A.Sheikhab, G.H.Bhata, R.Palitc, R.N.Alia S.Frauendor 'Microscopic study of doublet bands in odd–odd A = 100 nuclei', Nucl. Phy. A 933, January 2015, pp 123-134.

[35] Decowski P., W. Grochulski, A. Marcinkowski, K. Siwek, and Z. Wilhemi 1968, 'On superconductivity effects in nuclear level density', Nucl. Phys. A110, pp. 129.

[36] Diebel M., D. Glas, U. Mosel and H. Chandra 1980, 'Yrast lines of light nuclei (A = 24–60)', Nucl. Phys. A333, pp. 253.

[37] Dudouet J., A. Lemasson. G. Ducheneet al. 2017, '$^{96}$Kr$^{60}$–Low-Z Boundary of the Island of Deformation at N=60', Phy. Rev. Let. 118, pp. 162501.

[38] E. Cheifetz, R. C. Jared, S. G. Thompson, and J. B. Wilhelmy 1970, 'Experimental Information Concerning Deformation of Neutron Rich Nuclei in the A∼100 Region', Phys. Rev. Lett. 25, pp. 38.

[39] Ebert J. 2012, R. A. Meyer, and K. Sistemich, 'Nuclear Structure of the Zirconium Region': Proceedings of the International Workshop (Springer Science & Business Media, Berlin/Heidelberg).

[40] Egido J.L., L.M. Robledo and V. Martin 2000, 'Behavior of Shell Effects with the Excitation Energy in Atomic Nuclei', Phys. Rev. Lett. 85, pp. 26.

[41] Egido J. L., P. Ring and H. J. Mang 1986, 'Temperature-dependent Hartree-Fock-Bogoliubov calculations in hot rotating nuclei', Nucl. Phys. A451, pp. 77.

[42] Eisenberg J.M. and W. Greiner 1976, Microscopic theory of Nucleus (North Holland, Amsterdam) p. 399.

[43] Ericson T., 'The statistical model and nuclear level densities', Adv. Phys. 9, (1960) 425.

[44] F.K. Wohn, J. C. Hill, R. F. Petry, H. Dejbakhsh, Z. Berant, and R. L. Gill 1983, 'Rotational Structure and Nilsson Orbitals for Highly Deformed Odd-A Nuclei in the A∼100 Region', Phys. Rev. Lett. 51, pp. 873.

[45] Faessler, K.R. Sandhya Devi, F. Grummer, K.W. Schmid, and R.R. Hilton 1976, 'Backbending: Coriolis antipairing or rotational alignment?', Nucl. Phys. A256, pp. 106.

[46] Faessler, R.R. Hilton and K.R. Sandhya Devi 1976, 'Microscopic Determination of Nuclear Deformation Energy Surfaces at Very High Spins', Phys. Lett. 62B, pp. 133.

[47] Federman and S. Pittel P. 1977, 'Towards a unified microscopic description of nuclear deformation', Phys. Lett. B 69, pp. 385.

[48] Federman P. and S. Pittel 1978, 'Hartree-Fock-Bogolyubov study of deformation in the Zr Mo region', Phys. Lett. B 77, pp. 29.

[49] Feynman R.P. 1972, Statistical Mechanics (Benjamin, Massachusetts) 1.

[50] Fowler R.H. 1936, Statistical Mechanics, (Cambridge University Press, NewYork) pp. 27-30.

[51] Gaardhoje J. J 1992, 'Nuclear structure at high excitation energy studied with giant resonances', Annu. Rev. Nucl. Part. Sc. 42, pp. 483-536.

[52] Gaardhoje J. J. 1992, 'Nuclear Structure at High Excitation Energy Studied with Giant Resonances', Annu. Rev. Nucl. Part. Sc. 42, pp. 483-536.

[53] Gaardhoje, J.J. A.M. Bruce and B. Herskind, 1988 'Nuclear collective motion under extreme conditions: The GDR at very high spin and temperature', Nuci. Phys. A482, pp. 121-139.

[54] Glasstone S. 1973, 'Theoretical Chemistry', (Affiliated East-West, New Delhi) pp. 347.

[55] Goodman AL. 1986, 'Finite-temperature Hartree-Fock-Bogoliubov calculations in rare earth nuclei', Phys. Rev. C34, pp. 1942.

[56] Goodman AL. 1986, 'Temperature-induced deformation in $^{148}$Sm', Phys. Rev. C33, pp. 2212.

[57] Goodman AL. 1988, 'Temperature-dependent shape transition in $^{166}$Er', Phys. Rev. C38, pp. 977.

[58] Gottschalk P.A. and T. Ledergerber 1977, 'Shell-correction approach to nuclear state densities and the competition between fission and neutron emission of $^{210}$Po', Nucl. Phys. A278, pp. 16.

[59] Heyde K. and J. L. Wood 2011 'Shape coexistence in atomic nuclei' 'Rev. Mod. Phys. 83, pp. 1467-1522.

[60] Hotchkis M. A. C., J. L. Durell, J. B. Fitzgerald, A. S. Mowbray, W. R. Phillips, I. Ahmad, M. P. Carpenter, R. V. F. Janssens, T. L. Khoo, E. F. Moore, L. R. Morss, P. Benet, and D. Ye 1991, 'The strongly deformed nucleus $^{100}$Sr', Nucl. Phys. A 530, pp. 111.

[61] Huizenga J.R. and L.G. Moretto 1972, 'Nuclear Level Densities', Ann. Rev. Nucl. Sci. 22, pp. 427.

[62] Huizenga J.R. 1972, 'Proceedings of the Statistical Properties of Nuclei' (edited by J.B. Garg, Plenum Press, New York,) pp. 425.

[63] Ignatyuk A.V., G.N. Smirenkin, A.S. Tishin. 1975, 'Phenomenological description of the energy dependence of the level density parameter', Yad. Fiz. 9, pp. 425.

[64] Inglis D.R. 1954, 'Particle Derivation of Nuclear Rotation Properties Associated with a Surface Wave', Phys. Rev. 96, pp. 1059.

[65] Irvine J.M. 1972, Nuclear Structure Theory (Pergamon Press, New York).

[66] Johansson S. A. 1965, 'Gamma de-excitation of fission fragments: (II). Delayed radiation', Nuc. Phy. 64, pp.147.

[67] Kirchuk E and P. Federman 1993, 'Physical Nuclear deformation in the mass-80 and mass-100 regions', Phys. Review C, 47(2), pp. 2.

[68] Lalkovski S. and P. Van Isacker 2009, 'IBM-1 calculations towards the neutron-rich nucleus $^{106}$Zr', Phys. Rev. C 79, pp. 044307.

[69] Leider R.M. and H.Ryde 1978, 'Advances in nuclear physics', (ed by E.Vogt and M. Baranger, New York) vol. 10, pp. 1.

[70] Mamta Aggarwal 2016, 'Shape Transition to a Rare Shape Phase of Prolate Non-collective in A=100 Isobars Journal of Nuclear Physics', Material Sciences, Radiation and Applications -3(2), pp. 179.

[71] Mei H., J. Xiang, J. M. Yao, Z. P. Li, and J. Meng 2012, 'Rapid structural change in low-lying states of neutron-rich Sr and Zr isotopes', Phys. Rev. C 85, pp. 034321.

[72] Moretto L.G. 1971, 'Pairing correlation in excited nuclei with non-zero angular momentum', Phys. Lett. 35B, pp. 379; Phys. Lett. 34B, (1971) 191; Nucl. Phys. A180, (1972) 337; Phys. Lett. B38, (1972) 393; Nucl. Phys. A436, (1985) 14.

[73] Nanai, B.B. Back, D.J. Hofman, G. Hackman, D. Ackermann, Y. Alhassid 1999, 'Exclusive studies of the GDR in excited nuclei', Nucl. Phys. A649, pp. 153c.

[74] Neergard K. and V.V. Pashkevich 1975, 'Shell corrections to the deformation energies of very high spin nuclei (I $\lesssim$ 100)', Phys. Lett. 59B, pp. 218.

[75] Neergard K., H. Toki, M. Polszjczak and A. Faessler 1977, 'Very high spin Strutinsky calculations with a woods-saxon potential', Nucl. Phys. A287, pp. 48.

[76] Nerlo-Pomorska B., J. Sykut 2005, 'Temperature Dependence of the Nuclear Shell Energies', Acta Physica Polonica B 36, pp. 1377.

[77] Nilsson S. G. 1955, 'Binding states of individual nucleons in strongly deformed nuclei', Mat. Fys. Medd. Dan. Vid. Selsk. 29(16), pp. 1955

[78] Nilsson S.G., C.F. Tsang, A. Sobiczewski, Z. Szymanski, S. Wycech, G. Gaustafson, I.L. Lamm, P. Moller and B. Nilsson 1969, 'On the nuclear structure and stability of heavy and superheavy elements', Nucl. Phys. A131, pp. 1.

[79] Park, J.A.B. Garnsworthy, R. Krucken, C. Andreoiu, G.C. Ball, P.C. Bender, A. Chester, A. Close, P. Finlay, P. E. Garrett, et al., 2016, 'Shape coexistence and evolution in $^{98}$Sr', Phys. Rev. C 93, 014315.

[80] Pathria R.K. 1972, 'Statistical Mechanics' (Pergamon Press, New York,) pp. 85.

[81] Pereira J et al. 2009, 'β-decay half-lives and β-delayed neutron emission probabilities of nuclei in the region A≲110 relevant for the r process', Phys. Rev. C 79, pp. 035806.

[82] Petrovici A, K W Schmid and A Faesslerv 2011, 'Self-consistent description of shape coexistence in the A~100 Zr nuclei', Journal of Physics: Conference Series 312, pp. 092051.

[83] Pinston, J. Genevey, G.S. Simpson, W. Urban 2005. 'Shape coexistence in odd and odd-odd nuclei in the A~100 region', AIP Conference Proceedings. 798 (798), pp.149-156,

[84] Poloszajctak M., K.R. Sandhya Devi and A. Faessler 1977, 'Microscopic Determination of Energy Surfaces at Very High Spin States', Z. Phys. A282, pp. 267.

[85] Pomorski K, B Nerlo-Pomorska, A Surowiec, M Kowal 2000, 'Light-particle emission from the fissioning nuclei $^{126}$Ba, $^{188}$Pt and $^{266,272,278}_{110}$: theoretical predictions and experimental results', Nucl. Phys. A679, pp. 25.

[86] Pomorski K. 2004, 'A Particle number conserving shell-correction method', Phys. Rev. C70, pp. 044306.

[87] Quentin K.A. and H. Flocard 1978, 'Self-Consistant Calculations of Nuclear Properties with Phenomenological Effective Forces', Annu. Rev. Nucl. Part. Sc. 28, pp.523.

[88] Rajasekaran M. and V. Devanathan 1981, 'Nuclear Level Density and the Mass Distribution of Fission Fragments', Phy. Rev. C24(6), pp. 2606.

[89] Rajasekaran M. and V. Devanathan 1982, 'A New Formula for Nuclear Level Density', Phys. Lett. 113B, pp. 433.

[90] Rajasekaran M., N. Arunachalam and V. Devanathan 1987, 'Effect of high spin states on fusion in heavy ion collisions', Phys. Rev. 36, pp. 1860.

[91] Rajasekaran M., N. Arunachalam, T. R. Rajasekaran, and V. Devanathan 1988, 'Shell effects in hot isobaric nuclei', Phys. Rev. C38, pp. 1926.

[92] Rajasekaran M., T. R. Rajasekaran, and N. Arunachalam 1988, 'Nuclear Level Density Parameter - Its Dependence on Spin and Temperature', Phys. Rev. C37, pp. 307.

[93] Rajasekaran M., T. R. Rajasekaran, N. Arunachalam and V. Devanathan 1988, 'Neutron Separation Energy and Emission Probability at High Spins', Phys. Rev. Lett. 61, pp. 2077.

[94] Ramamoorthy V.S., S.S. Kapoor and S.K. Kataria 1970, Excitation Energy Dependence of Shell Effects on Nuclear Level Densities and Fission Fragment Anisotropies Phys. Rev. Lett. 25, pp. 386; S.K. Kataria and V.S. Ramamorthy, Nucl. Phys. A349, (1980) 10; V.S. Ramamoorthy and Y.R.Waghmare, Pramana 20, (1983) 5213.

[95] Regis J.-M., J. Jolie, N. Saed-Samii, N. Warr, et al. 2017, 'Abrupt shape transition at neutron number N=60: B(E2) values in $^{94,96,98}$Sr from fast $\gamma$–$\gamma$ timing', Phys. Rev. C 95, pp. 054319.

[96] Rodriguez T. R. 2014, 'Structure of krypton isotopes calculated with symmetry-conserving configuration-mixing methods', Phys. Rev. C 90, pp. 034306.

[97] Rodriguez-Guzman R., P. Sarriguren, and L. M. Robledo 2010, 'Systematics of one-quasiparticle configurations in neutron-rich odd Sr, Zr, and Mo isotopes with the Gogny energy density functional', Phys. Rev. C 82, pp. 044318.

[98] Rodriguez-Guzman R., P. Sarriguren, L. M. Robledo, and S. Perez-Martin 2010, 'Nuclear Theory Charge radii and structural evolution in Sr, Zr, and Mo isotopes', Phys. Lett. B 691, pp. 202.

[99] Rodriguez-Guzman R.,1 P. Sarriguren,1 and L. M. Robledo 2010, 'Signatures of shape transitions in odd-A neutron-rich rubidium isotopes', Phy. Rev. C 82, pp. 061302(R).

[100] Rodriguez-Guzman, P. Sarriguren, L. M. Robledo, and S. Perez-Martin 2010, 'Charge radii and structural evolution in Sr, Zr, and Mo isotopes' Phys. Lett. B 691, pp.202.

[101] Rodriguez-Guzman, R. P. Sarriguren, and L. M. Robledo 2010, 'Systematics of one-quasiparticle configurations in neutron-rich odd Sr, Zr, and Mo isotopes with the Gogny energy density functiona', Phys. Rev. C 82, pp.044318.

[102] Roubin de, D. Atanasov, K. Blaum, S. George, F. Herfurth, D. Kisler, M. Kowalska, S. Kreim,D. Lunney, V. Manea, E. Minaya Ramirez,M. Mougeot, D. Neidherr, M. Rosenbusch,L. Schweikhard, A. Welker, F. Wienholtz, R. N. Wolf, and K. Zuber 2017, 'Nuclear deformation in the A≈100 region: Comparison between new masses and mean-field predictions', Phy. Rev. C 96, 014310.

[103] S. A. Johansson 1965, 'Gamma de-excitation of fission fragments: (II). Delayed radiation Nucl. Phys. 64, pp. 147.

[104] Sano M. and S. Yamasaki 1963, 'Phase Transition and Level Density of Atomic Nuclei' Prog. Theor. Phys. 29, pp. 397-414.

[105] Santhosh Kumar S., A. Victor Babu, P. Preetha and T. R. Rajasekaran 2015, 'Structural Changes of Hot Rotating Neutron Deficient Doubly Magic Nucleus 100Sn', Asian Journal of Science and Applied Technology, 4(1), pp. 21.

[106] Sarriguren P. 2015, 'β-decay properties of neutron-rich Ge, Se, Kr, Sr, Ru, and Pd isotopes from deformed quasiparticle random-phase approximation', Phys. Rev. C 91, pp. 044304.

[107] Sarriguren P. 2015, 'β-decay properties of neutron-rich Ge, Se, Kr, Sr, Ru, and Pd isotopes from deformed quasiparticle random-phase approximation', Phys. Rev. C 91, pp. 044304.

[108] Schussler F.J., A.PinstonE. Monnand A. Moussa G. Jungab E. Koglinab B. Pfeifferab R. V. F.Janssens J. van Klinken 1980, 'Discovery of a very low-lying $0^+$ state in $^{98}$Sr and shape coexistence implication in $^{98}$S', Nucl. Phy. A 339, pp. 415.

[109] Seeger P.A. 1970, Proceedings of the International Conference on the Properties of Nuclei far from the Region of Beta-Stability, Switzerland, Vol. I, pp. 217.

[110] Shanmugam G., P.R. Subramanian, M. Rajasekaran and V. Devanathan 1978, Proceedings of the International Conference on Nuclear Interactions, Canberra, Australia, Lecture Notes in Physics, Vol.92, edited by B.A. Robson (Springer, Heidelberg, 1979) pp. 433.

[111] Sheline R., I. Ragnarsson, and S. Nilsson 1972, 'Shell structure for deformed nuclear shapes', Physics Letters B 41, pp. 115.

[112] Shizuma K., H. Ahrens J. P. Bocquet N. Kaffrell B. D. Kern H. Lawin R. A. Meyer K. Sistemich G. Tittel Trautmann 1984, 'Odd neutron nuclei near A=100: Rotational bands in$^{103}$Mo and $^{105}$Mo populated in the $\beta^-$ decays of$^{103}$Nb and$^{105}$Nb', Z. Phys. A - Atoms and Nuclei 315, pp. 65-75.

[113] Sieja, K. F. Nowacki, K. Langanke, and G. Martnez Pinedo 2009, 'Shell model description of zirconium isotopes', Phys. Rev. C 79, 064310.

[114] Sirag M. M. 2015, 'Investigation of Nuclear Shape Phase Transitions in the A∼100 Region Using the Interacting Boson Model', Chinese Journal Of Physics, 53, pp. 7.

[115] Skalski J, Heenen P H and Bonche P 1993, 'Shape coexistence and low-lying collective states in A ≈ 100 Zr nuclei', Nucl.Phys. A 559, pp. 221.

[116] Skalski J., S. Mizutori, and W. Nazarewicz 1997, ‘Equilibrium shapes and high-spin properties of the neutron-rich $A \approx 100$ nuclei’, Nucl. Phys. A 617, 282-315.

[117] Smith G., J. L. Durell, W. R. Phillips, W. Urban, P. Sarriguren, and I. Ahmad 2012, ‘Lifetime measurements and nuclear deformation in the A≈100region’, Phys. Rev. C 86, pp. 014321.

[118] Snover, K.A. 1986 ‘Giant Resonances in Hot Nuclei’, Ann. Rev. Nuci. Part. Sci. 36, 545-603.

[119] Soloviev V.G. 1976, ‘Theory of Complex Nuclei, (Pergamon Press, New York) pp. 20.

[120] Sotty C. et al. 2015, ‘$_{37}Rb^{60}$: The Cornerstone of the Region of Deformation around A ∼100’, Phy. Rev. Lett. 115, pp. 172501-6.

[121] Strutinsky V.M. 1967, ‘Shell effects in nuclear masses and deformation energies’, Nucl. Phys. A95, pp. 420-442.

[122] Sumikama T., K. Yoshinaga, H.Watanabe, S. Nishimura, Y. Miyashita, K. Yamaguchi, K. Sugimoto, J. Chiba, Z. Li, H. Baba, et al. 2011, ’tructural Evolution in the Neutron-Rich Nuclei $^{106}$Zr and $^{108}$Zr’, Phys. Rev. Lett. 106, 202501.

[123] Thomas T., K. Nomura, V. Werner, T. Ahn, N. Cooper, H. Duckwitz, M. Hinton, G. Ilie, J. Jolie, P. Petkov, et al. 2013, ‘Evidence for shape coexistence in $^{98}$Mo’, Phys. Rev. C 88, pp. 044305.

[124] Urban W. J. L. Durell, A.G. Smith, W.R. Phillips, M.A. Jones, B.J. Varley, T. Rząca Urban, I. Ahmad, L.R. Morss, M. Bentaleb 2001, ‘Medium-spin structure of $^{96,97}$Sr and $^{98,99}$Zr nuclei and the onset of deformation in the A∼100 region’, Nucl. Phys. A689, pp. 605.

[125] Urban W. ,J. A. Pinston J. Genevey T. Rzaca-Urban A. Złomaniec G. Simpson J. L. Durell W. R. Phillips A. G. Smith B. J. Varley I. Ahmad N. Schulz 2004, ‘The ν9/2[404] orbital and the deformation in the A ∼ 100 region’, Eur. Phys. J. A 22, pp. 241.

[126] Vidya DEVI 2013, 'Structure and odd-even staggering of Mo, Ru, and Pd even-even nuclei in the framework of IBM-1', Turkish Journal of Physics, 37, pp.330- 347.

[127] Wadsworth R., et al. 2009, 'Spectroscopy Of N ~ Z Nuclei Below Mass 100', Acta Physica Polonica B Vol. 40 (3), pp. 611.

[128] William Jr. F.C., 'An Iterative Method for the Calculation of Nuclear Level Densities', Nucl. Phys. A133, (1969) 33; G. Chan and J.R. Huizenga, Nucl. Phys. A187, (1982) 225.

[129] Xiang J., Z. P. Li, Z. X. Li, J. M. Yao, and J. Meng 2012, 'Covariant description of shape evolution and shape coexistence in neutron-rich nuclei at N≈60', Nucl. Phys. A 873, pp.1.